Oxygen and Hydrogen Isotopic Characterization of Groundwaters of India: Insights into Hydrogeological Processes

Thesis submitted to

Indian Institute of Technology Gandhinagar, India

for the degree of
Doctor of Philosophy
in
Earth Sciences
by

Amit Pandey
(Roll no. 17330005)

Supervised by

Prof. R. D. Deshpande

Geosciences Division
Physical Research Laboratory, Ahmedabad

August 2022

Dedicated to

My Parents and Teachers

DECLARATION

I declare here that this thesis report represents my own ideas in my own words, and I have included others' ideas with appropriate citations from original sources. I also declare that I have followed all principles of academic honesty and integrity and have not misrepresented, fabricated, or falsified any idea/fact/source/data in my submission. I understand that any violation of the above can cause disciplinary action by the Institute and can also evoke penal action from the sources that have thus not been properly cited or from whom proper permission has not been taken when needed.

Amit Pandey
Roll no. 17330005

Date: 03/08/2022

Discipline of Earth Sciences

Indian Institute of Technology Gandhinagar, Gujarat-382355

CERTIFICATE

It is to certify that the research work contained in the thesis titled "**Oxygen and Hydrogen Isotopic Characterization of Groundwaters of India: Insights into Hydrogeological Processes**" by Mr. Amit Pandey (Roll no: 17330005) has been carried out under my supervision and this work has not been submitted elsewhere for a degree. I have read this dissertation, and in my opinion, it is fully adequate, in scope and quality, for the degree of Doctor of Philosophy.

Date: 03/08/2022

Prof. R.D. Deshpande
(Thesis Supervisor)
Geosciences Division
Physical Research Laboratory
Ahmedabad, India

Acknowledgements

At this moment when I am winding up my Ph.D. thesis, I wish to express a few words of gratitude to these people who gave their unconditional support with dedicated spirit and have been part of my life as teachers, friends, and colleagues.

First and foremost, I owe a deep sense of gratitude to my thesis supervisor Prof. R.D. Deshpande for his guidance, continuous support, enduring encouragement, and tolerance he has shown me all throughout. He helped me to develop critical scientific thinking and gave valuable advice to improve my presentation skills to carry out scientific research. Under his guidance, I have learned the importance of ethics in science which one needs to maintain. I thank him for his patience while correcting my manuscripts and thesis. I must confess that those were the most difficult times for both of us.

The work reported here is carried out under the aegis of a National Programme on Isotope Fingerprinting of Waters of India (IWIN), funded jointly by the Department of Science and Technology (DST), Govt. of India vide Grant No. IR/ S4/ESF-05/2004, and the Physical Research Laboratory (PRL). The DST and PRL are acknowledged with thanks for all their support in carrying out this study. The groundwater samples along with hydrogeological information from different locations were provided by Central Groundwater Board (CGWB). We would like to thank Shri B.M. Jha, Chairman, CGWB, Dr. Dipankar Saha, Member CGWB, and Dr. Uma Kapoor, Scientist, CGWB, and the CGWB Coordinator for IWIN National Programme. I would also like to thank the scientists, hydrogeologists, and field team members of the CGWB without them nationwide sampling was not possible.

I would also like to express my sincere regard to my Doctoral Student Committee (DSC) members, Prof. M. G. Yadava, Prof. Sanjeev Kumar, and Dr. Harish Gadhavi, for their critical evaluation and crucial comment during the discussion. I would also like to extend my deepest gratitude to geoscience faculty members at PRL, Prof. J. S. Ray, Dr. A.D. Shukla, Prof. N. Rastogi, Dr. Arvind Singh, Dr. A. K. Sudheer, Dr. V. Goswami, and Dr. A. H. Laskar and others who attended my talk in Tuesday seminar and gave their valuable inputs and comments. The focus on work could be maintained as the other issues were always taken care of by PRL. I thank the Director for providing the facilities. Without the help extended *by members from administrative staff, library, computer center, workshop, maintenance, purchase, stores, accounts, medical, housekeeping, canteen, and office, life would not have been as convenient here.*

Further, I am thankful to Mr. Virendra Padhya and Dr. Raicy for their tireless support during fieldwork and for helping me in sample analysis and Dr. A. K. Sudheer for analysis and interpretation of major ions. I am thankful to IWIN family members Aakash, Rouf, Naveen, Saranya, Ashwini, Vishwa, Vaishnavi, and Mahesh Bhai who have made the experience of working in the lab fun and joyful. I am immensely thankful to Harsh, Swagatika, Siddharth, Kimi, and Juhi for their last moments of help without that I am unable to submit my thesis timely.

I would like to acknowledge Ikshu, Anirban, Bivin, Venkatesh, Anil, Chandana, Iftikar, Manu, Kiran, Niharika, Naman, Harsh, Aashish, Abdur, Deepika, Nisha, Deepak, Sanjeet, Deva, Ajayeta, Chandrima, and Shreya who have been wonderful seniors and friends. I am lucky to enjoy friendships with a new spectrum of people during my five years of life at PRL. Atif, Rajesh, Partha, Himanshu, Milan and a whole host of others too numerous to mention have helped me in course of my study.

My parents and family members continue to be an anchor of stability and support in my studies and my life. I am deeply grateful to them.

Abstract

Groundwater is the largest freshwater reservoir on Earth which sustains major water requirements for drinking, agriculture, and industrial usage. Groundwater also maintains the health of the riverine ecosystem by providing water through base flow. For India, Groundwater is even more important as it supports > 60% of irrigated agriculture and >85% of drinking water supplies. With ~250 km^3 of annual extraction, India is the large extractor of groundwater in the world. Although groundwater is known to be a limited natural resource, India depends heavily on it due to erratic and unevenly distributed rainfall and heterogeneous surface water availability. High dependency on groundwater has led to indiscriminate exploitation of groundwater in India over the last several decades, which has gradually resulted in various groundwater-related issues such as depletion in groundwater levels and severe scarcity, quality deterioration by geogenic and anthropogenic contaminants, high cost of pumping deeper groundwater, and marine water intrusion along the coastline. Groundwater is also lost to the sea through submarine groundwater discharge (SGD) along some stretches of India's 7500 km long coastline. Superimposed on these problems are the climate-change-related adverse impacts on groundwater resources.

Since groundwater is a precious but threatened natural resource of India, it is very important to understand hydrogeological processes concerning groundwater recharge. Groundwater recharge is conventionally estimated in India using the Groundwater Level Fluctuation Method and the Rainfall Infiltration Factor Method. These methods do not provide scientific information about the hydrogeological processes and factors concerning surface water groundwater interactions that govern groundwater recharge. Having this knowledge is important to take more informed policy decisions about groundwater development and management.

In the above backdrop, the broad scientific objective of this doctoral research is to understand the surface water-groundwater interaction and to identify the underlying processes and factors such as the effects of hydrogeology, lithology, orography, drainage, evaporation, and proximity to surface water bodies, the southwest and the northeast monsoon systems, vapour sources. Oxygen and hydrogen isotopic composition ($\delta^{18}O$, δD and d-excess) are useful tracers to characterize different water sources (groundwater, river, surface reservoirs, rain) and to understand their interaction and mixing. In this doctoral research, seasonal variation in $\delta^{18}O$, δD, and d-excess of groundwater have been examined and interpreted in conjunction with the

isotopic composition of its complimentary components (rainwater, river water, surface reservoirs) and other hydrogeological and meteorological aspects. While this thesis is largely based on the use of stable isotope composition of groundwater, other methodological components also include isotope mass balance, a two-component mixing model, backward wind trajectory analyses, and uncertainty analyses to strengthen the isotope-based inferences.

As the major scientific outcome of this doctoral research, it has been possible to broadly identify different regions in India where groundwaters are recharged by different types of recharge source waters (e.g., monsoonal rains, canal waters, surface waters, deeper groundwaters) and due to different types of recharge mechanisms (e.g., preferential recharge pathways, preferential sources, irrigation return flow). Overall, this doctoral research provided important new hydrological insights into the surfacewater-groundwater interaction in different parts of India.

This is the most extensive groundwater isotopic study ever carried out in India based on more than 5000 groundwater samples over one seasonal cycle of pre-monsoon and post-monsoon collected under the aegis of a multi-institutional collaborative national programme on isotope fingerprinting of waters of India (IWIN).

The general findings from this doctoral research are provided in one of the chapters on seasonal isoscapes ($\delta^{18}O$ and δD) of groundwater in India and underlying hydrogeological processes. The finer details emerging from certain states in India have been presented in subsequent chapters. In one of the chapters, the changes in the isotopic composition of groundwater within a decade have also been examined for a particular region. The last chapter of this thesis will discuss the limitations of this research and the future scopes of research emerging from this thesis.

Contents

Acknowledgements **ix**

Abstract **xi**

Abbreviations **xvi**

CHAPTER 1 1

Introduction **1**
Motivation 3
Objectives 4

CHAPTER 2 5

Methodology **5**
2.1 IWIN National Programme 5
2.2 Sampling locations and collection protocols 6
2.3 Isotope analysis 8
2.4 Isotope rationale/ systematics 11
2.5 Isotopes in precipitation 15
2.6 Isotopes in groundwater 16
2.7 Additional data used 17

CHAPTER 3 20

Seasonal isoscapes (δ^{18}O and δD) of groundwater in India and underlying hydrogeological processes **20**
3.1. Introduction 20
3.2 Study area 21
3.3 Results and Discussion 23
3.4 Conclusion 34

CHAPTER 4 35

Surface water - groundwater interaction in semi-arid western India (Gujarat) **35**
4.1 Introduction 35
4.2 Study area 36
4.3 Results and Discussion 38
4.4 Conclusion 48

CHAPTER 5 50

Long-term variation in groundwater dynamics in Gujarat **50**
5.1. Introduction 50
5.2 Study area 51
5.3 Results and Discussion 52
5.4 Conclusion 58

CHAPTER 6 59

Groundwater dynamics in coastal southwestern India (Kerala) 59

6.1 Introduction 59
6.2 Study area 60
6.3 Results and discussion 63
6.4 Conclusion 74

CHAPTER 7 76

Seasonal recharge of groundwater and its spatiotemporal variation in central India (Madhya Pradesh) 76

7.1 Introduction 76
7.2 Study area 77
7.3 Results and Discussion 79
7.4 Conclusion 91

CHAPTER 8 92

Conclusion and Way Forward 92

8.1 Conclusion 92
8.2 Limitations 94
8.3 Future Scope 95

References 97

Abbreviations

agl	Above Ground Level
amsl	Above Mean Sea Level
AS	Arabian Sea BOB Bay of Bengal
BCM	Billion Cubic Meter
bgl	Below Ground Level
BOB	Bay of Bengal
CF	Continuous Flow
CGWB	Central Groundwater Board
GC	Gas Chromatography
GDP	Gross Domestic Product
GISP	Greenland Ice Sheet Precipitation
GMWL	Global Meteoric Water Line
GNIP	Global Network of Isotopes in Precipitation
GVA	Gross Value Added
GW	Groundwater
HYSPLIT	Hybrid Single Particle Lagrangian Integrated Trajectory Model
IAEA	International Atomic Energy Agency
IC	Ion Chromatography
IMWL	Indian Meteoric Water Line

IRMS	Isotope Ratio Mass Spectrometer
IWIN	Isotope Fingerprinting of Waters of India
LMWL	Local Meteoric Water Line
lps	Litre Per Second
NEM	Northeast Monsoon
RIF	Rainfall Infiltration Factor
SLAP	Standard Light Antarctic Precipitation
SWM	Southwest Monsoon
TDS	Total Dissolved Solids
VSMOW	Vienna Standard Mean Ocean Water

Chapter 1

Introduction

Groundwater is an important subsurface component of the hydrological cycle stored in the primary or secondary pore spaces of the aquifer. Globally groundwater is one of the largest freshwater reservoirs used for drinking purposes by billions of people. It plays a central role in sustaining agriculture and maintaining the health of the riverine ecosystem by providing water through base flow [*Alley & Leake*, 2004; *Winter*, 2007; *Gleeson et al.*, 2012; *Pohl et al.*, 2015; *Miller et al.*, 2016; *Mukherjee et al.*, 2018; *Yao et al.*, 2021]. In the absence of surface water, the groundwater is extracted for agriculture, domestic, and industrial purposes. Agriculture is the largest sector in terms of groundwater consumption. It consumes nearly 70% of the total groundwater abstraction globally and irrigates 40% of the global cultivated land [*Shiklomanov & Shiklomanov*, 1999; *Alley et al.*, 2002; *Siebert et al.*, 2010; *Rodell et al.*, 2018]. This freshwater reservoir also provides drinking water for half of the world's population and is used for the industrial sector [*Jackson, R B et al.*, 2001; *Carpenter et al.*, 2011; *Gleeson et al.*, 2012; *Famiglietti*, 2014; *Gleeson et al.*, 2016; *Mukherjee et al.*, 2020].

Higher dependency on groundwater leads to higher abstraction, which varies spatially and temporally depending on the surface water availability and water demand. Large-scale abstraction of groundwater, particularly for agricultural purposes, creates an imbalance in the natural recharge of groundwater and abstraction. The long-term imbalance in recharge and abstraction leads to the overexploitation of groundwater [*Custodio*, 2002; *Gleeson et al.*, 2010; *Wada et al.*, 2010]. In recent decades groundwater depletion due to overexploitation has been reported on a regional and global scale [*Rodell et al.*, 2009; *Wada et al.*, 2010; *Famiglietti et al.*, 2011; *Konikow*, 2011; *Mukherjee et al.*, 2020]. The maximum depletion in groundwater has been observed along High Plains and Central Valley aquifers in the United States, Northern Sahara and Nubian aquifers in Africa, North China Plain, most of the Middle East Aquifers in the Persian Peninsula, and the aquifers in the northwestern and eastern parts of India and Bangladesh [*Chakraborty et al.*, 2020; *Mukherjee et al.*, 2020; *Figueroa & Smilovic*, 2021]. This could lead to land subsidence, enhancement of hydrological drought, groundwater salinization, water scarcity, and water quality issues [*Bouwer*, 1977; *Gimenez & Morell*, 1997; *Barker et al.*, 2000; *Postel*, 2000; *Changming et al.*, 2001; *Singh & Singh*, 2002; *Chen, C et al.*, 2003; *Foster & Chilton*, 2003; *Konikow & Kendy*, 2005; *Salameh*, 2008; *Wada et al.*, 2010;

Margat & Van Der Gun, 2013; *Wada et al.*, 2013; *Van Loon*, 2015; *Mahmoudpour et al.*, 2016; *Yuan et al.*, 2017; *Bierkens & Wada*, 2019].

India is the largest groundwater extractor (~245 Billion cubic Meters (BCM) per year) in the world [*Scott & Shah*, 2004; *Fishman et al.*, 2011; *Mukherjee et al.*, 2015; *Mukherjee*, 2018; *Saha et al.*, 2018], accounting for ~17 % of the annual global groundwater extraction [*Döll et al.*, 2012] and 61% of annually replenishable groundwater (~398 BCM) resource of India [*Saha & Ray*, 2019]. The rate of increase in groundwater extraction in India is also the highest in the world [*Margat & Van Der Gun*, 2013]. Nearly 90% of the extracted groundwater in India is used for irrigation and agriculture [*Scott & Shah*, 2004; *Wada et al.*, 2012; *Saha & Ray*, 2019] which covers nearly 50% of the total irrigated area [*Scanlon et al.*, 2010] and employs almost 50% of the workforce in India and contributes to ~ 17% of its GDP [*Arjun*, 2013]. Thus, groundwater is the most important natural resource for India, the country where ~17% of the global population lives.

The groundwater availability and extraction are not uniformly distributed across the country. Although on average, ~ 61% of replenishable groundwater is being extracted annually in India, the extraction varies regionally and exceeds 100% in certain regions. This has resulted in groundwater mining and declining water levels [*Tiwari et al.*, 2009], with more than 10 m per year in some parts [*Rodell et al.*, 2009]. The deep static groundwaters recharged over millennial timescales are also being exploited in some parts of the country [*Pahuja et al.*, 2010; *Saha et al.*, 2018]. Satellite-based gravity anomalies have revealed that an enormous volume of water has been drained from certain parts of the Indian landmass [*Rodell et al.*, 2009; *Tiwari et al.*, 2009; *Chen, J et al.*, 2014; *Döll et al.*, 2014; *Bhanja et al.*, 2016; *Long et al.*, 2016; *Asoka et al.*, 2017; *Rodell et al.*, 2018; *Bhanja et al.*, 2020; *Salam et al.*, 2020; *Sarkar et al.*, 2020]. On the other hand, some studies have also shown a marginal rise in groundwater levels in certain parts of the country due to artificial recharge efforts by the government and society [*Bhanja et al.*, 2017; *Mukherjee*, 2018; *Bhanja et al.*, 2019; *Patel et al.*, 2020; *Saha et al.*, 2022]. The rainfall that recharges the groundwater on an annual basis is highly seasonal, spatially uneven, uncertain and unpredictable. Since groundwater is the only ubiquitous and perennial water source in the country, it is being exploited indiscriminately.

Due to its high dependency on groundwater, India is facing water scarcity and several groundwater related issues like overexploitation of the aquifers, water quality deterioration by geogenic and anthropogenic contaminants, and marine water intrusion due to groundwater exploitation along the coastline [*Prusty et al.*, 2020]. The groundwater is also believed to be getting lost through submarine groundwater discharge along certain stretches of India's ~7500 km long coastline [*Babu et al.*, 2009; *Krishan et al.*, 2015; *Prakash et al.*, 2018; *Manivannan & Elango*, 2019]. Superimposed on these problems are the climate change related impacts on groundwater resources. Relentless groundwater exploitation to meet increasing water demand has created severe problems related to the quantity and quality of available groundwater and the cost of extraction from deeper levels, with economic implications.

Due to diverse geohydrology, topography, meteorology, surface water balance, soil type, and vegetation cover across the country, the groundwater scenario, problems and solutions are regions specific and not the same for entire India as a single geographical unit. In the above scenario, for effective groundwater resource management, it is important to discern the region-specific contemporary geohydrological processes in terms of the groundwater recharge mechanism, the interaction between rainwater/surface water and groundwater, and to identify sources of groundwater recharge and estimate the relative contribution of different sources.

Motivation

- Groundwater is one of the largest freshwater reservoirs on the earth and sustains ecology and livelihood by fulfilling the water demand of people. Nearly 50% of the world population depends on groundwater

- 40% of the global cultivated land depends on groundwater for its water needs and provides food grains to the millions of people

- India is the largest extractor of groundwater in the world (~17% of the global groundwater extraction). The extraction varies spatiotemporally, and higher extraction leads to various geogenic contamination and mining of static groundwater

- Groundwater interacts with surface water bodies and rainwater. The interaction and exchange between the surface and groundwater varies spatiotemporally, depending on the hydrogeological settings of the region, and governs the groundwater availability

Objectives

- To understand the interaction between surface water and groundwater and its spatial heterogeneity
- To identify the areas in which groundwater receives the influx of freshwater
- To detect the source of groundwater recharge and their contribution

To achieve the above objectives, groundwater isotopic data from IWIN National Programme and newly collected data from Gujarat State were used. Details about the number of samples, their geographical locations, and protocols for sample collection and storage will be discussed in the next chapter.

Chapter 2

Methodology

To achieve the objectives outlined in Chapter 1, the isotopic composition of groundwater is used in conjunction with other parameters such as the isotopic composition of rainfall and surface water, hydrogeological settings and the meteorology of the region. This chapter discusses details of groundwater isotope data, the geographical location of groundwater samples, the protocols for sample collection and analyses. The fundamentals of isotope systematics used in this thesis are also discussed to relate groundwater's isotopic composition with that of rain and surface water bodies. The prime dataset used in this thesis is the unpublished data of the IWIN National Programme [*Deshpande & Gupta*, 2008; 2012], which is discussed in the following.

2.1 IWIN National Programme

With a view to discerning subtle hydrological processes involving the interaction and exchange of water between different hydrological components, a multi-institutional collaborative National Programme on Isotope fingerprinting of Waters of India (IWIN National Programme, 2008-2013) was conceived, formulated, and executed by the Physical Research Laboratory (PRL), Ahmedabad, in collaboration with 14 research and academic institutes and central agencies. Details about the IWIN Programmes are given Programme [*Deshpande & Gupta*, 2008; 2012]. The IWIN National programme was jointly funded by the Department of Science and Technology (DST), the Government of India and PRL. The mission of the IWIN National Programme was to isotopically characterise the entire hydrological system of India (i.e. marine waters of the Arabian Sea and the Bay of Bengal, precipitation, water vapour, surface waters, rivers, and groundwater) to discern various hydrological processes operating on different scale spatially and temporally and to quantify the mass exchange in them.

This doctoral study is based on the unpublished groundwater isotope data generated under the aegis of the IWIN Programme. The groundwater samples collected during the IWIN National Programme for the pre-monsoon (April-May) and post-monsoon (Oct-Nov) seasons across the country from different hydrogeological units were analysed for oxygen and hydrogen isotopes. This groundwater isotope data is interpreted in conjunction with other related parameters, such as the isotopic composition of rain and surface water, hydrogeological settings, and the meteorology of the region. Apart from the IWIN isotope data, the new groundwater and surface water samples were also collected from Gujarat state (2019-2020) for pre-monsoon and post-monsoon seasons and analysed for oxygen and hydrogen isotopes and major ions.

2.2 Sampling locations and collection protocols

- **IWIN samples**

During IWIN National Programme (2008-2013), shallow (first unconfined aquifer) groundwater samples were collected by the Central Groundwater Board (CGWB) from 2527 locations across India for pre-monsoon and post-monsoon seasons for one year covering different hydrogeological units (Fig 2.1 a & b).

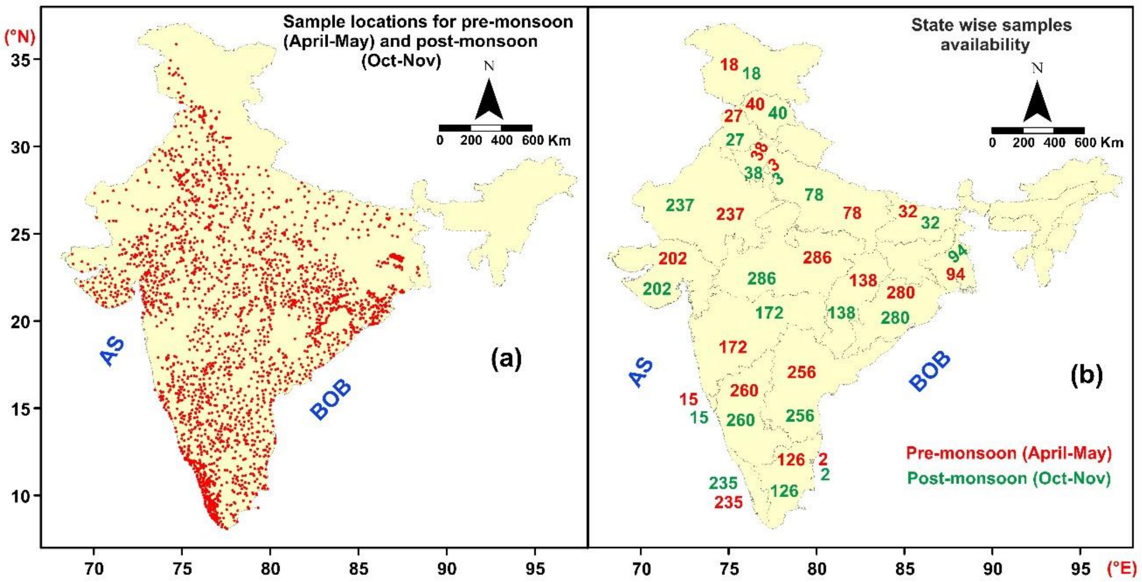

Fig 2.1: (a) Spatial distribution of sample locations; (b) State-wise sample availability.

The protocols followed for samplings are following:

- Most of the groundwater samples were collected from shallow unconfined aquifers.
- Samples from the handpumps were taken after purging them for 10-15 minutes to flush out the stagnant water in the pipes.
- Samples from dug wells were collected during peak hours of withdrawal when the inflow of pristine groundwater into the dug well is the maximum and the duration for possible evaporation before sampling is the minimum.

- Samples from the immediate vicinity of any surface water body (lake, stream, canal, etc.) were avoided.
- The sample bottles were thoroughly rinsed by the groundwater from the same source being sampled.
- No chemicals (acid/ preservative/ poison, etc.) were added to the groundwater samples.
- The groundwater samples were collected in 1-litre high-density plastic bottles and sealed with inner stub and pilferage-proof caps.
- A standardised IWIN sample code was written on the sampling bottle using a waterproof marker pen.
- The groundwater samples collected following the above protocol were transported to PRL, Ahmedabad for isotopic analyses.

A unique IWIN UMC Number (IWIN Unique Master Code) was given to every sample. The relevant information provided along with the samples from each station was recorded on a SQL-based internal server. Then after ensuring the integrity of each sample bottle in terms of its air-tightness, they were stored at 25 ⁰C temperature in the IWIN repository. Samples of doubtful integrity for sampling and storage were discarded.

- **New samples from Gujarat**

To understand the hydrogeological processes occurring in semi-arid western India, a new sampling campaign was undertaken in Gujarat state (2019-2020) to collect pre-monsoon and post-monsoon samples covering different hydrogeological units in Gujarat. Samples from 376 locations were collected for pre-monsoon and post-monsoon seasons (Fig 2.2). These samples were collected from shallow groundwater (263), deep groundwater (72), Narmada canal water (29), and surface water bodies such as reservoirs and lakes (12). The protocols followed during sampling are:

- Groundwater and Canal water samples were collected each from the 20km × 5km grid along the Narmada Canal to understand its influence on the groundwater in its vicinity.
- In the rest part of Gujarat state, samples were collected from every 25km × 25km grid.

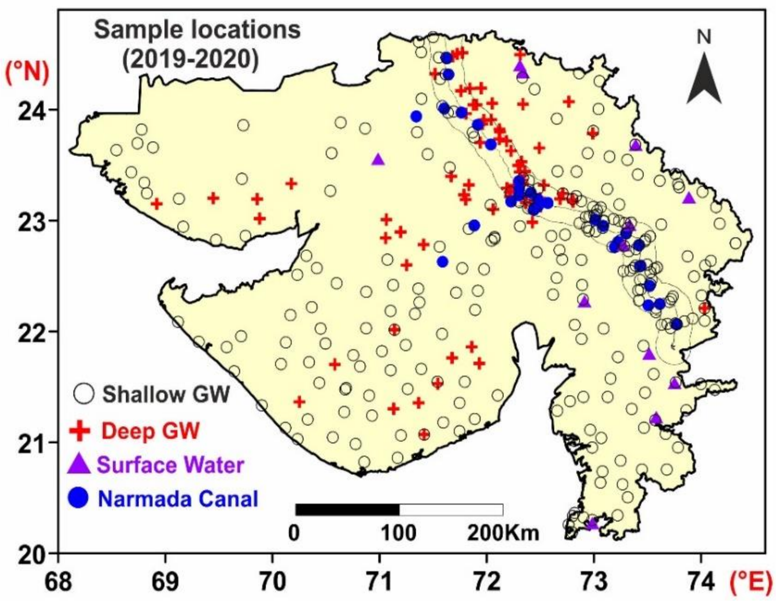

Fig 2.2: Groundwater and surface water sample locations.

- Groundwater samples were collected from a comparatively shallow aquifer (~500 feet) as well as the deep aquifer (up to ~2000 feet) after pumping out the stagnant water for 10 to 15 minutes.

- Surface water (including the Narmada canal) and dug well samples were collected by indigenously designed sample collectors from the deeper part of the water to avoid any spurious signature of evaporation.

- Samples were taken in 30 ml HDPE (High-Density Polyethylene) airtight sampling bottles after thoroughly rinsed and cleaned with the water from the same source.

- Samples were stored at 25°C in the IWIN repository to the analysis of stable isotopes and major ions.

2.3 Isotope analysis

The oxygen and hydrogen isotopic analysis of all samples (IWIN samples + Newly collected samples) was carried out using an Isotope Ratio Mass Spectrometer (IRMS) in continuous flow mode. Mass Spectrometry is a technique in which ions are separated based on their mass to charge ratios. In this study Thermo Scientific Delta-V-plus IRMS in continuous flow mode along with Gas bench II was used (Fig 2.3a). The IRMS consists of three major

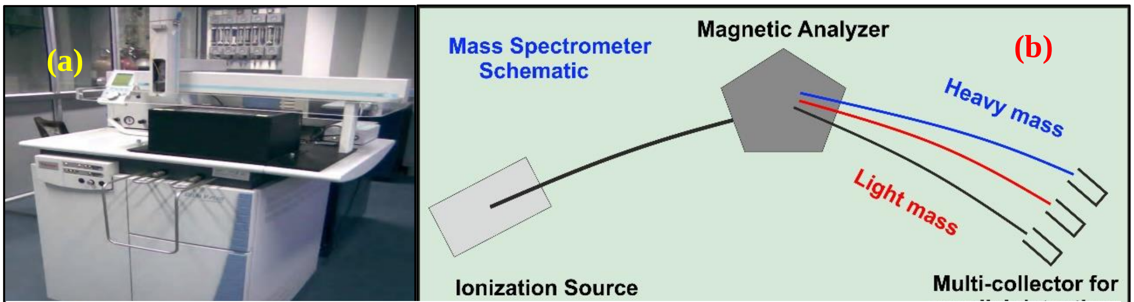

Fig 2.3: (a) Thermo Fisher Delta V+ IRMS at IWIN laboratory, PRL Ahmedabad; (b) Schematic of major components of a mass spectrometer.

components, namely, (i) source for ionizing the gaseous samples; (ii) magnetic analyser for separating the sample ion beams as per their mass to charge ratio; and (iii) detector comprising multiple ion collectors and detector electronics (Fig 2.3b).

A well-established gas equilibration method [*Epstein & Mayeda*, 1953] was used for isotopic analyses of water samples, in which water samples are equilibrated with CO_2 gas for $\delta^{18}O$ analysis and H_2 gas for δD. The equilibrated gas captures the isotopic imprints of water and introduced into the mass spectrometer for analysis.

The steps followed for the measurement of $\delta^{18}O$ and δD of water using the IRMS are listed below:

1. For $\delta^{18}O$ measurements, 12 ml exetainer (quartz vials) fitted with air tight-caps were flushed with a CO_2 gas mixture (99.7 % He + 0.3% CO_2) for 8 minutes using a specialised flushing needle with two openings, one of the openings forces mixture gas into the vial, and the air within is flushed out through the other opening.
2. For δD measurements, a 12 ml exetainer fitted with air-tight caps was flushed with a hydrogen gas mixture (98 % He + 2 % H_2) for 8 minutes using a similar needle.
3. As part of the established standardised laboratory procedure for oxygen and hydrogen isotope analyses using IRMS in Continuous Flow mode using Gas Bench in the IWIN IRMS laboratory [*Maurya et al.*, 2011], 300 μl of the sample was injected into the pre-flushed exetainer vials using the disposable syringe.
4. For $\delta^{18}O$ measurement, the vials were left for 16:00 hrs for equilibrium with CO_2 at 25ºC in thermostat sample tray of Gas bench II. The laboratory temperature was also maintained at 25ºC using air conditioners.
5. For δD measurement, the vials were left for 01:30 hrs with platinum catalytic rods for equilibrium with H_2 at 25ºC in thermostat sample tray of Gas bench II. The laboratory temperature was also maintained at 25ºC using air conditioners.
6. Equilibrated gas was then introduced to IRMS through the GC (Gas Chromatography) column of Gas bench II for isotope measurement.
7. In order to ensure the quality of isotope analyses, every batch of 80 samples included 21 aliquots of three secondary laboratory standards. The analytical reproducibility based on

8. the measurement of multiple aliquots of the laboratory standard in each batch was found to be better than 0.1‰ for $\delta^{18}O$ and 1‰ for δD.

- **IRMS calibration**

Table 2.1: Details of IWIN IRMS calibration and secondary laboratory standards.

IWIN Secondary Laboratory Standard	**IAEA, Vienna**			**PRL, Ahmedabad**		
		$\delta^{18}O$ (‰)	**δD (‰)**		**$\delta^{18}O$ (‰)**	**δD (‰)**
IWIN-1	**IWIN-1**	**-6.57**	**-40.5**	**IWIN-1**	**-6.54**	**-39.75**
Standard Deviation (± ‰)		0.07	0.71		0.07	0.91
No. of aliquots					10	7
IWIN-2	**IWIN-2**	**-11.09**	**-73.8**	**IWIN-2**	**-11.01**	**-73.96**
Standard Deviation (± ‰)		0.07	0.75		0.09	1.05
No. of aliquots					10	5
IWIN-3	**IWIN-3**	**15.1**	**36**	**IWIN-3**	**15.07**	**36.8**
Standard Deviation (± ‰)		0.09	0.64		0.1	1.49
No. of aliquots					10	7
IWIN-4	**IWIN-4**	**-2.29**	**-17.6**	**IWIN-4**	**-2.21**	**-17.25**
Standard Deviation (± ‰)		0.1	0.75		0.1	0.84
No. of aliquots					20	17
Sample Volume (µl)					300	300
Equil. Temp. (°C)					32	32
Equil. Duration (hh:min)					16:00	1:30
Name and isotopic composition of Secondary Lab. Standard(s) used as reference material for isotopic analyses				**Lab Std. for $\delta^{18}O$ and dD**	**$\delta^{18}O$ (‰)**	**δD (‰)**
				VSMOW	0.00 ± 0.03	0.01 ± 0.8
				SLAP	–55.37 ± 0.09	–425.46 ± 064
				GISP	–24.74± 0.08	–188.91 ± 0.78

As part of the IRMS calibration exercise under the IWIN National Programme, four secondary laboratory standards were prepared. Two secondary laboratory standards (IWIN-1 and IWIN-3) were synthesised at the IWIN-IRMS-PRL laboratory to have highly depleted as well as highly enriched isotopic compositions. This was achieved respectively by distillation and evaporation. The other two secondary standards (IWIN-2 and IWIN-4) were natural water samples of groundwater and river water respectively. A set of these four secondary laboratory standards were sent to the isotope hydrology laboratory of IAEA, Vienna, to provide certified isotopic values, which can be used to calibrate the IRMS under the IWIN National Programme. The $\delta^{18}O$ and δD analyses were performed at IAEA using both gas source IRMS and Laser Analysers (both LGR and Picaro), and average values were provided to IWIN, which were taken as the authentic certified value to be used as calibrated benchmark values with respect to which results of secondary laboratory standards are compared.

The IWIN IRMS laboratory at PRL was also independently calibrated with international standard reference materials (VSMOW, GISP and SLAP) obtained from IAEA. The secondary laboratory standards were analysed as samples in multiple aliquots in the IWIN-IRMS-PRL laboratory using VSMOW2, GISP and SLAP2 as the laboratory reference. The $\delta^{18}O$ and δD values of secondary laboratory standards obtained from IAEA and that of IWIN-IRMS at PRL are given in Table 2.1. The $\delta^{18}O$ and δD values of secondary laboratory standards obtained from IWIN-IRMS at PRL using the above protocols of isotope analyses are in perfect agreement with IAEA certified values, within a narrow range of ± 0.06‰ for $\delta^{18}O$ and ± 0.52‰ for δD.

2.4 Isotope rationale/ systematics

Isotopes are atoms of the same element with the same number of protons but different numbers of neutrons. Thus, isotopes have the same chemical properties but different physical properties. Isotopes are of two types: (i) radioactive (decay to stable daughter nuclides over time) and (ii) stable (do not decay). Stable isotopes of oxygen (^{16}O, ^{17}O, ^{18}O) and hydrogen (^{1}H and ^{2}H or D) are the important tracers used in hydrology to isotopically characterize water and understand the interaction and exchange processes occurring in different components of the hydrological cycle, as they are an integral part of the water molecule itself [*Clark & Fritz*, 1997; *Kendall & Mcdonnell*, 2012]. During phase change (solid↔liquid↔vapour) of water molecules in the course of the hydrological cycle, isotopic fractionation occurs, i.e. the heavier

Table 2.2: Stable isotopes of oxygen, hydrogen and isotopologues of water and their relative abundance.

Isotopes	**Natural abundance (%)**	**Atomic mass (amu)**	**Water Isotoplogues**	**Abundance (%)**
^{16}O (8p+8n)	99.762	15.9949146	$H_2{}^{16}O$	99.73
^{17}O (8p+9n)	0.038	16.9991315	$HD^{16}O$	0.015
^{18}O (8p+10n)	0.2	17.99916	$D_2{}^{16}O$	2.24 x 10^{-6}
Oxygen 15.9994(3) g·mol−1			$H_2{}^{17}O$	0.035
^{1}H (1p + 0n)	99.99	1.00782503	$HD^{17}O$	5.25 x 10^{-6}
^{2}H (1p + 1n)	0.02	2.01410177	$D_2{}^{17}O$	7.88 x 10^{-10}
Hydrogen 1.00794(7) g·mol−1			$H_2{}^{18}O$	0.2
			$HD^{18}O$	3.07 x 10^{-5}
			$D_2{}^{18}O$	4.6 x 10^{-6}

water isotopologues (isotopic molecular species of water) get preferentially partitioned and concentrated in the denser phase having a comparatively smaller degree of freedom for molecular movement due to difference in their molecular masses, and consequently their physical properties (e.g. bond strength, rotational, vibrational and translational frequencies, density, collision frequency and vapour pressure). Therefore, by monitoring the relative abundances of isotopologues in different components of the hydrological cycle, various hydrological processes can be traced and understood. The different combinations of these isotopes form different isotopologues of water. Table 2.2 enlists all the water isotopologues along with their natural abundances[*Clark & Fritz*, 1997].

- **Expressing isotopic composition**

The isotopic composition of water samples is expressed as the ratio of deviation of abundance ratio (R) of less abundant to more abundant isotope in the sample from that of the international standard reference material such as VSMOW (Vienna Standard Mean Oceanic Water) to the standard. Isotopic composition is expressed in δ notation in per mil (‰) unit.

$$\delta = \left(\frac{R_{sample}}{R_{standard}} - 1\right) \times 10^3 \ (‰)$$

Where R = $^{18}O/^{16}O$ for oxygen or $D/^{1}H$ for hydrogen isotopic composition, respectively for the $\delta^{18}O$ and δD.

- **Isotope fractionation**

The differential partitioning of isotopes between two interacting phases during a phase

Table 2.3: Values of constants in the empirical equation for the computation of equilibrium fractionation [Majoube [1971]] for ^{18}O and D.

	C1	C2	C3
^{18}O	1.137×10^3	-0.4156	-2.066×10^{-3}
D	-24.884×10^3	-76.248	-52.612×10^{-3}

change reaction is known as isotopic fractionation. The isotope fractionation occurs because of the difference in atomic mass and consequently their physical properties. In the case of water, when water molecules move from one phase to another (liquid↔solid↔vapour), water isotopologues get preferentially partitioned between the two phases resulting in isotopic fractionation. The isotopic fractionation is quantitatively expressed in terms of fractionation factor (α) as the ratio of isotopic abundance ratios of two co-existing phases:

$$\alpha_{Liquid}^{Vapour} = \frac{R_{Vapour}}{R_{Liquid}}$$

where R = $^{18}O/^{16}O$ or $D/^{1}H$ for oxygen and hydrogen isotopic fractionation.

In per mil (‰) notation fractionation factor (α) is represented by another term (ε) which is also referred to as enrichment factor or simply fractionation given by:

$$\varepsilon = (\alpha - 1) \times 10^3$$

Depending on the physical conditions during a phase change reaction, water isotopologues may undergo equilibrium and kinetic fractionation as described below:

1. Equilibrium fractionation

Equilibrium fractionation occurs when there is thermodynamic equilibrium between two interacting phases in a closed system, i.e. the rate of the forward and backward reaction is equal. Several laboratory experiments have been undertaken to empirically determine the value of the equilibrium fractionation factor for different temperature ranges [*Clark & Fritz*, 1997]. *Majoube* [1971] gave an empirical formula for the computation of equilibrium fractionation (α_{eq}) as follows:

$$\ln(\alpha_{eq}) = \frac{C_1}{T^2} + \frac{C_2}{T} + C_3$$

Where C_1, C_2, and C_3 are constants (table 2.3) for temperature (T in Kelvin) above 273.15 K. Several researchers have provided empirical equations for computing fractionation factors for different phases and different temperature ranges [*Merlivat & Nief*, 1967; *O'neil*, 1968; *Suzuoki & Kimura*, 1973]. *Horita &Wesolowski* [1994] have integrated available empirical values and given a formula valid from 0 ºC to 374 ºC temperature range as follows:

$$10^3 \ln\alpha_{(l-v)}(\delta^{18}O) = 6.7123\left(\frac{10^3}{T}\right) - 1.6664\left(\frac{10^6}{T^2}\right) - 7.685 + 0.35041\left(\frac{10^9}{T^3}\right)$$

$$10^3 \ln\alpha_{(l-v)}(D) = 1158.8\left(\frac{T^3}{10^9}\right) - 1620.1\left(\frac{T^2}{10^6}\right) + 794.84\left(\frac{T}{10^3}\right) - 161.04 + 2.9992\left(\frac{10^9}{T^3}\right)$$

Equilibrium fractionation is a temperature-dependent phenomenon, and the magnitude of fractionation is inversely related to temperature.

2. Kinetic fractionation

In kinetic fractionation (non-equilibrium), the reaction rate is higher in one direction compared to another. Non-equilibrium conditions and resultant unidirectional reaction can arise due to several factors such as a sudden change in the temperature or sudden addition/removal of the mass of reactant/product in the open system or sudden change in temperature and pressure in the closed system. However, the most common cause of kinetic fractionation in the hydrological cycle is the diffusion of vapour mass from higher to lower concentrations across the gradient within the undersaturated air column. Lighter isotopic molecules have higher diffusive velocities compared to their corresponding heavier isotopic molecules, and this velocity is affected by the molecular resistance offered by humidity in the medium through which vapour mass is diffusing. Therefore, isotopes get differentially partitioned between two reservoirs between which mass flux occurs. *Gonfiantini* [1986] gave approximate empirical formulations for the computation of kinetic enrichment ($\Delta\varepsilon$) as follows:

$$\Delta\varepsilon^{18}O = 14.2 \times (1-h); \Delta\varepsilon^{2}H = 12.5 \times (1-h)$$

Where h is the fractional relative humidity (i.e. values of h ranging from 0 to1).

2.5 Isotopes in precipitation

- **Global Meteoric Water Line**

The Global Meteoric Water Line (GMWL) is the observed relationship between $\delta^{18}O$ and δD of global precipitation. Originally this relationship was given by *Craig* [1961] based on the isotopic composition of surface water samples ($\delta D = (8\times\delta^{18}O+10)$. However, *Rozanski et al.* [1993] redefined GMWL based on the isotopic composition of precipitation samples collected from 219 GNIP (Global Network of Isotopes in Precipitation) stations as:

$$\delta D = (8.17 \pm 0.07)\delta^{18}O + (11.27 \pm 0.65)$$

The above-redefined relationship between the $\delta^{18}O$ and δD suggests that despite huge spatial variability in climatic conditions and geographical features of the globe, $\delta^{18}O$ and δD correlate and behave in a fairly predictable manner. The slope of GMWL is the manifestation of the ratio of equilibrium fraction for ^{18}O and D ($\varepsilon D/\varepsilon^{18}O$), which ranges between ~8.2 to 9.5 for temperatures ranging from 0ºC to 30ºC. The intercept of ~10 in GMWL indicates the presence of additional deuterium in the natural hydrological cycle and suggests the involvement of kinetic fractionation during the evaporation process. If the entire rain-forming mechanism were under equilibrium conditions, then the $\delta^{18}O$ and δD relationship would have been $\delta D = \sim 8(\delta^{18}O) + 0$. However, the non-zero intercept indicates kinetic fractionation mainly due to the atmospheric humidity gradient in the source region during evaporation.

The GMWL is an average of many Local Meteoric Water Lines (LMWLs), which may differ from GMWL due to variations in the local geographical and hydro-meteorological conditions. The deviation of LMWL from GMWL is used advantageously to understand the local hydro-meteorological processes.

- **The deuterium excess (d-excess)**

Whenever there is kinetic fractionation involved, the net ratio of fractionation of D to ^{18}O is different from 8 because, unlike equilibrium fractionation, the magnitude of kinetic fractionation for ^{18}O is more compared to that for D. Therefore, during the evaporation process, the residual liquid gets relatively more enriched in ^{18}O compared to D. Correspondingly, the resultant vapour gets relatively more enriched in D compared to ^{18}O. Therefore, the rain generated from such a vapour also contains the excess of D over what can be accounted for by equilibrium fractionation between water and vapour. Considering this fact, *Dansgaard* [1964] defined a new parameter, called d-excess (also referred to as d) to quantitatively express the kinetic effect in fractionation as:

$$d - excess = \delta D - (8 \times \delta^{18}O)$$

The benefit of the d-excess parameter is that it can be computed and interpreted for each individual water sample (rain event, groundwater, surface water), whereas only one intercept value of the $\delta^{18}O$ - δD regression line can be computed for the entire data set used in the regression.

2.6 Isotopes in groundwater

Groundwater recharge occurs when surface water percolates downwards through an overlying unsaturated zone and becomes part of the groundwater stored in the aquifer. The recharge could be diffused (mostly from precipitation) or focused (from surface water such as lakes, reservoirs, and rivers) [*Allison*, 1988; *Nimmo et al.*, 2005; *Healy*, 2010; *Simmers*, 2013]. During groundwater recharge, the isotopic signature of source water is transferred to groundwater, and these signatures are analysed and interpreted to understand: (1) the groundwater-surface water interaction [*Herczeg et al.*, 1992; *Hunt et al.*, 2005; *Aggarwal et al.*, 2009; *Yang et al.*, 2012; *Lin & Garzione*, 2017]; (2) the groundwater recharge dynamics [*O'driscoll et al.*, 2005; *Yeh et al.*, 2011; *Keesari et al.*, 2017; *Schilling et al.*, 2021]; (3) estimate the contribution of point source and precipitation to groundwater recharge [*Liu & Yamanaka*, 2012; *Hameed et al.*, 2015; *Jesiya & Gopinath*, 2019; *Jung et al.*, 2019]; and (4) determine the effect of evaporation on groundwater systems [*Hendry & Schwartz*, 1988]. The isotopic composition of groundwater recharged by rain is expected to be comparable to the amount-weighted average isotopic composition of annual precipitation[*Clark & Fritz*, 1997]. However, any deviation observed in the isotopic composition of groundwater from that of the rain can be ascribed to various factors, including evaporation from groundwater, the seasonal differences in recharge source; lateral movement of groundwater; recharge from a point source; paleo-groundwater recharged by precipitation under different climate conditions; or mixing of groundwaters with different origins and histories [*Jasechko*, 2019].

2.7 Additional data used

- **Major ions**

Groundwater chemistry mainly depends on the mineralogical composition of the aquifer through which it flows. As groundwater laterally moves from recharge area to discharge area, various hydrogeochemical processes occur which govern the hydrogeochemistry of groundwater [*Lakshmanan et al.*, 2003; *Elango & Kannan*, 2007]. The hydrogeochemical processes and hydrogeochemistry of groundwater vary spatiotemporally depending upon the geology and aquifer characteristics [*Lakshmanan et al.*, 2003]. These variations are used to understand; (1) rock water interaction [*Elango & Kannan*, 2007; *Subramani et al.*, 2010]; (2) dissolution, ion exchange and residence time [*Apodaca et al.*, 2002; *Li et al.*, 2013]; (3) evaporation from groundwater [*Loni et al.*, 2015; *Rajmohan et al.*, 2021]. In this thesis, major ions dissolved in groundwater were measured using the ion chromatography technique that is discussed below:

- **Ion chromatography**

Ion chromatography (IC) is the technique used for separating and analyzing the major ions in water samples. The ions are separated based on their retention time. The separation depends on the molecular weight or charge of the compounds or ions. In IC, two columns are used. One consists of cation exchange resin, and the second consists of anion exchange resin. The mobile phase used for the cation column is methane sulphonic acid (MSA), and that for the anion column is the mixture of sodium carbonate/bicarbonate. The exchanges of ions between the stationary phase and mobile phase occur in the column, and they are separated from the column based on their retention time. The detector used in the IC is the conductivity detector. The detail of IC can be seen in *Kumar, R V S* [2018].

The analysis of cations (Na^+, K^+, Ca^{2+}, and Mg^{2+}) and anions (Cl^-, SO_4^{2-} and NO_3^-) in water samples were performed with a dual-channel Ion Chromatograph (Dionex, ICS-5000, DC). Samples were first diluted with Milli-Q water (Resistivity: 18.2 MΩ cm) as per their TDS (Total Dissolved Solids) and were transferred to pre-cleaned 2 ml vials and used for analysis on Ion Chromatograph. The instrument is well calibrated before the analysis using external standards of both cations and anions. A mixture of sodium carbonate (Na_2CO_3) and sodium bicarbonate ($NaHCO_3$) was used as an eluent for the study of anions and an anion self-regenerating suppressor (ASRS) was used to suppress the conductivity. For the analysis of cations, methane sulphonic acid (MSA) was used as an eluent, and the conductivity was suppressed with the help of a cation self-regenerating suppressor (CSRS). The anions and cations were separated using analytical and guard columns [*Banks et al.*, 1998; *Jackson, P E*, 2000; *Morales et al.*, 2000; *Rastogi et al.*, 2016; *Sudheer et al.*, 2016].

- **Air Trajectory Model**

Groundwater in any region has a strong dependence on the rainfall in that region. The isotopic composition of rainfall depends on geographical and meteorological factors and the moisture source. Therefore, for interpreting the isotopic composition of groundwater in certain regions receiving rains from different directions, it may be useful to track the air parcel trajectory.

To track the history of air parcel containing the moisture for precipitation for the concerned region, 120hrs back wind trajectories were generated using Hybrid Single-Particle Lagrangian Integrated Trajectory (HYSPLIT) model downloaded from http://ready.arl. noaa.gov/HYSPLIT.php [*Draxler & Rolph*, 2003; *Stein et al.*, 2015]. The Hybrid Single-Particle Lagrangian Integrated Trajectory Model (HYSPLIT) is a complete system for computing simple air parcel trajectories, as well as complex transport, dispersion, chemical transformation, and deposition simulations [*Soderberg et al.*, 2013; *Wu et al.*, 2015; *Bagheri et al.*, 2019; *Esquivel-Hernández et al.*, 2019; *Sun et al.*, 2019; *Oza et al.*, 2020a]. One of the most important applications of HYSPLIT is the back-trajectory analysis to determine the origin of air masses, its progressive movement from the source region to the receptor region, and change in the sources of water vapour. Hence, it is important to understand vapour source dynamics. The HYSPLIT model has been used in this study to relate the observed isotopic variation in groundwater with variation in vapour sources and mixing of different vapour masses that causes the precipitation.

The percentage contribution of various moisture sources in precipitation is computed using specific humidity provided by HYSPLIT. Variation in specific humidity (q) provided by HYSPLIT along the trajectory is used as an indicator of moisture uplift through convective evaporation or moisture drop through precipitation [*Sodemann et al.*, 2008; *Oza*, 2020]. The underlying assumption here is that the change in moisture over the course of time ($\Delta q/\Delta t$) is the result of net evaporation (E) or precipitation (P) only. The following steps were followed for the computation of moisture source contribution:

1. Masks for ocean and land filters were created using the polygon function in MATLAB software.
2. An algorithm checks if the trajectory is picking up moisture from the ocean or land by tracing specific humidity (q).
3. All addition or removal of moisture from the vapour parcel travelling along the trajectory was computed at an interval of 1 hr. Change in q is attributed to moisture pickup or rainfall.
4. While causing rainfall, q from land or ocean is reduced in proportion to their content in the vapour parcel.

Step number 4 is repeated until the 0th hour, and the final fraction represents oceanic and land-derived moisture contribution.

Chapter 3

Seasonal isoscapes ($\delta^{18}O$ and δD) of groundwater in India and underlying hydrogeological processes

3.1. Introduction

The stable isotopes of oxygen and hydrogen ($\delta^{18}O$, δD) are useful tracers to understand the patterns and processes in the hydrological cycle [*Deshpande et al.*, 2003; *Gupta et al.*, 2005b; *Mcguire & Mcdonnell*, 2007; *Deshpande et al.*, 2010; *Gat*, 2010; *Maurya et al.*, 2011; *Lin & Garzione*, 2017; *Bowen et al.*, 2019; *Gautam et al.*, 2020; *Oza*, 2020]. The isotopic compositions ($\delta^{18}O$, δD) of different components of the hydrological cycle reveal the physical processes related to its formation and transport [*Craig*, 1961; *Dansgaard*, 1964; *Gat*, 1996; *West, A et al.*, 2014]. These physical processes impart specific isotopic composition to water in that component and cause its spatial variation [*Craig*, 1961; *Gat*, 1996; *Bowen & Revenaugh*, 2003].

In groundwater, these isotopes are used to understand groundwater movement and mixing [*Adams et al.*, 2001; *Weyhenmeyer et al.*, 2002; *Wilcox et al.*, 2004; *Nakaya et al.*, 2007; *Liu & Yamanaka*, 2012], to identify the sources of groundwater recharge and their relative contributions [*Maurya et al.*, 2011; *Yeh et al.*, 2014b; *Hameed et al.*, 2015; *Swetha et al.*, 2020], and the interaction between surface water and groundwater [*Hunt et al.*, 2005; *Yeh et al.*, 2011; *Yang et al.*, 2012; *Hao et al.*, 2019; *Krishan et al.*, 2020a]. In particular, spatial variation in the isotopic composition of groundwater can be used to delineate water flow systems and quantify mass-balance relationships in the hydrological investigation [*Clark & Fritz*, 1997; *Coplen et al.*, 2000; *Jung et al.*, 2022]. The spatial variation in the isotopic composition of groundwater (isoscape) depends on the input signal, i.e. the isotopic composition of precipitation, hydrogeological setting, evapotranspiration rate, and the heterogeneous characteristics of the recharge area [*O'driscoll et al.*, 2005; *Gleeson et al.*, 2009; *Song et al.*, 2009; *Raidla et al.*, 2016]. In the absence of spatially distributed large-scale precipitation data, the isoscape of shallow groundwater can be used as a precipitation indicator [*Darling et al.*, 2003; *Kortelainen & Karhu*, 2004; *Wassenaar et al.*, 2009; *West, A et al.*, 2014], apart from this, these isoscapes are used to visualize the large-scale hydrological process on a different scale (regional, continental or global) [*West, J B et al.*, 2009; *West, A et al.*, 2014]. The isoscapes are used in some other studies, such as animal migration [*Rubenstein & Hobson*, 2004]and leaf water isotope [*West, J B et al.*, 2008].

This study is based on a large number of shallow groundwater samples (N = 5054, 2527 for pre-monsoon and 2527 for post-monsoon) collected across India for the pre-monsoon (April-May) and post-monsoon (October-November) seasons covering major hydrogeological units in the country, under the aegis of the IWIN National programme [*Deshpande & Gupta*, 2008; 2012]. The details about the study area, sampling location, and important findings of this study are discussed below.

3.2 Study area

India is the largest south Asian country covering nearly 3.06×10^{6} km^2 area, surrounded by ocean water on three sides, namely, the Arabian Sea in the west (AS), the Bay of Bengal (BOB) in the east, and the Indian Ocean in the south (Fig 3.1). The northern part of the study area is surrounded by Himalayan mountains; these mountains are the source of some of the major river systems in India. The southwestern margin of the study area has north-south trending Western Ghats that act as a water divide for the rest of the southern part of the study area below 20° latitude. The study area receives nearly 1090 mm of average annual precipitation [*Parthasarathy & Yang*, 1995], but the precipitation is spatially heterogeneous. For instance, the northeast part receives more than 2000 mm of rainfall while the northwestern

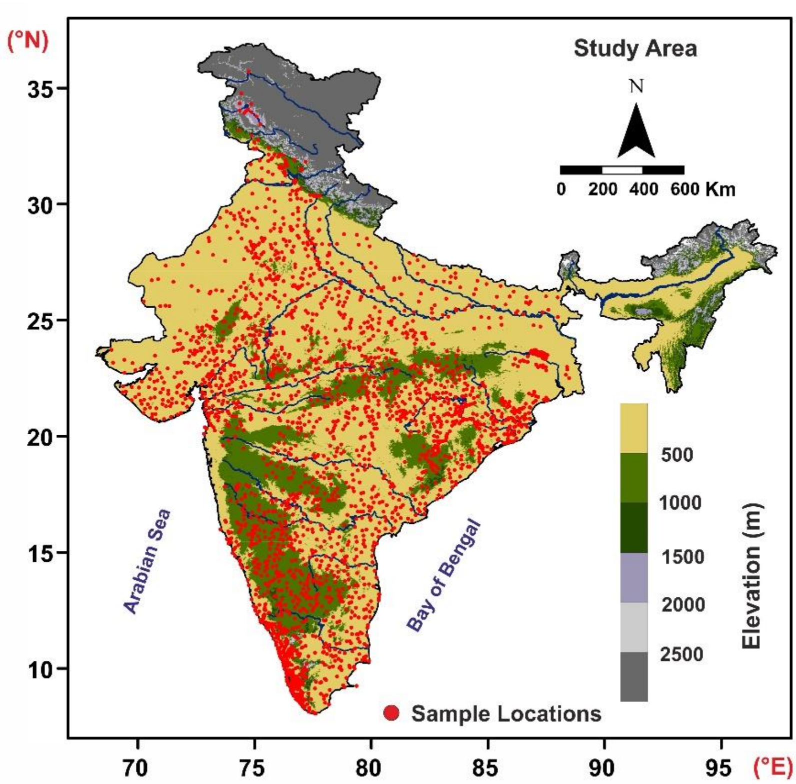

Fig 3.1: Elevation profile of the study area along with sample locations.

part gets nearly 700 mm of rain [*Kumar, K R et al.*, 1992]. Climatic condition is quite diverse in India. According to the Koppen climatic classification based on seasonal precipitation and temperature patterns, India has six different climatic zones, namely: montane, humid subtropical, tropical wet and dry, tropical wet, semi-arid, and arid. The long-term (1901-2012) average annual temperature of the country is ~24ºC with a maximum average temperature of ~27ºC during Jun-Sep and minimum average temperatures of ~19ºC during Jan-Feb. For details of the climate record, a reference is made to the India Meteorological Department website (www.mausam.imd.gov.in). Agriculture is the main source of income for 58% of the country's population and covers nearly 60% of the geographical area, and it contributes 16% of countries total GVA (http://www.Indiabudget.gov.in). Agriculture is highly water-intensive, and 90% of the extracted groundwater (249 BCM) is used for irrigation (CGWB annual report 2017).

- **Hydrogeology**

India has a diverse hydrogeological setting which governs groundwater occurrence and movement (Fig 3.2). Based on hydrogeology, India has 14 principal aquifer systems and 42

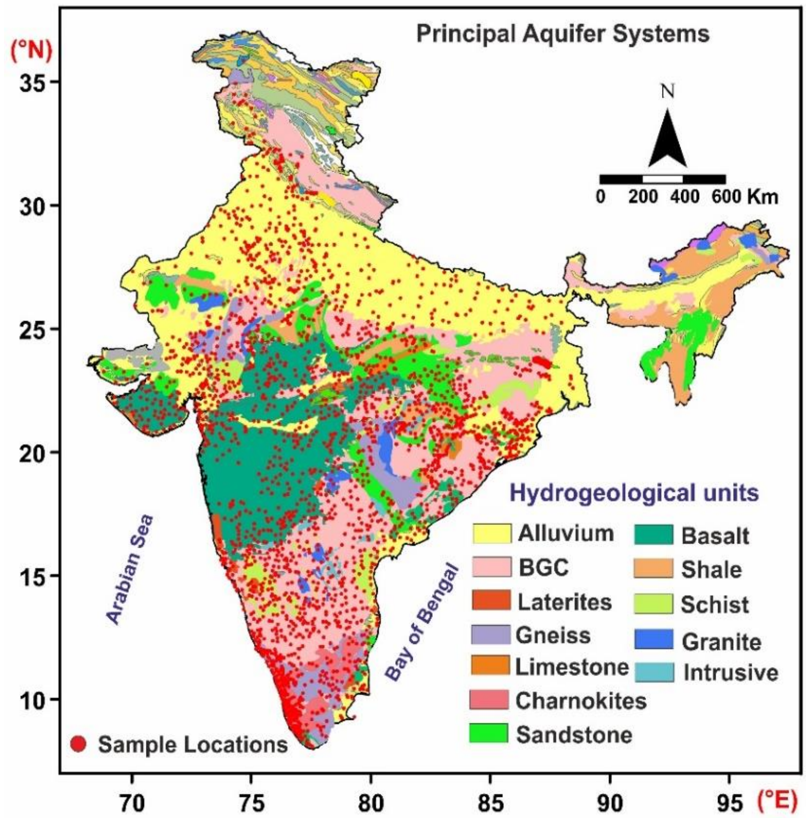

Fig 3.2: Map showing the hydrogeological setting of India along with sample locations, redrawn from https://indiawris.gov.in/wris/#/Aquifer.

major aquifers. The northern part of India is covered by Indo-Gangetic Alluvium, which gradually merges with cratonic provinces of central and south India, fluvio-aeolian deposits of the west and the basaltic province of the Deccan plateau [*Saha & Ray*, 2019]. The geographical extent of Alluvial aquifers is the highest in the country (31% of the total area). They form multilayered aquifers with a high yield of ~70 litres/sec and aquifer transmissivity of ~1000 to 5000 m^2/day [*Saha et al.*, 2010]. These aquifers are available in Uttar Pradesh, Bihar, West Bengal, Assam, Odisha, Gujarat and Rajasthan. The Banded Gneissic Complex (BGC) and Gneiss cover around 20% of the country's area and are available in almost all the peninsular states and the Himalayan states. The weathered upper part and the fracture zone below it forms the potential aquifer. The transmissivity of these aquifers remains mostly within ~100m^2/day and sometimes goes up to ~600 m^2/day. Basalt covers around 17% area of the country and is mainly spread over Maharashtra, Madhya Pradesh, Gujarat, Rajasthan and Karnataka. The weathered zones of the top flow (thickness ~15 m to ~40 m), the vesicular zones of the successive flows below, and the intertrappeans form the basaltic aquifers. Transmissivity of these aquifers remain mostly within ~70m^2/day. Sandstone aquifer covers around 8% area in the country and is available in Chhattisgarh, Andhra Pradesh, Madhya Pradesh, Gujarat, Karnataka and Rajasthan. Shale aquifer accounts for around 7% of the area, and Limestone aquifer covers a very small area of around 2% of the country, rest 15% of the study area is covered by aquifers namely; Schist, Granite, Quartzite, Charnockite, Khondalite, Laterites and Intrusive. The details of these aquifers can be seen in Aquifer Information and Management System (https://www.aims-cgwb.org/principal-aquifer-systems-india.php) as well as in [*Saha & Ray*, 2019].

3.3 Results and Discussion

- **δ^{18}O vs δD and d-excess vs δ^{18}O relationships**

The δ^{18}O - δD regression lines for pre-monsoon and post-monsoon groundwater samples collected from 2527 locations across India are shown in Fig 3.3a along with IMWL (Indian Meteoric Water Line) for South West Monsoon Season [*Oza*, 2020]. The statistical description of δ^{18}O, δD, and d-excess for pre-monsoon and post-monsoon seasons are given in Table 3.1. The slope of GW samples for pre-monsoon (6.3 ± 0.1) and post-monsoon (6.4 ± 0.1) seasons are similar but lower than the slope of IMWL (7.8 ± 0.1). The d-excess vs δ^{18}O scatter plots for pre-monsoon and post-monsoon groundwater samples are given in Fig 3.3b. The lower regression line slopes of post-monsoon groundwater compared to the meteoric water line and the decreasing trend of d-excess with increasing δ^{18}O indicate that post-precipitation and pre-recharge evaporation is the dominant mechanism controlling groundwater isotopic composition [*Deshpande et al.*, 2003]. The lower regression line slopes of pre-monsoon groundwater suggest post-recharge evaporation from groundwater or recharge by evaporated surface water sources.

Groundwater recharge from precipitation is expected to have an isotopic composition close to the amount weighted mean of precipitation, but it can show much variability depending on post-precipitation modifications either before recharge or after recharge [*Rozanski*, 1985; *Ingraham & Taylor*, 1991]. It is seen in Fig 3.3a &b that some of the samples marked by ellipse-

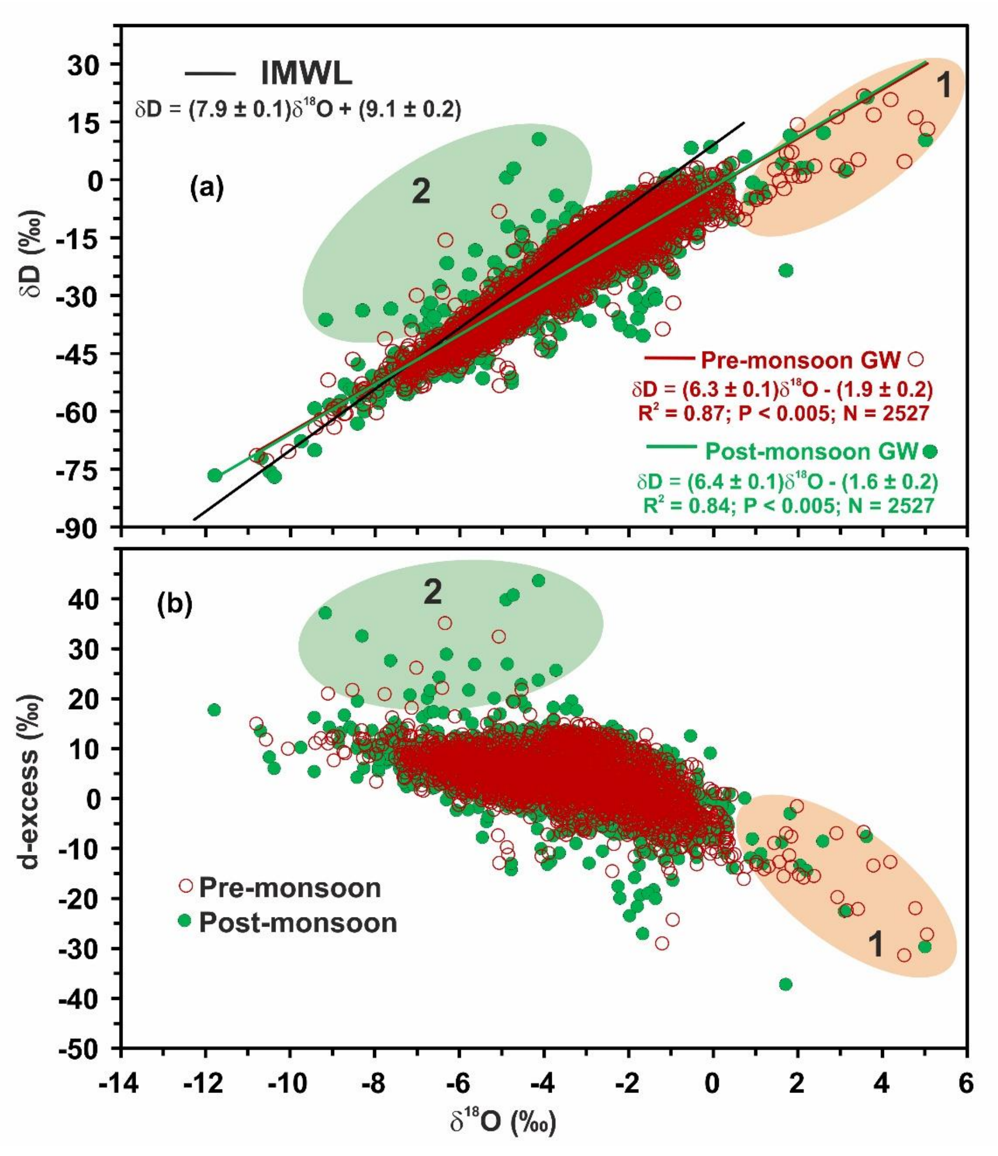

Fig 3.3: (a) Seasonal regression line for GW along with IMWL, (b) scatter plot of d-excess vs $\delta^{18}O$ with the season. The samples falling within the ellipses are isotopically distinct from the rest and governed by some other processes discussed in the main text.

1 have higher $\delta^{18}O$ (> 0‰) and lower d-excess (< -5.0‰), while samples marked by ellipse-2

have higher d-excess (> 15.0‰). The groundwater samples with such extreme $\delta^{18}O$ and d-excess values samples are scattered in the study area and are not associated with specific hydrogeological settings or climatic conditions. The samples falling in ellipse-1 are mostly pre-monsoon samples indicating the recharge from point sources such as lakes, reservoirs, and ponds that are prone to a higher extent of evaporation being open surface sources. The groundwater samples falling in ellipse-2 are mostly post-monsoon samples suggesting event-based recharge or recharge by a peculiar type of precipitation in certain regions with higher d-excess values. Higher d-excess values (>15 ‰) in precipitation are reported in certain geographical areas such as western Himalayas, NE India and Kerala [*Warrier et al.*, 2010; *Jeelani et al.*, 2013; *Hameed et al.*, 2015; *Jeelani & Deshpande*, 2017; *Oza et al.*, 2022]. Higher d-excess in groundwater was also reported earlier in the Karnataka region [*Gupta et al.*, 2005b].

Table 3.1: Statistical summary of $\delta^{18}O$, δD, and d-excess for pre-monsoon and post-monsoon groundwater

	Pre-monsoon			**Post-monsoon**		
Statistical parameters	**$\delta^{18}O$**	**δD**	**d-excess**	**$\delta^{18}O$**	**δD**	**d-excess**
Mean	-3.6	-25	4.0	-3.8	-26	4.4
Standard Error	0.0	0	0.1	0.0	0	0.1
Median	-3.5	-24	4.3	-3.8	-25	4.4
Mode	-3.6	-11	4.9	-3.7	-36	5.2
Standard Deviation	1.9	13	5.5	1.8	12	5.6
Range	15.9	94	66.5	16.8	98	80.8
Minimum	-10.8	-73	-31.3	-11.8	-77	-37.2
Maximum	5.1	22	35.1	5.0	21	43.7
Count	2527	2527	2527	2527	2527	2527

- **Seasonal isoscapes of $\delta^{18}O$, δD, and d-excess**

Spatial variations in $\delta^{18}O$, δD, and d-excess of groundwater across the country during the pre-monsoon and the post-monsoon seasons are shown respectively in Fig. 3.4, Fig 3.5 and Fig 3.6, based on seasonal groundwater samples collected from 2527 locations across the country. Major observations regarding the spatial variations in the isotopic composition of groundwater, and the inferences drawn by comparing these seasonal and spatial variations with isotopic composition of the southwest monsoon (SWM) and northeast monsoon (NEM) rainfall [*Oza*, *2020*], are discussed in the following. It should however be realized that the inferences drawn here based on large-scale spatial variation are indicative in nature,

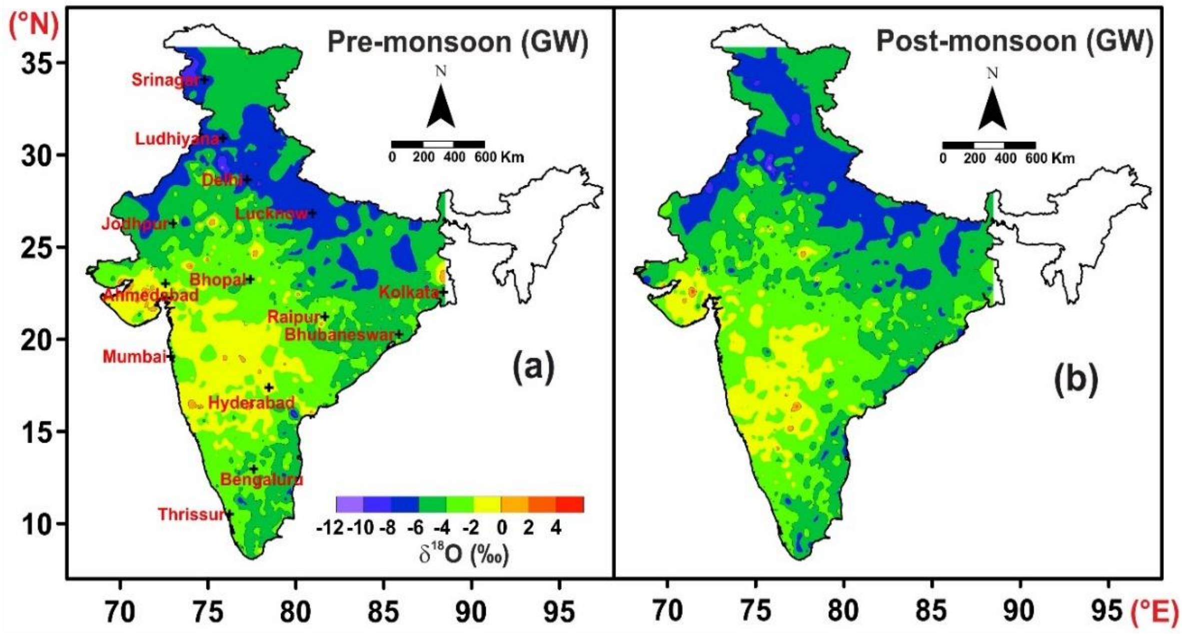

Fig 3.4: (a) Pre-monsoon and (b) post-monsoon contour maps showing spatial variation in groundwater $\delta^{18}O$ (‰). The isotopic depletion trend is observed from SW to NE direction. Names of the important cities are marked in pre-monsoon map as reference locations for discussing the geographical variation.

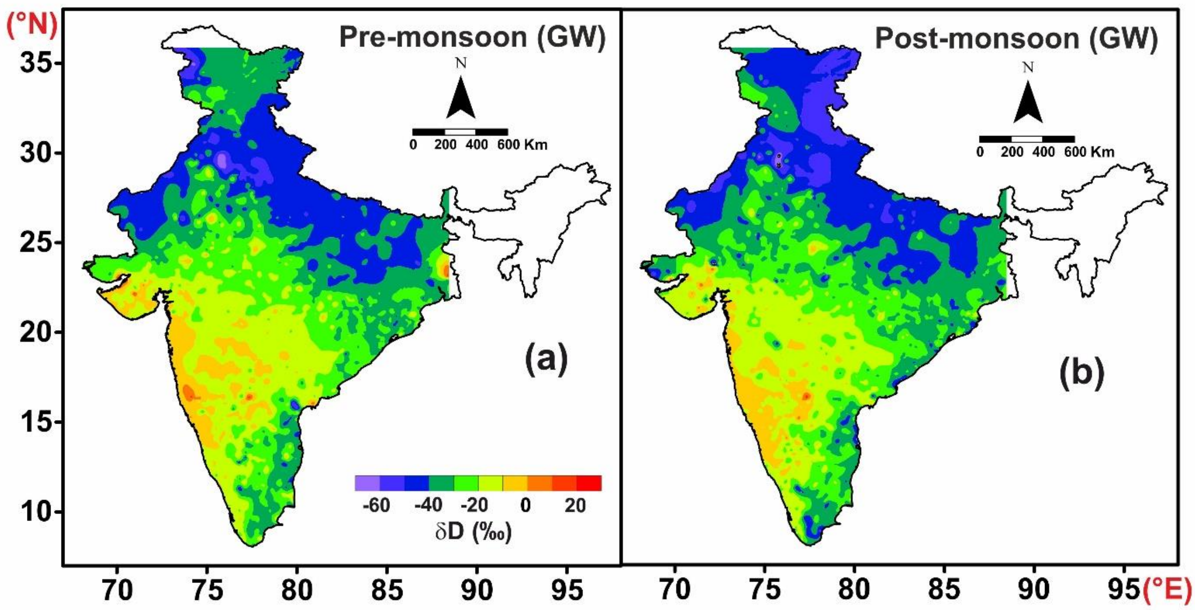

Fig 3.5: Seasonal contour map showing spatial variation in groundwater δD (‰). The most enriched values are observed along the western coast while depleted values are associated with high-altitude areas in the north, Ganga plain, and the western side Of Rajasthan. A similar trend is visible in $\delta^{18}O$ also.

and more conclusive inferences are drawn from the region-wise studies namely for western India (Gujarat), Central India (Madhya Pradesh), and Southwestern India (Kerala) which are discussed in subsequent chapters. Major observations and inferences are:

- Comparison of pre-monsoon and post-monsoon contour maps for $\delta^{18}O$ (Fig 3.4a and b) and also δD (Fig 3.5a and b) reveals that the isoscape of groundwater changes seasonally, with groundwater in the almost entire country becoming isotopically lighter during post-monsoon season. This isotopic depletion in the post-monsoon season indicates that groundwater is recharged by SWM rainfall in the majority of the geographical area in the country.

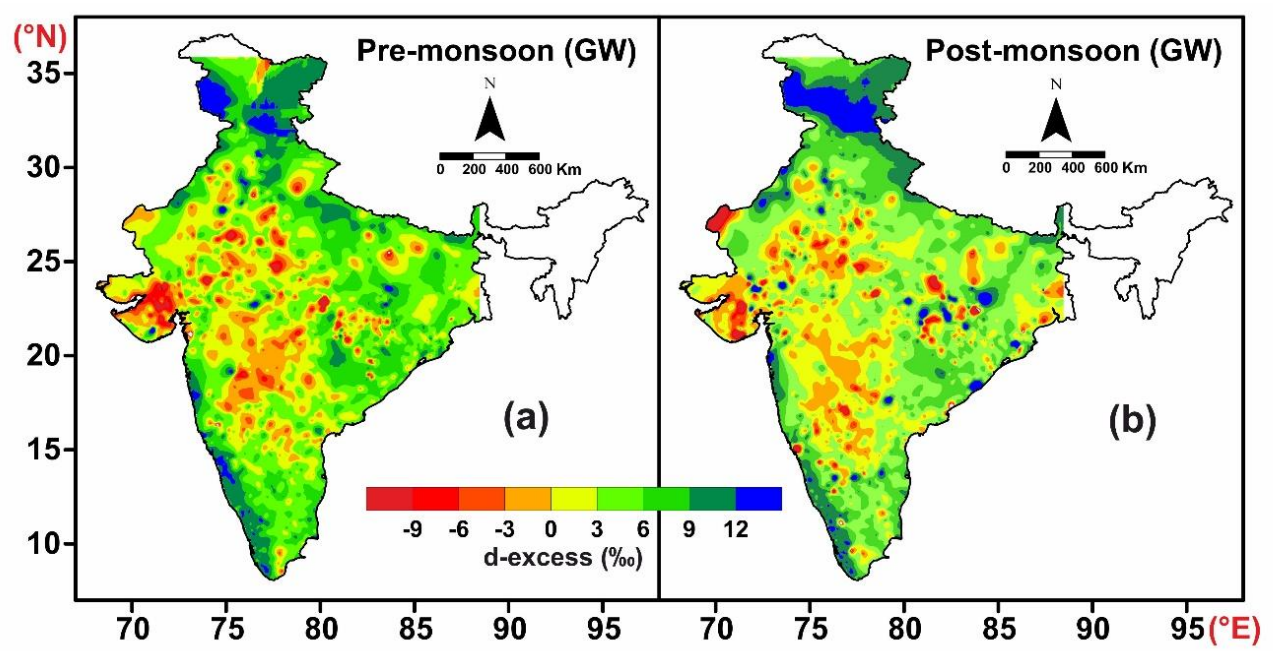

Fig 3.6: Spatial variation in d-excess of groundwater for pre-monsoon and post-monsoon seasons. The d-excess does not show any directional change as observed in $\delta^{18}O$ and δD. The lower d-excess (<-3‰) is visible in patches while the higher d-excess (≥ 10‰) is observed along the Western Ghats and around Srinagar.

- The contour maps of spatial variation in $\delta^{18}O$ (Fig 3.4) and δD (Fig 3.5) in groundwater for pre-monsoon and post-monsoon seasons show a general depletion trend from southwest to northeast direction which is comparable with similar geographical variation in amounted weighted average $\delta^{18}O$ of SWM rainfall [*Oza*, 2020], although the rainfall is isotopically lighter compared to groundwater. This similarity between the spatial trends in groundwater and the SWM rainfall suggests that SWM is the major source of groundwater recharge. The observation that groundwater is isotopically enriched compared to precipitation suggests that the post-precipitation modification in the isotopic composition of the recharge source is caused by evaporation prior to GW recharge.

- There are certain geographical areas in which there is no major isotopic depletion during the post-monsoon season. These regions are the one in which groundwater is recharged during the pre-monsoon season by sources which are isotopically lighter (e.g., Canal water sourced from Himalayan regions) and hence have isotopically lighter signatures during pre-monsoon season. Such regions are recharged by SWM rainfall which might be isotopically heavier or comparable to pre-monsoon groundwater. Therefore, seasonal isotopic change is not observed prominently. This fact has been examined subsequently by studying the map of seasonal differences in $\delta^{18}O$.

- In the southeastern part of India (below 15°N latitude, on the eastern side of Bengaluru; see Fig 3.4a for location), groundwater has depleted $\delta^{18}O$ (-4.0‰ to -6.0‰) and δD (-30‰ to -40‰) compared to the SWM rainfall $\delta^{18}O$ (-2.0‰ to -4.0‰) [*Oza*, 2020]. This depletion in groundwater isotopic composition suggests SWM rainfall may not be the dominant source of groundwater recharge in this region.

- The groundwater in a large area (15°- 24°N) surrounded by the landmark cities of Mumbai, Ahmedabad, Bhopal, Raipur and Hyderabad (see Fig 3.4a for locations) has an enriched isotopic composition during the pre-monsoon season ($\delta^{18}O$ 0.0‰ to -2.0‰) which gets isotopically depleted during the post-monsoon season ($\delta^{18}O$ -2.0‰ to -4.0‰) but it is still enriched compared to the SWM the rainfall ($\delta^{18}O$ -4.0‰ to -6.0‰) [*Oza*, 2020]. The depletion in $\delta^{18}O$ of groundwater in the post-monsoon season suggests the groundwater recharge by the SWM rainfall during the intervening period between pre- and post-monsoon sampling seasons.

- Groundwater in the western part of Rajasthan (northwest to Jodhpur city, Fig3.4a) has depleted $\delta^{18}O$ (-6.0‰ to -8.0‰) during the pre-monsoon season compared to SWM rainfall (-4.0‰ to -6.0‰) [*Oza*, 2020] which indicates different groundwater recharge sources in this area. In this area, inter-basin transfer of water takes place (Sutlej and Beas river water diverted in this area) through Indira Gandhi Canal (India's largest canal) for irrigation purposes. This water is highly depleted in $\delta^{18}O$ (~ -11.0‰) [*Pande et al.,* 2000] and the irrigation return flow of this water seems to give rise to a depleted isotopic signature to pre-monsoon groundwater. Since the SWM rain is not as depleted as the canal water, the groundwater recharged during the post-monsoon season is not further depleted compared to the pre-monsoon season. On the contrary, the groundwater recharged by relatively enriched rainwater (compared to canal water) can only shift the groundwater isotopic composition towards more enriched values.

- The groundwater in the Indo-Gangetic plain covered by recent alluvium has in general depleted isotopic composition ($\delta^{18}O$ -6.0‰ to -8.0‰) both during pre-monsoon and post-monsoon seasons. This can be ascribed to groundwater recharge by isotopically depleted rain during SWM season, which is known to in general isotopically depleted due to the continental effect in rainfall received from the Bay of Bengal branch of SWM [*Bhattacharya et al.*, 2003; *Kumar, B et al.*, 2010; *Oza*, 2020]. The isotopically depleted groundwater during the pre-monsoon season suggests that groundwater during non-rainy pre-monsoon months is recharged by the network of rivers (Ganga and the Indus along with their tributaries; Beas, Yamuna, Gomti, Ravi, Chambal, Sutlej and Chenab) in the Indo-Gangetic plains, many of which carry the water derived by glacial and snow melt in the warm seasons. Higher glacial melt contribution in the rivers draining the Himalayas is already reported [*Maurya et al.*, 2011].
- The spatial variation in d-excess of pre-monsoon (Fig 3.6a) and post-monsoon (Fig 3.6b) groundwater can help to identify the regions in which groundwater is considerably evaporated (d-excess < 0 ‰) either due to pre-recharge evaporation of infiltrating rainwater, or due to evaporation from groundwater table through the capillary fringe zone, or preferential recharge by substantially evaporated surface water source (lake, pond, surface reservoir). It is also seen that area of such highly evaporated groundwater reduces during the post-monsoon season and the d-excess values increase, but even during the post-monsoon season, the d-excess remains lower than the surrounding regions. It means that these regions with lower d-excess might indicate stressed groundwater resources and negative water balance. A large part of the country shows groundwater d-excess values between 0‰ to 9‰. Since lower d-excess is a powerful indicator of evaporation, isoscapes of groundwater d-excess values provide a first-order idea about the evaporative regime and the stress on groundwater resources. Some of the samples have higher d-excess (≥10‰), these samples are falling on the western side of the Western Ghats where huge rainfall (~ 3000mm) and proximity to the sea cause higher d-excess in rainfall which is eventually reflected in groundwater. There are some isolated patches of groundwater with higher d-

excess (>12 ‰). Such higher d-excess values cannot be ascribed to any post-precipitation process; hence, it is inferred that such high d-excess values represent the signatures inherited from the rainfall recharging the groundwater. A higher d-excess in rainfall (except in the western Himalayas) is known to arise due to the contribution of recycled vapour. Extensive recycling of continental vapour is already known to be a major hydrometeorological process operating in India [*Oza et al.*, 2020a; *Oza et al.*, 2020b; *Oza et al.*, 2022]. Therefore, the observed high d-excess in groundwater can be interpreted as the manifestation of vapour recycling in the groundwater.

- **Seasonal variation in $\delta^{18}O$ of groundwater**

In the intervening period between the pre-monsoon and the post-monsoon seasons, the study area receives copious rainfall from SWM. It was shown earlier that SWM rainfall is

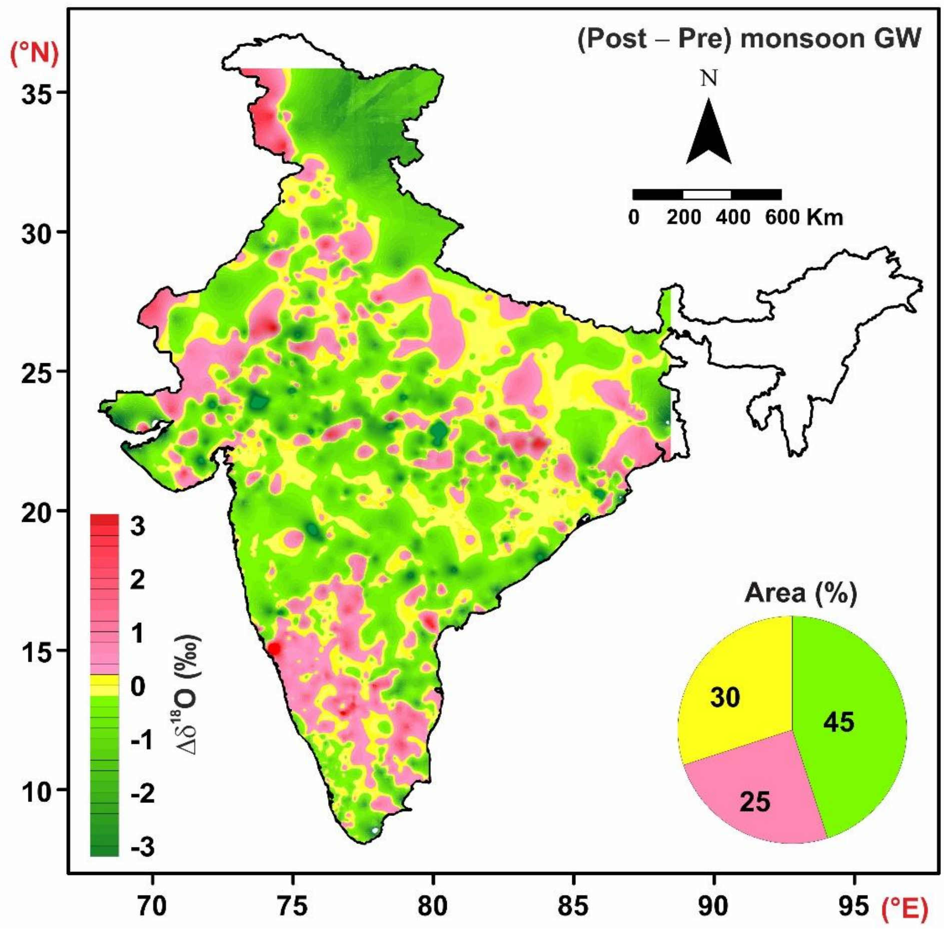

Fig 3.7: Geographical distribution of seasonal variations in $\delta^{18}O$ ($\Delta\delta^{18}O$ = Post-monsoon $\delta^{18}O$ – Pre-monsoon $\delta^{18}O$). The negative value of $\Delta\delta^{18}O$ means that post-monsoon groundwater is isotopically depleted compared to pre-monsoon groundwater, and indicates groundwater recharge by SWM rainfall.

isotopically depleted compared to the pre-monsoon GW in most parts of the country, barring a few exceptions. Therefore, the region in which groundwater is recharged by the SWM rainfall is expected to become isotopically depleted during the post-monsoon season compared to the pre-monsoon season. This fact about seasonal variation can be advantageously used to identify the areas which are recharged by the SWM rainfall, and also to identify the regions in which some source other than the SWM rainfall is playing an important role in seasonal groundwater recharge. With the above scientific logic, to identify the areas in which groundwater is recharged seasonally by the SWM rainfall or another source, the geographical distribution of seasonal variations in $\delta^{18}O$ ($\Delta\, \delta^{18}O$ = Post-monsoon $\delta^{18}O$ – Pre-monsoon $\delta^{18}O$) is plotted in Fig 3.7. The negative value of $\Delta\delta^{18}O$ means that post-monsoon groundwater is isotopically depleted compared to pre-monsoon groundwater, and indicates groundwater recharge by SWM rainfall. On the other hand, the positive value of $\Delta\delta^{18}O$ indicates that post-monsoon groundwater is isotopically enriched compared to pre-monsoon groundwater. This could be due to groundwater recharge by isotopically depleted source water, such as canal water sourced from higher altitude areas or long-distance transport of water of different meteorological origin, through preferential migratory pathways such as faults and fractures.

To evaluate the seasonal differences in $\delta^{18}O$ (Fig 3.7), 2σ standard deviations of analytical precision (2σ i.e. ±0.2‰ for $\delta^{18}O$) of isotope measurement is considered as the significant threshold difference in $\delta^{18}O$ [*Mao et al.*, 2021]. It means that if the seasonal difference ($\Delta\delta^{18}O$) is within ±0.2‰, it is not considered to be significant, and the interpretative significance is assigned only if the $\Delta\delta^{18}O$ value is beyond ±0.2‰. The samples showing a seasonal variation of more than ±0.2‰ are considered as an actual variation influenced by seasonal recharge of groundwater rather than differences ascribable to instrumental uncertainty. Based on the seasonal difference in groundwater $\delta^{18}O$, the study area is categorized into no variation (within ±0.2‰), positive variation (> 0.2‰), and negative variation (< -0.2‰). The samples showing no variation indicate that groundwater recharge takes a longer time than pre-monsoon (April-May) to post-monsoon (October-November) time difference, even for shallow groundwater, and accounts for 30% of the geographical area in the contour map (Fig 3.7).

The samples showing positive $\Delta\delta^{18}O$ represent about 25% of the geographical area and indicate that pre-monsoon GW is depleted compared to post-monsoon GW, which is possible when pre-monsoon GW is recharged by a depleted source, which could be: (1) recharge from the NEM rainfall; (2) irrigation return flow from deeper paleo-groundwater used for irrigation;

and (3) recharge from water originating in different geographical or climatic setting and transported to the location under consideration through rivers, canals or other preferential migratory pathways such as faults and fractures. Most of the area showing positive $\Delta\delta^{18}O$ is associated with the region in which the stage of groundwater development for dynamic groundwater resource is more than 100%, i.e., to fulfil the water demand, deeper groundwater is extracted here [*Saha & Ray*, 2019].

The samples showing negative $\Delta\delta^{18}O$ represent about 45% of the geographical area and indicate that pre-monsoon GW is isotopically enriched compared to post-monsoon GW. The observed isotopic enrichment in pre-monsoon GW compared to post-monsoon season can be ascribed to (1) evaporation from groundwater through the capillary fringe zone; (2) pre-recharge evaporation from infiltrating rainwater; (3) groundwater recharge during pre-monsoon seasons from evaporated point sources such as the open lakes, ponds, and reservoirs. The isotopic depletion in post-monsoon is possible only when pre-monsoon GW mixes with isotopically depleted new water mass which is freshly recharged during and after SWM rainy season and forms the post-monsoon GW, which becomes isotopically depleted compared to pre-monsoon season. From the above scientific logic, it is suggested that nearly 45% of the geographical area receives seasonal recharge from SWM rain. The detailed region-specific causes of seasonal variation are discussed in the upcoming region-wise chapters.

- **Schematic models for seasonal isotopic variations**

In order to explain the observed seasonal variation in the isotopic composition of groundwater, we propose the following four schematic models (Fig 3.8).

1. Preferential migratory pathways

The faults, fractures, and planes of weakness are the preferential migratory pathways through which movement of water can take place laterally or vertically and contribute to groundwater recharge. Engineered canals are also another preferential migratory pathway. Through all these preferential pathways, water from some distant location in a different geographical, climatic, altitudinal or hydrometeorological zone can be transported to a particular area under consideration. The influence of such pathways plays a more important role during non-rainy seasons when autochthonous water for recharge may not be available locally, but allochthonous water transported through these pathways may be available for groundwater recharge.

2. **Point source of recharge**

The lakes, ponds, and surface reservoirs are point sources of water for groundwater recharge. These sources also assume prominence during the non-rainy season when rainwater is not available for diffused recharge from everywhere. These sources can feed the groundwater if hydrogeology allows it. Such open surface reservoirs undergo continuous evaporation and have isotopically enriched isotopic composition. If groundwater is recharged by such point sources, particularly during the non-rainy pre-monsoon season, it will impart its isotopically enriched signature to pre-monsoon groundwater. This isotopic signature will change if there is fresh input of rainwater during and after the rainy season.

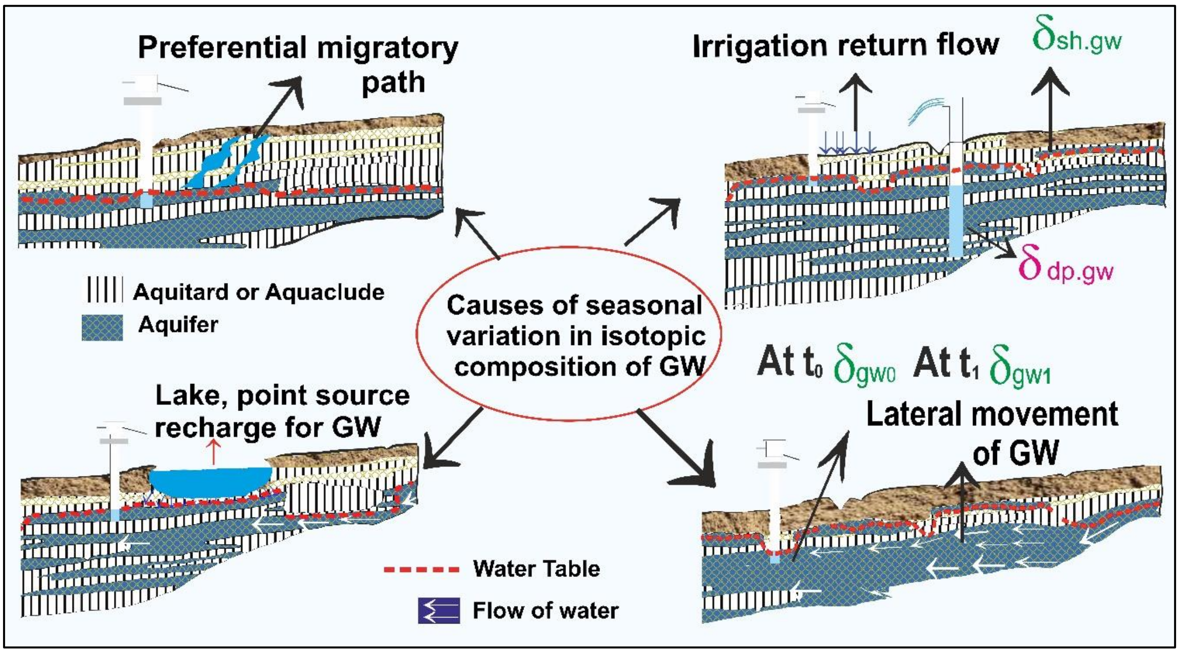

Fig 3.8: Schematic models explaining the observed seasonal isotopic difference.

3. **Irrigation return flow**

In heavily irrigated areas, irrigation return flow can also impart a characteristic isotopic signature to groundwater, particularly in the pre-monsoon season when rainwater is not available, and irrigation through groundwater or canal water is prominent. Irrigation return flow can impart conspicuous isotopic composition to groundwater in regions where deep paleo-waters are extracted from depth for irrigation (such as in the state of Gujarat). The dep paleo waters recharged during different climatic regimes are expected to have a different isotopic character compared to the contemporary rainwater. Similarly, water in the canals transporting rainwater from the different climatic regimes is also expected to have a different isotopic character compared to local rainwater. The Influence of such water sources through irrigation return flow might be one of the reasons for the observed seasonal isotopic difference.

4. **Lateral flow of groundwater**

Groundwater in shallow aquifers is known to have a finite horizontal flow velocity. Therefore, it is logical to consider that when shallow groundwater is sampled from a particular location after an interval of about six months, the water mass from a certain distance has arrived at the sampling location, depending on the horizontal flow velocities. If there is geographical heterogeneity in the recharge source, it may result in an isotopic difference between the two samples. Among all the four possibilities, this one is the least probable. Nonetheless, there exists a possibility of such a situation.

3.4 Conclusion

This chapter presents the first ever seasonal isoscapes of shallow groundwater across the country. Seasonal variation in the isotopic composition of groundwater is compared with the isotopic composition of rainfall available in the literature [*Oza*, 2020]. Using seasonal differences in the isotopic composition of groundwater, various recharge sources and geohydrological processes responsible for the observed isotopic variation are suggested. The isotopic signatures are interpreted in terms of recharge from SWM and NEM rainfall, allochthonous water transported through preferentially migratory pathways such as faults, fractures and canals, and recharge from open surface water bodies such as lakes, ponds, and surface reservoirs. The seasonal variation in $\delta^{18}O$ indicates that 45% of the geographical area receives seasonal recharge from SWM rainfall, 25% of the geographical area shows positive variation indicating groundwater recharge during the pre-monsoon season, and the rest 30% of the geographical area shows no variation suggesting non-occurrence of the seasonal recharge or slow recharge taking place over a longer period beyond the seasonal time gap of about six months. The seasonal isoscapes provide an overview of broad processes operating in the different parts of the country. These isoscapes have been examined in great detail for certain states and described in the subsequent chapters.

Chapter 4

Surface water - groundwater interaction in semi-arid western India (Gujarat)

4.1 Introduction

Groundwater is the world's largest accessible source of fresh water, providing 36% of the world's drinking water and nearly 42% of the water for irrigation [*Taylor et al.*, 2013]. The dependency on groundwater is more in semi-arid and arid regions, which cover nearly 1/3rd of the continental area globally [*Huang & Pang*, 2012], as surface water resources are generally scarce and highly unreliable in these regions [*Taylor et al.*, 2013]. The higher dependency on groundwater poses a threat of overexploitation and contamination of this freshwater reservoir [*Currell et al.*, 2010; *Huang & Pang*, 2012].

One such water-stressed region that depends mainly on groundwater and faces consequences of overexploitation is the state of Gujarat, located in the semi-arid western India, the tenth most populous Indian state with an estimated population of ~60 million (~5% of the Indian population). About 60% of the state's total area (~1.96×10^5 km^2) is drought-prone due to various unfavourable factors such as erratic rainfall, rocky terrain, desert region, lack of perennial rivers, salinity ingression, and deteriorating groundwater quality due to overexploitation [*Bandyopadhyay et al.*, 2020]. Given the above scenario, providing adequate water on a sustainable basis for various requirements (agricultural, industrial and domestic) of the rural and urban population is a significant problem in Gujarat. To mitigate this problem, it is necessary to understand groundwater recharge characteristics, its geographical variation, and factors controlling the interaction between surface water and groundwater. To understand the groundwater recharge processes, isotope tracers have been widely used as the stable isotopic composition of groundwater recharge through direct infiltration of precipitation water will reflect that of local precipitation[*Clark & Fritz*, 1997]. Apart from that, variations in stable oxygen and hydrogen isotopic composition (δ^{18}O and δD) of groundwaters have been advantageously used to understand a variety of hydrogeological processes across the world [*Gat*, 1971; *Vogel & Van Urk*, 1975; *Förstel & Hützen*, 1983; *Frits et al.*, 1987; *Clark & Fritz*, 1997; *Deshpande et al.*, 2003; *Gupta & Deshpande*, 2005b; a; *Mukherjee et al.*, 2007; *Lawson* *et al.*, 2008; *Kendall & Mcdonnell*, 2012; *Govender et al.*, 2013; *Liotta et al.*, 2013; *Hameed et al.*, 2015; *Zhao et al.*, 2018; *Joshi et al.*, 2021] including in India.

This study is based on shallow groundwater samples collected for pre-monsoon (207) and post-monsoon (204) seasons across Gujarat during the IWIN National Programme. The specific objectives of the present study are (1) to identify various probable freshwater sources during different seasons (pre-monsoon, post-monsoon) which are feeding the groundwater and to estimate their seasonally varying relative contribution to groundwater recharge; (2) to delineate the areas primarily recharged by monsoonal rain, and those receiving irrigation return; (3) identify the areas from where surplus groundwater is lost into the sea. In the present study, the isotopic composition of groundwater and its spatiotemporal variation in conjunction with the isotopic composition of rain [*Oza*, 2020] and hydrogeological parameters have been used to achieve these objectives.

4.2 Study area

- **Location, Climate and Physiography**

This study was undertaken in Gujarat (Fig 4.1), located in semi-arid western India, encompassing an area (20.07 - 24.70 °N; 68.17 - 74.48 °E) of nearly 1.96×10^5 km^2, with 1600 km long coastline in the west. Typically, there are four seasons in this region, namely: summer (March-May), monsoon (June-September), autumn (October) and winter (November-February). The state of Gujarat has varied climates ranging from sub-humid and semi-arid to arid type. Maximum rainfall of ~200 cm is recorded in the southern part with a decrease from south to north, and a minimum of ~30 cm precipitation is observed in Kachchh. The annual average rainfall in the state is ~90 cm, almost entirely received within ~30 rainy days during the four months of the Indian Summer Monsoon (ISM). The rainfall details can be

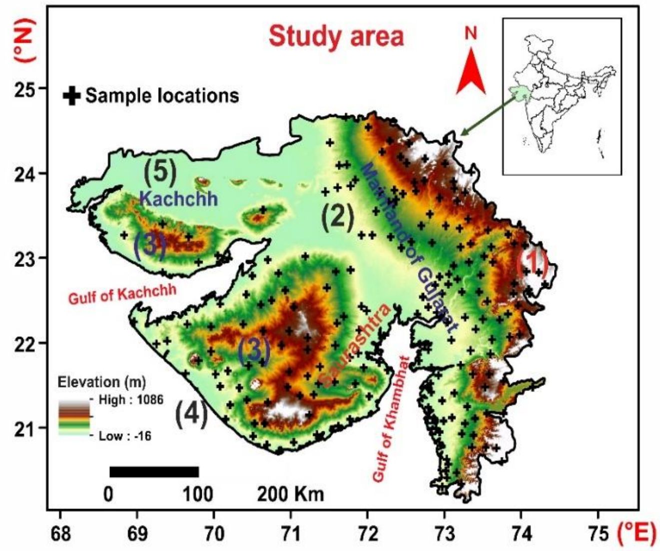

Fig 4.1: The study area has five physiographic divisions namely: (1) Eastern hilly tract (2) Alluvial plain in mainland Gujarat (3) Hilly regions of Saurashtra and Kachchh (4) Coastal alluvial (5) Marshy saline desert.

seen [*Mohanty et al.*, 2015; *Dave & James*, 2017]. Different parts of Gujarat have diverse ecosystems, such as deserts, scrublands, grasslands, deciduous forests, wetlands, mangroves, estuaries, and gulfs.

The study area (Fig 4.1) has been divided into five major physiographic zones [*Mehr*, 1995; *Chamyal et al.*, 2003], namely: (1) The Eastern hilly tract (~300m to ~1086m Above Mean Sea Level or amsl) forms a significant hydrological divide. Most rivers in Gujarat originate from the hills in the east and flow towards the south and southwest. It has four inter-state, west to southwest flowing rivers in mainland Gujarat: the Sabarmati, the Mahi, the Narmada and the Tapi; (2) Alluvial Plains extend from south to north extreme. The alluvial plains also extend westwards to the desert of Little Rann of Kachchh and Banni area; (3) Uplands (~150m to 500m amsl) of Kachchh-Saurashtra comprising sedimentary and volcanic rocks. The Girnar is an isolated mountain (1069m amsl) in the Saurashtra region; (4) The low-lying (~3m to ~25m amsl) coastal tract in the Saurashtra and Kachchh extends from the Rann of Kachchh through the Little Rann Kachchh and low-lying delta region of numerous rivers draining into the Gulf of Khambhat region; (5) Marshy to saline deserts named Rann of Kachchh and Little Rann of Kachchh extending into the saline tracts around the Gulf of Kachchh. This vast expanse of salts mixed with clay lacks vegetation or habitation. The general elevation of this zone varies between 1 to 4m amsl.

- **Aquifer setting**

The state has unconsolidated, semi-consolidated, and fissured geological formations that act as potential groundwater aquifers and have distinct hydrogeological characteristics (Fig 4.2). The unconsolidated formation lies in a large area extending from Banaskantha in the north to Surat and Valsad in the south, forming the state's largest and most potential groundwater aquifer. These aquifers are extensively thick,

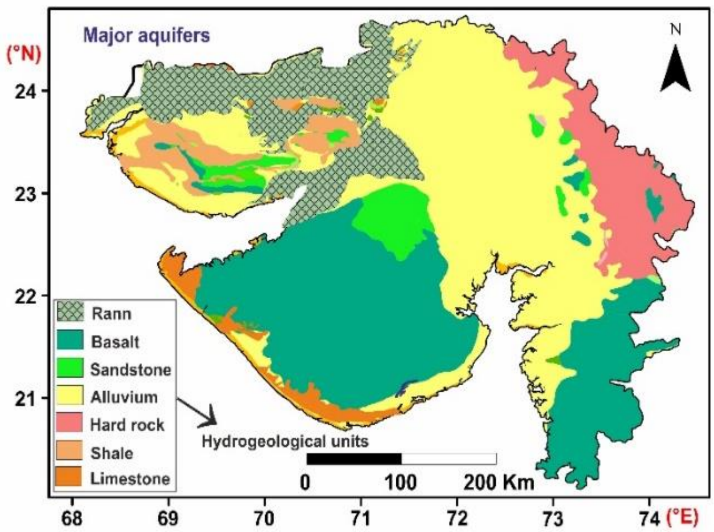

Fig 4.2: Hydrogeological settings of Gujarat.

hydraulically connected and have high hydraulic conductivity (5 to 20 m/d) and yield (10 to 40 lps) (CGWB Report 2015-16). The semi-consolidated formations lie primarily in the Kachchh area and the northeastern part of Saurashtra (Surendranagar District). These formations form discontinuous aquifers and have a moderate yield (<15 lps) and hydraulic conductivity (2 to 10 m/d). The fissured formation covers the Saurashtra and eastern side of mainland Gujarat. Groundwater occurs in the shallow weathered zone and deep fracture in these formations. They have a meagre yield (2 to 15 lps). Further details of aquifer properties can be found in the CGWB report 2015-16 for Gujarat State (http://cgwb.gov.in/Regions/GW-year-Books/GWYB-2015-16/GWYB%20WCR%202015-16.pdf).

4.3 Results and Discussion

Interpretation of groundwater isotopic data in conjunction with published data on the isotopic composition of rain reveals important new scientific insights discussed in the following.

Pre-monsoon groundwater samples have a wide range of $\delta^{18}O$ (-5.5‰ to 4.1‰; avg. -1.9 ± 1.6‰) and δD (-36.6‰ to -17.6‰; avg. -14.5 ± 9.5‰) values. Similarly, the post-monsoon groundwater samples also have a wide range of $\delta^{18}O$ (-9.7‰ to 4.9‰; avg. -2.3 ± 1.6‰) and δD (-77.2‰ to 9.9‰; avg. -17.8 ± 10.8‰) values. The d-excess of pre-monsoon groundwater samples ranges from -22.5‰ to 10.35‰ with an average of 0.2 ± 5.5‰, and that for post-monsoon groundwater range from -29.4‰ to 13.5‰ with an average of 0.7 ± 5.2‰. Between the pre-monsoon and the post-monsoon seasons, the study area receives rainfall during the southwest monsoon season, whose $\delta^{18}O$ values range between -13.2‰ to 3.7‰ with an amounted weighted average of -4.1 ± 3.3‰, and δD values range from -92.0‰ to 33.0‰ with an amounted weighted average of -24.0 ± 26.0‰ for a long-term monitoring station at Ahmedabad [*Oza*, 2020]. The SWM rain at this monitoring station has d-excess ranging from -6.0‰ to 23.0‰, with an amounted weighted average value of 9.0 ± 4.0 ‰. The average $\delta^{18}O$ of post-monsoon groundwater (GW) lies between pre-monsoon GW and the South West Monsoon (SWM) rainfall, indicating that SWM seasonally recharges post-monsoon GW. Above seasonal variations have been examined in detail below.

- **$\delta^{18}O$ - δD regression lines**

Fig.(4.3a) shows the $\delta^{18}O$ vs δD regression line for pre-monsoon and post-monsoon GW samples and also for the rainfall (i.e. local meteoric water line - LMWL) representative for the Gujarat state [*Oza et al.*, 2020b]. The $\delta^{18}O$ - δD regression line equation for the pre-monsoon groundwater samples is: $\delta D = (5.4 \pm 0.2) \times\delta^{18}O - (4.7 \pm 0.4)$, and for the post-monsoon groundwater samples is: $\delta D = (6.1 \pm 0.2) \times\delta^{18}O - (3.6 \pm 0.5)$. The LMWL for Gujarat state [$\delta D = (7.8 \pm 0.1) \times \delta^{18}O + (8.0 \pm 0.1)$]; [*Oza et al.*, 2020b] is comparable to the global meteoric water line (GMWL: slope ~ 8 and intercept ~10). The $\delta^{18}O$ - δD regression lines for

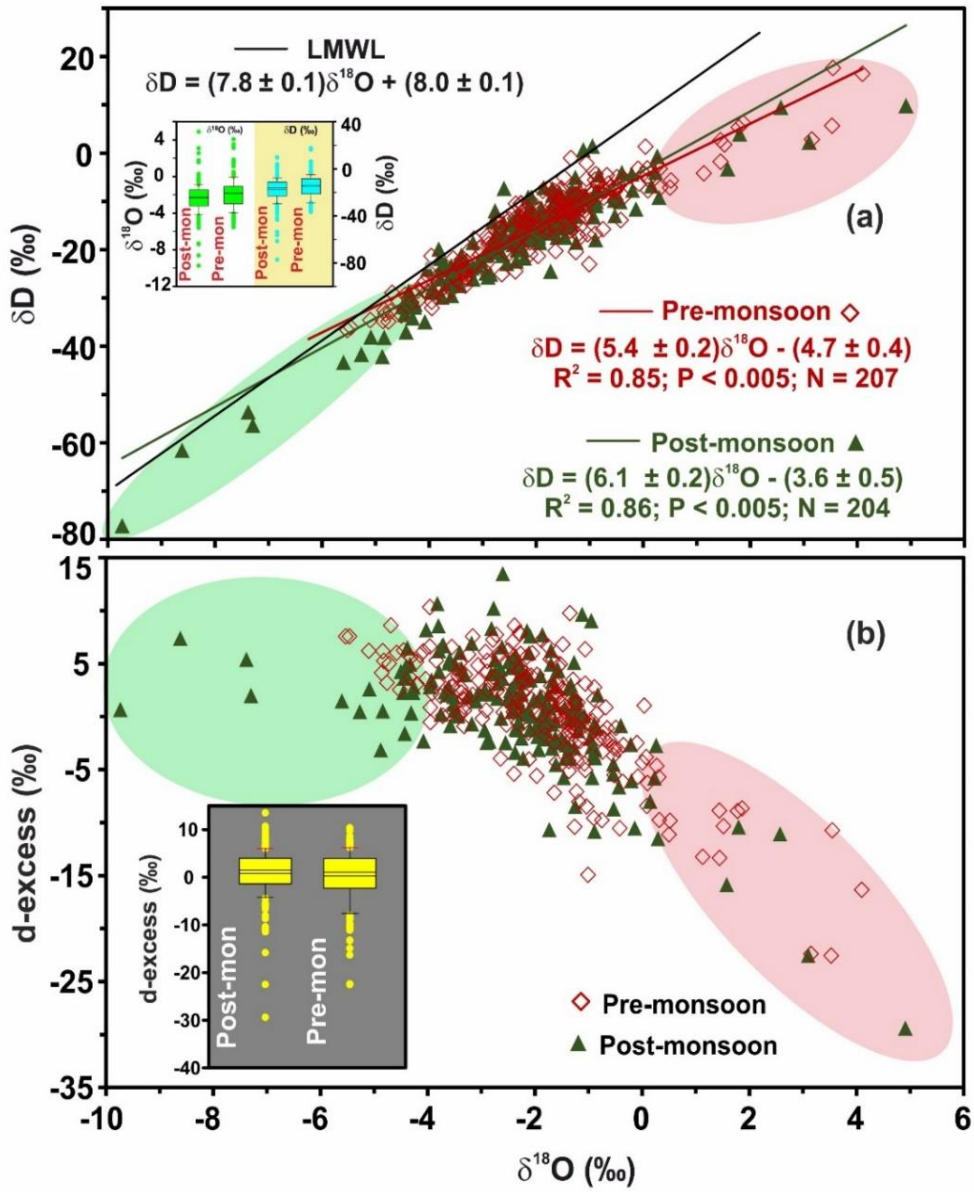

Fig 4.3: (a) The plot of δD vs $\delta^{18}O$ for shallow unconfined groundwater sampled during pre-monsoon and post-monsoon seasons along with LMWL based on rainfall samples at Ahmedabad (b) A plot of d-excess versus $\delta^{18}O$. The samples with extreme values are marked by ellipses, which are associated with conspicuous hydrological processes as discussed in the text.

pre-monsoon and post-monsoon groundwater samples have different values of slope and intercept, which are statistically significant. This conveys that the isotopic signature of groundwater changes seasonally. It is important to notice and realise that the seasonal change in groundwater isotopic composition evident from regression lines for the two seasons can be missed out if only mean values of the pre-monsoon and post-monsoon datasets are considered or only the statistical distribution from the box and whisker plot (inset in Fig 4.3a) is considered. A close comparison of the seasonal regression lines (Fig 4.3a) reveals that the $\delta^{18}O$ - δD regression line slope for post-monsoon GW (6.1 ± 0.2) is lower than that of the LMWL (7.8 ± 0.1), indicating that rainwater undergoes considerable evaporation before and during infiltration while it becomes groundwater. The combined effect of the local atmospheric and shallow surface processes is known to result in the evaporation of rainwater before groundwater recharge [*Gupta & Deshpande,* 2005b]. Another observation is that the slope of $\delta^{18}O$ - δD regression for pre-monsoon GW (5.4 ± 0.2) is lower than that of post-monsoon (6.1 ± 0.2). This indicates that the isotopic composition of groundwater changes during a long non-rainy, dry, pre-monsoon season. There are no major water sources that can recharge the groundwater during the pre-monsoon season. A major portion of the study area is in the arid to semi-arid region, as a result of which groundwater undergoes considerable evaporation via fractures, fissures and capillary fringe zones during pre-monsoon. This is manifested in pre-monsoon GW's lower slope than preceding post-monsoon GW. There are already reports of evaporation of groundwater even from a depth of more than 20 m [*Coudrain et al.*, 2003]. However, it is possible in certain localised areas that groundwater in the pre-monsoon season is recharged by small and shallow surface water bodies subjected to continuous evaporation during the non-rainy period.

Fig. (4.3b) shows the scatter plot of $\delta^{18}O$ vs d-excess. In both the pre-monsoon and the post-monsoon seasons, the d-excess is found to decrease with increasing $\delta^{18}O$. An increasing $\delta^{18}O$ associated with decreasing d-excess is a signal of evaporation [*Deshpande et al.*, 2003]. About 35% of the groundwater samples, even in the post-monsoon season, have negative values of d-excess, which indicates perpetual evaporation of groundwater during the preceding non-rainy period and intense evaporation of rainwater before recharge, even during the rainy season. In the pre-monsoon season proportion of samples with negative d-excess increases to 40%. From Fig 4.3a and 4.3b, it is seen that the $\delta^{18}O$ of the majority (~85%) of groundwater samples for both seasons lie between 0 to -4.0‰. Only ~7% of pre-monsoon samples and ~9 % of the post-monsoon samples are isotopically depleted compared to the amount weighted mean $\delta^{18}O$ of SWM rain samples (-4.1 ‰). These isotopically depleted samples (identified by a green ellipse in Fig 4.3a and b also have their d-excess values different from the general trend of $\delta^{18}O$ vs d-excess (Fig 4.3b). Contrary to expectation, these isotopically depleted samples are located in arid to semi-arid regions of Kachchh and Northern Gujarat (Fig 4.1), where evaporative isotopic enrichment is expected to be more than other regions due to higher aridity and should result in higher values of $\delta^{18}O$. The occurrence of isotopically depleted groundwater in these arid regions indicate the following three possibilities: (1) different source water brought in through engineered inter-basin transfer is feeding the groundwater; (2) shallow aquifers are being recharged by irrigation return flow of old /deep groundwaters extensively extracted for irrigation in this region, and (3) event-based preferential recharge during extreme rain events.

During both pre-monsoon and post-monsoon seasons, certain samples have enriched $\delta^{18}O$ (0 to 4.9‰) and much lower d-excess (-10 to -25‰). These samples with positive $\delta^{18}O$ values and low d-excess values (identified by a pink ellipse in Fig 4.3a and b) are from locations close to the coastal area and inner parts of Saurashtra (Fig 4.1). Although these groundwater locations have proximity to the Arabian Sea, the seawater intrusion cannot be responsible for the enriched isotopic composition of groundwater to such an extent because the Arabian Sea is known to have $\delta^{18}O$ values of 0.9 ± 0.3‰ and d-excess values of 1 ± 1‰ in the coastal area [*Deshpande et al.*, 2013]. Thus, the observed enriched isotopic signature ($\delta^{18}O$: 0 to 4.9‰ and d-excess: -10 to -25‰) in groundwater cannot be ascribed to seawater intrusion but is possible only when recharge occurs through intensely evaporated surface water. Therefore, it is inferred that hypersaline waters of numerous salt pans recharge such highly evaporated groundwaters in coastal areas. This inference is supported by the fact that there are several salt pans in the coastal regions [*Charatkar et al.*, 2005; *Andharia*, 2013].

- **Spatial variation in $\delta^{18}O$ and d-excess**

Fig. (4.4 a&b) and Fig (4.5 a&b) show maps of the spatial distribution of $\delta^{18}O$ and d-excess of shallow groundwater sampled in pre-monsoon and post-monsoon seasons. The observed spatial distribution of groundwater with different isotopic compositions across the study area can be explained in the light of various factors such as the isotopic composition of rain, the latitude effect, the aquifer types, and proximity to the Arabian Sea.

In the pre-monsoon season, most enriched values of $\delta^{18}O$ (0 to 4.1‰) were observed in the coastal region of south Gujarat, the coastal region of Saurashtra, in the vicinity of the Gulf of Kachchh, and the low-lying track linking the Gulf of Khambhat and the Gulf of Kachchh

(Fig 4.4a). These higher $\delta^{18}O$ values in the pre-monsoon season can be ascribed to evaporation from shallow GW and localised recharge from the evaporated surface water sources during the non-rainy season. These two factors are justifiable because of the prevalent aridity in the region during the non-rainy season. The highly depleted $\delta^{18}O$ (< -4.0‰) values were observed in the pre-monsoon season in the northern parts of Gujarat, spanning from northwestern to northeastern parts. These depleted $\delta^{18}O$ values were associated with relatively higher altitude regions in the north, northeast and eastern parts of Gujarat, which is also known for intense agricultural practices dependent on deeper groundwaters. Such depleted $\delta^{18}O$ values of groundwater, even in pre-monsoon, indicates a contribution from a different source than the rain and the local surface water. Because there is extensive pumping of deeper groundwater for irrigation, it is possible that the deeper and old groundwater formed in the different climatological regimes, with depleted isotopic composition, which is extracted for irrigation now, recharges the shallower groundwater as irrigation return flow.

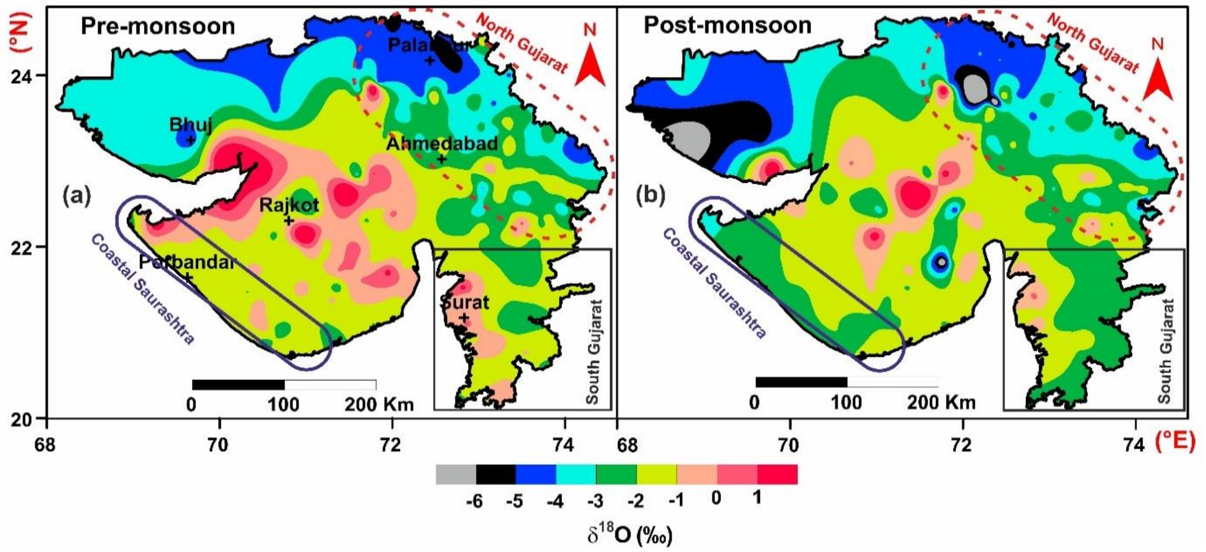

Fig 4.4: The spatial distribution of $\delta^{18}O$ in groundwater is plotted for (a) pre-monsoon season (b) post-monsoon season. The encircled area depicts the change in the isotopic composition of groundwater in two different seasons from the same location. The rectangle south of 22°N in South Gujarat identifies the region for which isotope mass balance has been done to estimate the flux of surface water-groundwater interaction and exchange.

In the post-monsoon season, groundwater $\delta^{18}O$ varies spatially and has different isotopic composition than pre-monsoon (Fig 4.4b). South Gujarat and Saurashtra show no variation with latitude, while north Gujarat shows decreasing trend from lower to higher latitude region (Fig 4.4b). The western coast of Saurashtra shows depleted $\delta^{18}O$ compared to pre-monsoon as well as compared to the rest part of Saurashtra (marked in a blue ellipse in Fig 4.4a and b). This can be ascribed to recharge from southwest monsoon rain. Based on the observed isotopic difference between western coastal Saurashtra and the rest of Saurashtra (Fig 4.4b), it can also be inferred that the recharge process in western Saurashtra is relatively faster compared to the rest of Saurashtra. This is justifiable as the coastal part of Saurashtra is covered with coastal alluvial (rainfall infiltration factor, RIF = 0.2) and limestone (RIF = 0.06) while the rest part of Saurashtra is covered with basaltic rock (RIF=0.02, Fig 4.2) (GEC report, 2015: http://cgwb.gov.in/Documents/GEC2015_Report_Final%2030.10.2017.pdf). The higher RIF causes faster recharge [*Mao et al.*, 2021]. In south Gujarat, the coastal alluvial aquifer shows enriched $\delta^{18}O$ compared to the hard rock aquifer on the eastern side (Fig 4.4b). The isotopic depletion ($\delta^{18}O \leq -2.0‰$) in the eastern part of south Gujarat is the combined effect of relatively higher altitude (up to 900m) and fast recharge through secondary migratory pathways. Northern Gujarat is mostly covered with quaternary alluvium except the eastern margin (Fig 4.2), which shows a depleting trend in $\delta^{18}O$ from lower latitude to higher latitude during post-monsoon season.

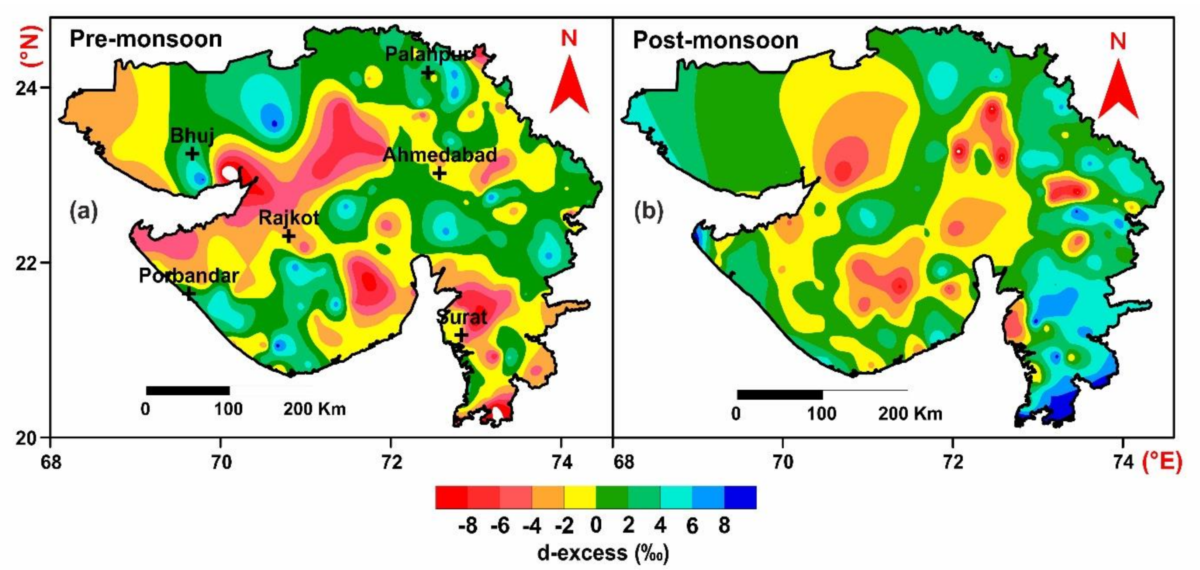

Fig 4.5: Spatial distribution of d-excess in shallow groundwater is plotted (a) for pre-monsoon season and (b) for the post-monsoon season. The spatial distribution of d-excess values is different for both seasons suggesting different processes governing the d-excess values. For the pre-monsoon season these factors could be evaporation and recharge from point sources while for the post-monsoon season these values are dominantly governed by recharge from SW monsoon rainfall.

The inverse relationship between $\delta^{18}O$ and d-excess (Fig 4.3b) is also reflected in the spatial variation in $\delta^{18}O$ (Fig 4.4a&b) and d-excess (Fig 4.5a&b) for pre-monsoon and post-monsoon seasons. The higher d-excess (0 to 10‰) is mainly observed in mainland Gujarat's north and middle parts. Apart from that, a few coastal Saurashtra areas also show a higher d-excess during pre-monsoon. In the post-monsoon season, except for some parts of mainland

Gujarat and Saurashtra, the entire region offers a relatively higher d-excess indicating the change in the groundwater mass because of freshwater influx after the rainy season.

- **Seasonal variation in $\delta^{18}O$ and d-excess**

The seasonal variation in groundwater $\delta^{18}O$ and d-excess can be comprehended by computing the difference between the post-monsoon and pre-monsoon groundwater isotopic composition ($\Delta\delta = \delta_{post\text{-}monsoon} - \delta_{pre\text{-}monsoon}$). A seasonal difference of ±0.2‰ in $\delta^{18}O$ has been

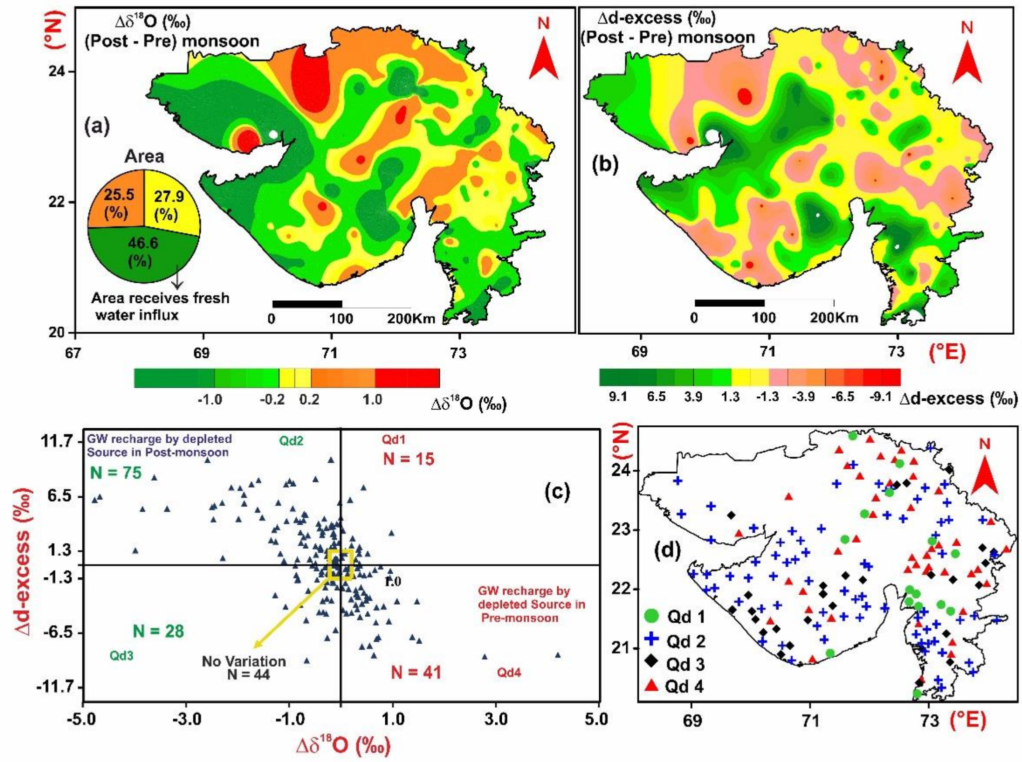

Fig 4.6: A plot showing seasonal difference (Δ = Post-monsoon minus Pre-monsoon) for (a) $\delta^{18}O$ (i.e. $\Delta\delta^{18}O_{post-pre\text{-}monsoon}$), and (b) for d-excess (i.e. Δd-excess $_{post-pre\text{-}monsoon}$) of Groundwater. The values of seasonal variation in $\delta^{18}O$ ($\Delta\delta^{18}O$) and d-excess (Δd-excess) are plotted in (c). Geographic locations of samples falling in the different quadrants of (c) are plotted in (d).

considered to be a significant (i.e. 2σ measurement precision of ±0.1‰ for $\delta^{18}O$) threshold value in this study, similar to other previous studies [*Mao et al.*, 2021]. A seasonal difference of ±1.3‰ in d-excess is considered to be significant, based on the error propagated in the computation of d-excess from the precision of $\delta^{18}O$ (±0.1‰) and δD (±1‰). The marked seasonal differences in $\delta^{18}O$ and d-excess beyond the above threshold values are considered indicators of some natural processes changing the isotopic composition of groundwater. During the rainy season between pre-monsoon and post-monsoon periods, the study area receives rainfall from SWM, which has lower $\delta^{18}O$ (and higher d-excess) compared to the pre-monsoon groundwater. Therefore, depending upon the fresh rainwater influx, post-monsoon GW is expected to show variations in $\delta^{18}O$ and d-excess concerning pre-monsoon GW. The groundwaters receiving substantial fresh rainwater influx before the post-monsoon sampling are expected to have lower $\delta^{18}O$ (and higher d-excess).

To understand the possible causal factors for the observed seasonal isotopic differences, the spatial variation in seasonal differences, i.e. $\Delta\delta^{18}O$ is plotted in Fig 4.6a, for Δd-excess is plotted in Fig 4.6b. The values of $\Delta\delta^{18}O$ and Δd-excess are plotted in x-y coordinates in Fig 4.6c. The geographic locations of samples falling in the different quadrants of Fig 4.6c are plotted in Fig 4.6d. It is observed from Fig 4.6a that nearly 47% of the study area shows lower $\delta^{18}O$ in post-monsoon groundwater compared to pre-monsoon values (i.e. -ve values of $\Delta\delta$) which suggest recharge from isotopically depleted fresh rainwater. On the other hand, nearly 25% of the geographical area shows higher $\delta^{18}O$ in post-monsoon groundwater compared to pre-monsoon values (i.e. +ve values of $\Delta\delta$), this is possible only if there is continuous localised recharge from isotopically enriched surface water, even during the rainy season when isotopically depleted rainfall occurs in other areas. More insights are obtained when seasonal variations in both $\delta^{18}O$ and d-excess are simultaneously considered (Fig 4.6c). It is seen that most of the samples (>50%) fall in Qd2 and Qd4, where $\delta^{18}O$ and d-excess have an inverse correlation. The samples (N = 75) falling in Qd2 have -ve variation in post-monsoon $\delta^{18}O$ and +ve variation in post-monsoon d-excess compared to pre-monsoon values, this indicates that groundwater undergoes evaporation during the pre-monsoon season, which leads to the enrichment of $\delta^{18}O$ and lowering of d-excess, while in the post-monsoon season, fresh rainwater influx (with lower $\delta^{18}O$ and higher d-excess) depletes the $\delta^{18}O$ and increases the d-excess. Samples (N= 41) falling in Qd4 (Fig 4.6c) have +ve variation in post-monsoon $\delta^{18}O$ and -ve variation in post-monsoon d-excess compared to pre-monsoon values. These samples are located mainly in the arid to semi-arid, water-stressed northern Gujarat (above 22°N), which is known for the presence of deep, static palaeowater with up to >35ka age [*Agarwal et al.*, 2006]. The deeper static palaeowater is extensively pumped to meet the agriculture and domestic water demand [*Gupta & Deshpande*, 2005b; *Shah*, 2014]. The +ve seasonal difference ($\Delta\delta^{18}O$) indicates groundwater recharged by an isotopically depleted water source during the pre-monsoon season, although this season is devoid of precipitation. As stated earlier, deeper static water is extensively used for irrigation, and it could be isotopically depleted due to the following three reasons: (1) lateral flow of groundwater recharged in the high altitude regions in NE Gujarat; (2) deeper groundwater recharged during different climatic regime when isotopically depleted winter rains have been inferred in this region [*Agarwal et al.*, 2006]; (3) Himalayan rivers draining into Arabian sea passing through this region [*Sengupta et al.*, 2020]. Based on the above evidence, we inferred that the observed +ve $\Delta\delta^{18}O$ and -ve Δd-excess could be due to the pumping of isotopically depleted deeper groundwater for irrigation and its return flow to relatively shallower aquifers.

A small number of samples also fall in Qd1 (~7%) and Qd3 (~14%), where $\delta^{18}O$ and d-excess in post-monsoon show variation in a similar direction compared to pre-monsoon values, i.e. both $\Delta\delta^{18}O$ and Δd-excess have +ve values, or both have -ve values. Samples falling in Qd1 show positive variation in post-monsoon $\delta^{18}O$ and d-excess compared to pre-monsoon values which means both the isotopic parameters shift towards lower values during pre-monsoon. In contrast, samples falling in Qd3 have negative variation in post-monsoon $\delta^{18}O$ and d-excess compared to pre-monsoon values, suggesting both the parameters shift towards lower values in the post-monsoon season. Based on available evidence, it is impossible to ascertain the exact causal mechanism for observed seasonal variation in this small proportion of samples. Since there is no conclusive evidence, it can only be conjectured based on the overall scheme of facts that isotopically different water mass, either originating as rain in the high-altitude region or during different climatic regimes, contributes substantially to either of the seasons.

- **Groundwater recharge in South Gujarat**

South Gujarat (south of 22°N latitude in mainland Gujarat; Fig 4.4) receives an annual rainfall of ~1034 mm during SWM from June to September, a fraction of which recharges the groundwater, which sustains the agriculture and fulfils the domestic and industrial water demand. South Gujarat has been marked in Fig 4.4a&b by a rectangle south of 22°N. A two end-member mixing model is used to calculate the contribution of SWM rainfall to groundwater recharge in south Gujarat. The contributions are calculated using the standard mass balance equations used in several earlier studies [*Phillips*, 2001; *Hameed et al.*, 2015; *Sakakibara et al.*, 2017]:

$$\delta_{pre}\, M_{pre} + \delta_{rain}\, M_{rain} = \delta_{post} \;\ldots\ldots\ldots\ldots\ldots\; Eq.1$$

$$Where$$

$$M_{pre} + M_{rain} = 1 \ldots\ldots\ldots\ldots\ldots Eq. 2$$

Where δ_{pre} is the $\delta^{18}O$ of pre-monsoon groundwater and M_{pre} is the mass fraction of pre-monsoon groundwater, δ_{rain} is the $\delta^{18}O$ of rainwater for SWM and M_{rain} is the mass fraction of rainfall, δ_{post} is the $\delta^{18}O$ of post-monsoon groundwater, which is the admixture of pre-monsoon groundwater and the rainfall. From the above equation, the percentage contribution of rain in groundwater is calculated using the following equation:

$$\text{Rainwater contribution in (\%)} = \left\{\frac{\delta_{post} - \delta_{pre}}{\delta_{rain} - \delta_{pre}}\right\} \times 100 \ldots\ldots\ldots Eq. 3$$

Table 4.1: The fraction of rain in groundwater of South Gujarat were calculated using two end-member mixing model.

Groundwater recharge from SWM in South Gujarat	
Post-monsoon GW $\delta_{post}{}^{18}O$ (‰)	-1.9
Pre-monsoon GW $\delta_{pre}{}^{18}O$ (‰)	-1.2
Mumbai rain $\delta_{rain}{}^{18}O$ (‰)	-2.3
Rainwater contribution with uncertainty using formulations of Genereux (1998)	(0.7 ± 0.1) ~70%

The end member values of $\delta^{18}O_{pre}$ = -1.2‰ and $\delta^{18}O_{post}$ = -1.9 ‰ are taken respectively as the average pre-monsoon and post-monsoon values for the groundwater samples from south Gujarat. The end member value of δ_{rain} = -2.3‰ is taken as the amount weighted average $\delta^{18}O$ of rainfall sampled at the coastal station of Mumbai in 2009. Uncertainty in rainwater contribution estimated using the above equations is calculated by the uncertainty propagation technique [*Genereux*, 1998]. The above end-member mixing model reveals that the post-monsoon groundwater mass consists of an admixture of 70% of rainwater which mixes with 30% of the pre-monsoon groundwater (Table 4.1). The uncertainty in the above-estimated rain fraction is 0.1 (i.e. 10%). As discussed in the following, these estimated mass fractions of rainwater and pre-monsoon groundwater can be advantageously used for the volumetric estimation of other hydrological components of south Gujarat.

According to Dynamic Groundwater Resources of India, 2011 [*Cgwb*, 2011], a report published by CGWB (Central Groundwater Board), water resources of the five districts (Surat, Valsad, Dang, Navsari, Tapi) in southern Gujarat, total dynamic groundwater resource available in south Gujarat is ~2.1 Billion Cubic Meter (BCM). Using the estimated mass fractions for rainwater (70%), it is estimated that 1.5 BCM (i.e. 70% of available groundwater resource of 2.1 BCM) is the volume of rainwater that percolates underground to recharge the groundwater in south Gujarat on an annual basis. The volume of rainfall in south Gujarat is 14.8 BCM, and the groundwater recharge volume is calculated as 1.5 BCM. Thus, the rainfall recharge is ~10% of the total rainfall. The estimated volume of pre-monsoon groundwater is ~0.6 BCM (i.e. 30% of available groundwater resource of 2.1 BCM). This estimate of pre-monsoon groundwater volume can be used to estimate the volume of water lost from dynamic groundwater systems. The groundwater withdrawal in south Gujarat is reported to be ~45%, according to the CGWB report (2011). On withdrawal of 0.9 BCM groundwater (i.e. ~45% of the total groundwater resource of 2.1 BCM), the remaining groundwater is expected to be 1.2 BCM (= 2.1 – 0.9 BCM). However, from isotope mass balance, it is estimated that pre-monsoon groundwater volume is only. ~0.6 BCM. The difference between the volume of water expected to remain (1.2 BCM) and the estimated volume of pre-monsoon groundwater (~0.6 BCM) from mass balance is 0.6 BCM (i.e. 1.2 – 0.6 = 0.6 BCM), which is lost from the dynamic groundwater resource. It can be inferred that this volume of water is lost into the Arabian Sea as submarine groundwater discharge (SGD). A recent study [*Bhagat et al.*, 2021] has also reported that groundwater lost as SGD into the Arabian Sea in Gujarat is maximum in southern districts. The importance of this computation is that it demonstrates how seasonal variation in isotopic composition can be advantageously used to provide a first-order volumetric estimate of surface water - groundwater interaction and exchange. This study also shows how seasonal isotopic variation can be used to provide estimates of the SGD.

4.4 Conclusion

The current study is based on seasonal differences in the stable isotopic composition of groundwater to understand the interaction and exchange between surface water and groundwater. Conventionally, the seasonal water level fluctuation is used to estimate groundwater recharge, and an increase in water level in the post-monsoon season is ascribed to fresh groundwater influx. However, the seasonal difference in water level depends on aquifer properties and seasonal variation in groundwater extraction. Therefore, the water level increase in the post-monsoon season does not necessarily represent the actual recharge.

This study reveals that groundwater shows seasonal variation in $\delta^{18}O$ and d-excess from pre-monsoon to post-monsoon. Groundwater in ~47% of the study area shows depletion in $\delta^{18}O$ in the post-monsoon season, which is ascribed to recharge by SWM rainfall. In contrast, groundwater in ~25% of the study area shows depletion in $\delta^{18}O$ during the pre-monsoon season, ascribed to recharge by irrigation return flow of deeper, static paleo-groundwater being mined for irrigation since there is no surface water or shallow groundwater available in the required quantity. About 28% of the study area doesn’t show any seasonal isotopic variation in shallow groundwater, suggesting negligible groundwater replenishment through seasonal recharge. The isotopic mass balance in conjunction with data on dynamic groundwater resources in South Gujarat suggests that ~28% (0.6 BCM) of the available dynamic groundwater in this region is lost as submarine groundwater discharges into the Arabian Sea. The deterioration in groundwater quality near the Gulf of Kachchh region is caused by recharge from hypersaline residual water in the salt pans and not due to seawater intrusion as was believed earlier.

Chapter 5

Long-term variation in groundwater dynamics in Gujarat

5.1. Introduction

Nearly 1/3rd of the terrestrial earth's surface is covered by arid and semi-arid regions [*Scanlon et al.*, 2006]. Gujarat, a semi-arid western Indian state, is one such region that receives low rainfall (average annual rainfall: ~900 mm) and has only 2% (37 BCM) of the country's total surface water reserve. Thus, groundwater faces the maximum burden of meeting the water demand, out of ~21.2 BCM of annual replenishable groundwater, ~13.6 BCM of groundwater is annually extracted in the state of Gujarat (http://cgwb.gov.in/Documents/Dynamic-GW-Resources-2011.pdf).

The availability of groundwater and its extraction in Gujarat is highly heterogeneous and some parts of it face higher groundwater withdrawal compared to annual recharge [*Saha & Ray*, 2019]. The imbalance in groundwater recharge and extraction causes not only the mining of static groundwater but also quality deterioration in shallow groundwater. To overcome the problems associated with groundwater availability, a huge engineered intervention was done in terms of the Sardar Sarovar Dam on the Narmada River and the associated Narmada Canal, which is the World's largest lined canal (~458 km), operational since 2008, and an entire network of major and minor canals measuring 74626 km in length (http://nca.gov.in/ssp_salient2.htm). The Narmada canal transfers water from the Narmada River flowing through South Gujarat with a sub-humid climate to North Gujarat having a semi-arid to arid climate [*Ray et al.*, 2009] to irrigate nearly 1.8 million hectares of land (https://sardarsarovardam.org/benefits-of-project.aspx). Despite its huge socio-economic relevance, detailed scientific studies assessing the effect of the Narmada Canal on the groundwater are very few.

To understand the changes in groundwater recharge sources for shallow GW over a period of one decade from 2009 to 2019, and the interaction between shallow and deep groundwater, field campaigns were carried out during 2019-2020 for pre-monsoon and post-monsoon seasons across Gujarat to collect samples from shallow GW, deep GW, Narmada Canal Water, and reservoirs water. These samples were analysed for oxygen and hydrogen isotopes as they are the natural tracers used to understand the interaction between different water masses [*Gat*, 1996; *Deshpande et al.*, 2003; *Kortelainen*, 2011; *Yeh et al.*, 2014b; *Mao* *et al.*, 2021] along with some of the major ions (anions- Cl^{-1}, SO_4^{-2}, NO_3^{-1} and cations NA^{+1}, Mg^{+2}, Ca^{+2}). To assess the change in groundwater dynamics, including the recharge sources and interaction between the surface water and the groundwater, 204 shallow groundwater samples collected during the year 2009 under the aegis of the IWIN National Programme and analysed for $\delta^{18}O$ and δD were compared with 262 shallow groundwater samples collected during 2019-2020.

5.2 Study area

- **Location, Physiography, and Climate**

Located in the western-most part of India, the study area of Gujarat covers nearly 6% (1.96 lakh square km) of the country's geographical area and accommodates ~5% of the country's population (http://gujenvis.nic.in /PDF/soe-land.pdf). On the eastern side, the study area is bounded by the Aravalli mountain ranges in north Gujarat and the Vindhyan hilly tract in south Gujarat. On the western side, it has a 1600 km long Arabian Sea coastline [*Shah et al.*, 2008]. The study area has five different physiographic divisions (Fig 5.1) given by [*Mehr*, 1995; *Chamyal et al.*, 2003], namely (1) the eastern hilly tract, with altitudes ranging between ~300m to ~1000m acts as major water divides; (2) the alluvial planes, are the low lying area in the middle of the study area; (3) upland area of Kachchh and Saurashtra comprising sedimentary and volcanic rocks; (4) the coastal low lying area, covered by coastal alluvial; (5) marshy to saline deserts named as Rann of Kachchh and Little Rann of Kachchh extending into the saline tracts around the Gulf of Kachchh. This vast expanse of salts mixed with clay, lacks vegetation or habitation. Typically, there are four seasons in this region, namely, summer (March-May), monsoon (June-September), autumn (October) and winter (November-February). The state of Gujarat has varied climates ranging

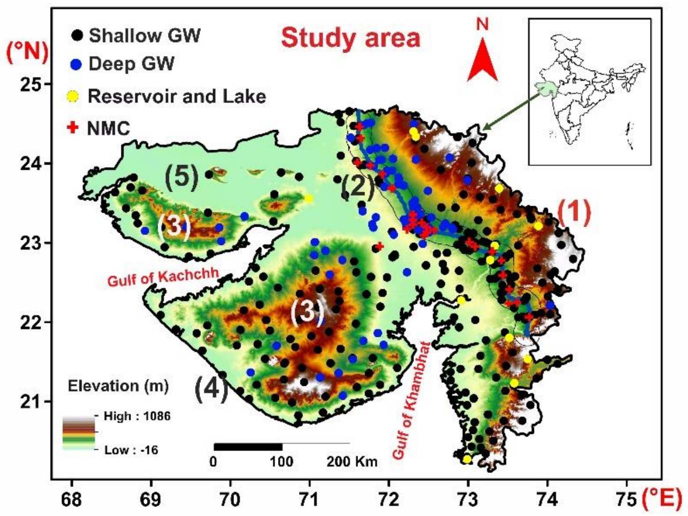

Fig 5.1: This figure represents the study area's elevation profile and sample locations. The samples were collected from different water masses (shallow GW, deep GW, reservoirs and lake, and Narmada canal). The 1,2,3,4,5 represents different physiographic units.

from sub-humid, semi-arid, and arid types spread over different regions. Northern Gujarat (above 23° latitude) has an arid climate, while South Gujarat (below 22° latitude, east of Gulf of Cambay) has a sub-humid climate, rest part of Gujarat having a semi-arid climate [*Ray et al.*, 2009]. Maximum rainfall of ~200 cm is recorded in the southern part and decreases from south to north, and a minimum of ~30 cm rainfall is observed in Kachchh [*Priyan*, 2015]. The annual average rainfall in the state works out to be ~90 cm, almost entirely received within ~30 rainy days during the four months of the southwest (SW) Indian Summer Monsoon (ISM).

- **Hydrogeology**

The larger part of the study area is covered by alluvial and basaltic rocks (Fig 5.2). The alluvial tract extending from north to south covers nearly 9000 km^2 of the area and constitutes the largest and the most potential groundwater reservoir in the state. It is a multilayered aquifer system, and most of the deep (> 500 feet) GW samples during 2019-20 were collected from the northern part of this aquifer along with shallow GW (Fig. 5.1). Basaltic rock covers nearly 74000 km^2 of the geographical area and forms a moderate quality aquifer in terms of water yield (5 to 15 lps). In this aquifer, shallow groundwater is present in the weathered zones, while deeper groundwater is present in fracture zones. Shallow GW samples were collected from this aquifer (Fig 5.1). The eastern and northern part is covered by Archean rocks with higher altitude, which causes higher runoff and lower groundwater recharge, making them a low potential zone for groundwater. The details of the aquifer characteristics are available in state-wise groundwater reports published by CGWB (http://cgwb.gov.in/GW-Year-Book-State.html).

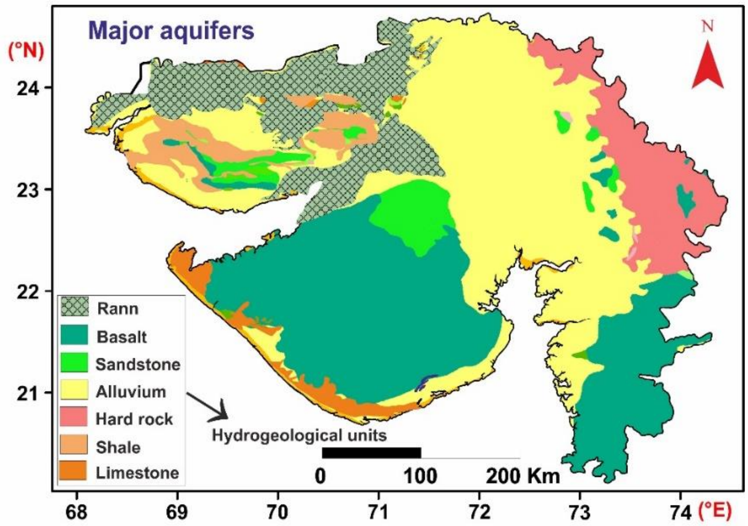

Fig 5.2: Hydrogeological seting of Gujarat.

5.3 Results and Discussion

- **δ^{18}O-δD Regression lines for shallow GW (2009 and 2019)**

The $\delta^{18}O$-δD regression line and d-excess vs $\delta^{18}O$ for shallow GW samples collected during IWIN National Programme, 2009 and those collected during 2019 for pre-monsoon and post-monsoon seasons are plotted in Fig 5.3a,b & a',b' along with LMWL available from [*Oza et al.*, 2020b]. The statistical description of the 2019 data is given in Table 5.1, while that for

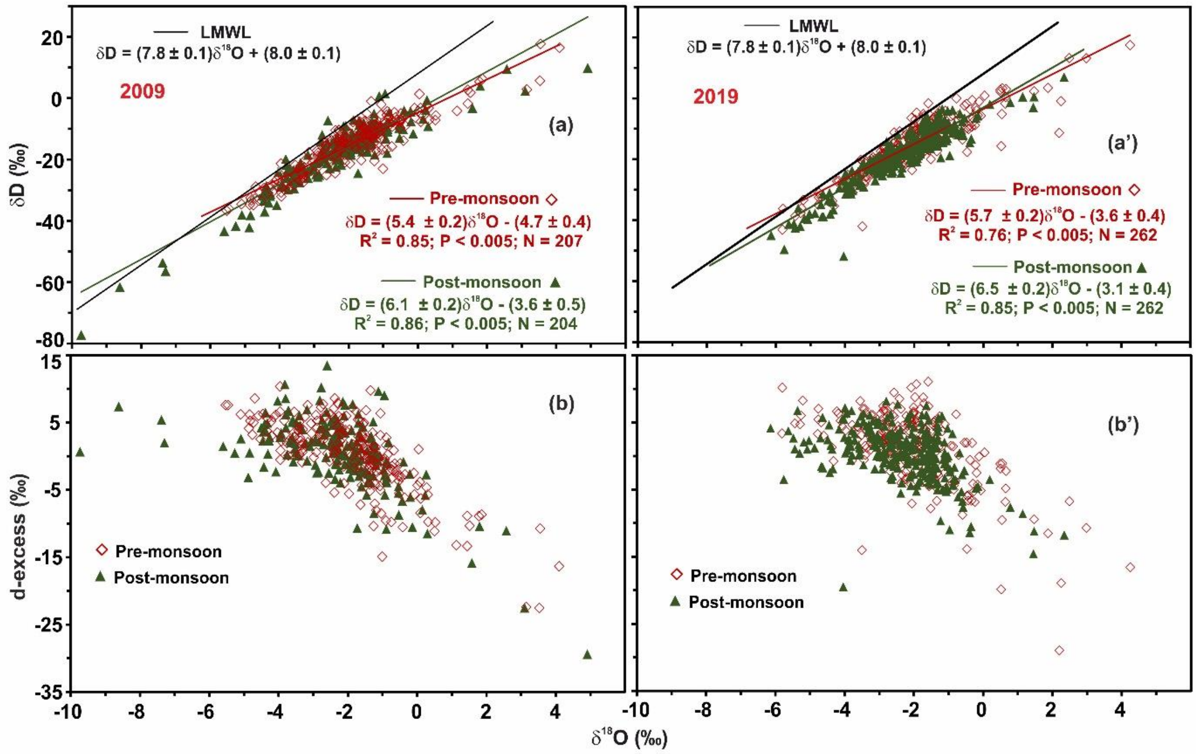

Fig 5.3: Relationship between δD-$\delta^{18}O$ and d-excess-$\delta^{18}O$ for pre-monsoon and post-monsoon shallow GW of 2009 and 2019 along with LWML.

2009 data was discussed earlier in Chapter 4 on the State of Gujarat. Major observations and inferences that are drawn based on the seasonal variation in the regression lines slope of the groundwater and the decreasing trend of d-excess with an increase in $\delta^{18}O$ are as follows:

A comparison of the regression lines slope for pre-monsoon and post-monsoon seasons reveal that groundwater mass changes isotopically in the post-monsoon season due to an influx of fresh rainwater. Post-monsoon groundwater has higher regression line slope compared to pre-monsoon groundwater, and the post-monsoon regression line slope value is closer to that of the local meteoric water line (LMWL), although less than the LMWL. The lower regression line slope for both the seasons compared to LMWL indicate an evaporative regime in the study area as a result of which groundwater is isotopically enriched compared to local rainwater. The evidence of evaporation can also be seen in the d-excess values of groundwater. Many of the samples have negative d-excess, which goes up to -20‰ (Fig 5.3 b'), while the local rainwater, which is the major groundwater recharge source, has positive d-excess [*Oza et al.*, 2020b]. This observation is valid both for 2009 and 2019, suggesting that there is no change in this pattern of seasonal changes during the interval of 10 years from 2009 to 2019. However, an important change in the isotopic signature of groundwater between the years 2009 and 2019 is that the value of the regression lines slope both for the pre-monsoon and the post-monsoon increased slightly in 2019 as compared to 2009. This suggests that the overall evaporative regime has become slightly milder and that groundwater is not getting as much evaporated in 2019 as it was in 2009. Another possibility is that, in addition to the rainfall, which is the major recharge source, the Narmada river bringing water from southern Gujarat into north Gujarat could also be contributing to groundwater recharge to a certain extent.

Table 5.1: Statistical description of $\delta^{18}O$, δD, and d-excess of pre-monsoon and post-monsoon shallow GW samples collected during 2019

	Pre-monsoon			**Post-monsoon**		
	$\delta^{18}O$	δD	d-excess	$\delta^{18}O$	δD	d-excess
Mean	-2.0	-15	1.1	-2.3	-18	0.3
Standard Error	0.1	1	0.3	0.1	1	0.2
Median	-2.0	-15	1.7	-2.2	-17	0.6
Mode	-2.9	-21	5.0	-1.3	-17	1.6
Standard Deviation	1.4	9	5.2	1.3	9	4.0
Range	10.1	61	40.1	8.5	59	27.7
Minimum	-5.8	-43	-29.0	-6.1	-52	-19.5
Maximum	4.3	17	11.1	2.3	7	8.2
Count	262	262	262	262	262	262

Another observation emerging by comparing isotopic values of 2009 and 2019 is that the range of $\delta^{18}O$ and δD values decreased in 2019. In 2009 the Pre-monsoon groundwater samples had a wide range of $\delta^{18}O$ (-5.5‰ to 4.1‰; avg. -1.9 ± 1.6‰) and δD (-36.6‰ to -17.6‰; avg. -14.5 ± 9.5‰) values. Similarly, the post-monsoon groundwater samples in 2009 have a wide range of $\delta^{18}O$ (-9.7‰ to 4.9‰; avg. -2.3 ± 1.6‰) and δD (-77.2‰ to 9.9‰; avg. -17.8 ± 10.8‰) values. Compared to 2009, in 2019, the $\delta^{18}O$ ranges from -5.8‰ to 4.3‰ with an average of -2.0 ± 1.4‰; and δD ranges from -43.0‰ to +17.0‰ with an average of -15.0 ± 9.0‰ in pre-monsoon. The post-monsoon values in 2019 range for $\delta^{18}O$ from -6.1‰ to 2.3‰ with an average of -2.3 ± 1.3‰; and δD ranges from -52.0‰ to +7.0‰ with an average of -18.0 ± 9.0‰. This reduction in the isotopic range in 2019 also supports the possibility that Narmada water transported through the canal is manifested in the change in the isotopic makeup of the groundwater.

- **Spatial variation in $\delta^{18}O$ from 2009-2019**

To discern the changes in groundwater recharge sources and hydrogeological processes concerning groundwater recharge, which might have occurred during the decadal interval from 2009 to 2019, the spatial variation of groundwater $\delta^{18}O$ during the post-monsoon seasons (after groundwater recharge) of 2009 and 2019 are plotted in Fig 5.4. The $\delta^{18}O$-δD regression line for the Narmada main canal water and the bivariant plot of Na/Cl vs electrical conductivity (EC) of groundwater samples collected within the buffer zone (Fig 5.1) of the Narmada main canal are plotted in Fig 5.5. The major observations and inferences drawn based on these two aspects are presented below.

There are three broad regions in Gujarat in which groundwater dynamics seems to have changed from 2009 to 2019. These regions are (1) Coastal Saurashtra; (2) North Gujarat; (3) South Gujarat. These regions have been identified and marked in Fig. 5.4. By comparing Fig 5.4a with 5.4b, it is clearly seen that over a period of one decade from 2009 to 2019, the groundwater in coastal Saurashtra and the eastern part of South Gujarat show a clear isotopic enrichment. The observed isotopic enrichment in groundwater indicates a lowering of groundwater recharge rates in 2019 compared to 2009. The lowering of the relative rate of groundwater replenishment is supported by the fact that the groundwater table has lowered, and groundwater extraction has increased in both these regions. This is also supported by the fact that industrialization and urbanization in both these areas have significantly increased during the last decade, and several commercial establishments and urban centres have come up along the Saurashtra coast and also south Gujarat, which is already known to be a pharmaceutical hub of Gujarat.

In contrast to isotopic enrichment observed in coastal Saurashtra and south Gujarat, the groundwater in north Gujarat shows isotopic depletion in 2019 compared to 2009. This isotopic depletion is more prominently observed on the western side of the Narmada canal. In this part of the region isotopically depleted Narmada canal water is used for agriculture. This water not only recharges the groundwater through irrigation return flow but also causes lower abstraction of groundwater for irrigation. This observation is also supported by the increased groundwater levels and reduced overall draft in north Gujarat [*Bhanja et al.*, 2017]. The combined effect of these could be responsible for the observed isotopic depletion in groundwater in an identified region of North Gujarat.

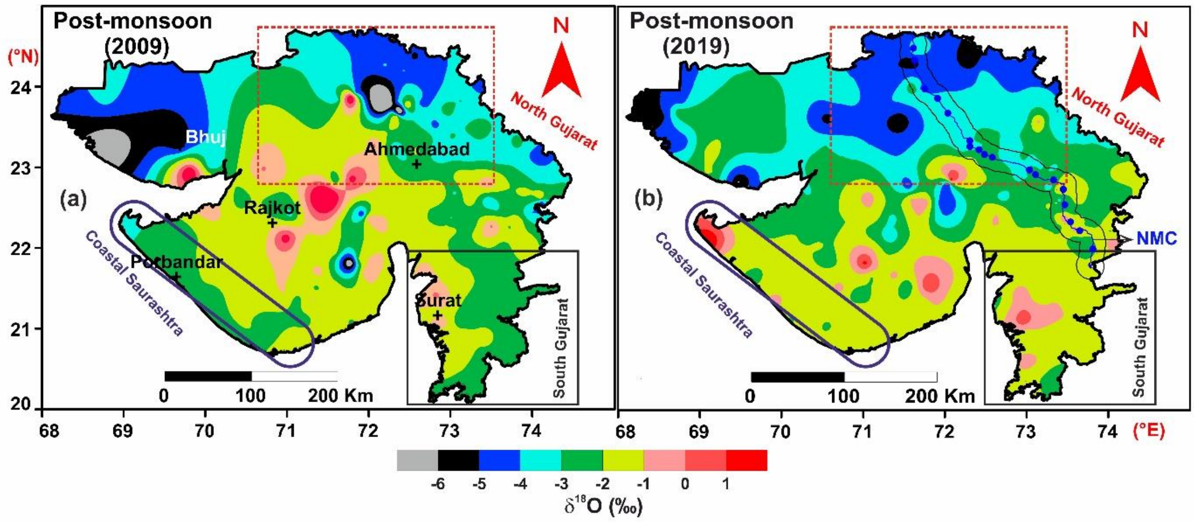

Fig 5.4: (a) Spatial variation of $\delta^{18}O$ in groundwater during post-monsoon season 2009, (b) Spatial variation of $\delta^{18}O$ in groundwater during post-monsoon season 2019. The marked regions are the identified areas where groundwater shows isotopic variation.

While it is difficult to quantify the effect of irrigation return flow on the groundwater availability in the region, there is indirect evidence, which suggests that the residence time of groundwater (aquifer-groundwater interaction time) in the regions fed by the Narmada canal

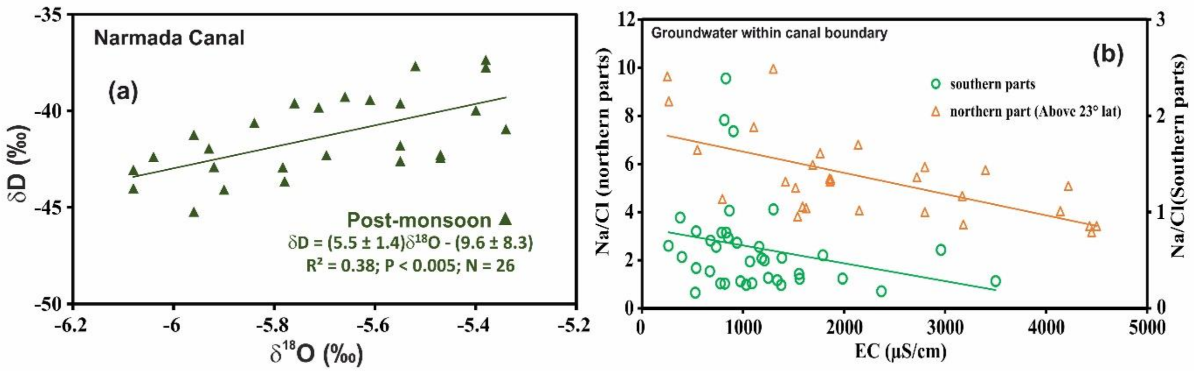

Fig 5.5: The regression line for Narmada main canal water, (b) the bivariant plot (Na/Cl vs EC) for groundwater samples collected within the buffer zone of the Narmada main canal (Fig 5.1).

could be more than those regions which are not fed by Narmada Canal. The bivariant plot of Na/Cl vs EC (Fig. 5.5b) shows that in the northern part of Gujarat, the Na/Cl ratio is higher compared to the southern part, although the alluvial aquifer remains the same (see Fig 5.2). The comparatively higher (>1) Na/Cl ratio is caused by longer residence time and increased silicate chemical weathering due to the interaction between groundwater and the aquifer matrix [*Stallard & Edmond*, 1983].

- **Interaction between shallow and deep GW**

The study area, Gujarat, has different aquifers (Fig 5.2), some of which have been examined to understand the interaction between the shallow and deep groundwater in them. There are sandstone aquifers in Kachchh and Surendranagar districts which are marked by ellipse-1 and ellipse-2 in Fig 5.6. Based on the information provided by the farmers and owners of these tube wells, the drilling depth of the borewells in these aquifers is nearly 700 feet. The depth of slotted angle pipes (screen depths) in these wells is not known. The multilayered alluvial aquifers system extending north-south has a few thousand years to a couple of tens of thousands of years [*Agarwal et al.*, 2006] old groundwater. The balance of dynamic groundwater resources in these aquifers is negative, i.e. extraction is higher than the recharge in the northern part of this aquifer [*Saha & Ray*, 2019], marked by ellipse-3 in Fig 5.6. The drilling depth of the borewells in alluvial aquifers ranges from 600 to 1000 feet. The basaltic aquifer covers the largest geographical area; the deeper groundwater (up to 800 feet) is taped in some parts of these aquifers marked by ellipse-4 in Fig 5.6.

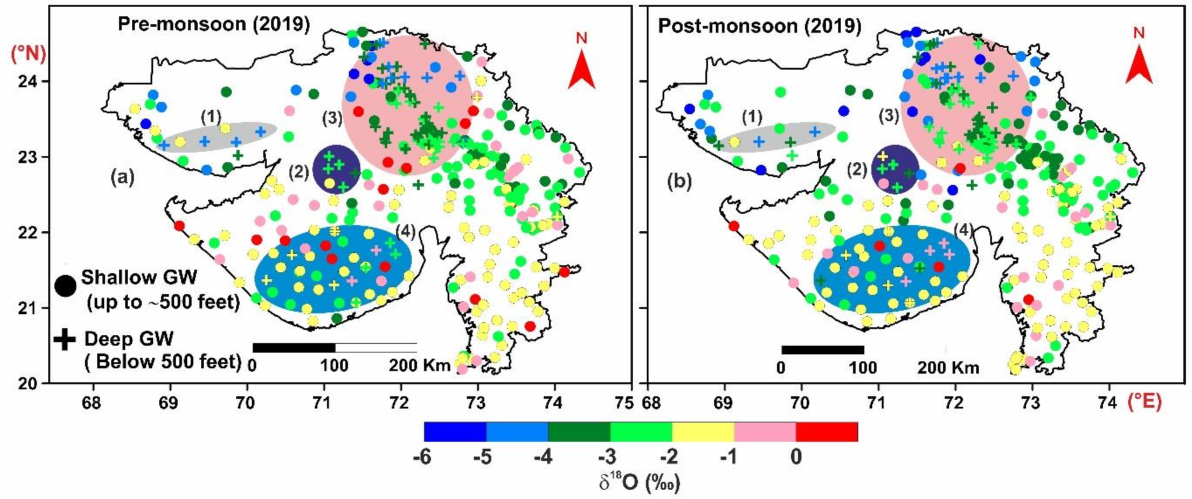

Fig 5.6: Bubble plot of shallow and deep groundwater for (a) pre-monsoon and (b) post-monsoon seasons. The marked regions are examined to understand the interaction between shallow and deep GW.

The $\delta^{18}O$ bubble plot of shallow (< 500 feet) and deep (> 500 feet) groundwater for pre-monsoon and post-monsoon seasons are given in Fig 5.6a and b. The deeper groundwater present in sandstone aquifers is isotopically lighter compared to shallow groundwater, and from pre-monsoon to post-monsoon, some of the borewells show enrichment in $\delta^{18}O$. This suggests that during the post-monsoon season, the contribution of shallow groundwater is more in the mixed water column of deeper wells. The deeper groundwater present in alluvial aquifers of northern Gujarat (ellipse-3) do not show any seasonal change. Although the deeper GW shows nearly 2‰ depletion from south to north in north Gujarat (ellipse-3) although the climate remains the same, this suggests that the groundwater recharge zone is different within the north Gujarat alluvial aquifers. The groundwater present in the basaltic aquifer, marked by ellipse-4, has a seasonal variation in shallow and deep GW. The variation is neither unidirectional nor the same for two different groundwater masses, which indicates that recharge sources and processes are different within the marked area.

5.4 Conclusion

This study used the variation in the isotopic composition of shallow groundwater over a period of a decade between 2009 and 2019, the isotopic composition of shallow and deep groundwater, and the Narmada canal water to find out the change in groundwater recharge sources; the interaction between shallow and deep groundwater; and the effect of the canal on groundwater. Groundwater in this area shows a slight increase in the $\delta^{18}O$-δD regression line slope for the same seasons between 2009 and 2019, indicating that the evaporative regime in this region has become slightly milder over a period of one decade from 2009 to 2019. Spatially variability in $\delta^{18}O$ during this time interval suggests that coastal Saurashtra and the eastern part of South Gujarat are negatively impacted in terms of recharge rate, while the impact of the Narmada canal in groundwater is visible in Northern Gujarat. The deeper groundwater present in the study area has a distinct isotopic composition compared to the shallow groundwater. This seasonal variability in the isotopic composition of deeper groundwater in ellipse-1 (Kachchh) and 2 (Surendranagar) indicates the seasonal influence of shallow groundwater in deeper wells while in northern Gujarat isotopic composition of deeper groundwater suggests the different recharge zones.

Chapter 6

Groundwater dynamics in coastal southwestern India (Kerala)

6.1 Introduction

Despite a high annual average rainfall (~3060 mm), Kerala, a coastal state of India, is a prominent water-stressed region [*Varma*, 2017]. This is primarily due to hydrogeological reasons compounded by the high population density, agrarian economy, impacts of climate change, and loss of freshwater as submarine groundwater discharge. A few studies were carried out in some of the river basins to understand surface water groundwater interaction and their contribution to groundwater recharge [*Kumar, U S et al.*, 2008; *Hameed et al.*, 2015; *Saranya et al.*, 2020; *Swetha et al.*, 2020] but detailed understanding of processes governing groundwater recharge, the effect of dual monsoon on groundwater recharge, and their contribution are lacking. The present study will give extensive geographical coverage (38863 km^2) of isotope characterisation of groundwater for pre-monsoon and post-monsoon seasons. This characterisation would enable us to understand the groundwater recharge mechanism, the interaction between rainwater/surface water and groundwater, and the identification of sources of groundwater recharge and their contribution. The scientific objectives of the present study are (1) to identify various probable freshwater sources during different seasons (southwest monsoon, and northeast monsoon) which can feed the groundwater and estimate their seasonally varying relative contribution to groundwater recharge; (2) to delineate the areas recharged by NEM rainfall; (3) to estimate the volume of freshwater transported from the land area into the ocean through subsurface pathways.

To achieve these objectives, stable isotopes of oxygen and hydrogen in conjunction with classical geohydrological data are used. Stable isotopes of oxygen (^{16}O, ^{18}O) and hydrogen (^{1}H, ^{2}H or D) in water have been used as a tracer to understand the origin of water, groundwater recharge mechanism, surface water groundwater interaction, and to delineate the mixing proportion of different end members [*Deshpande et al.*, 2003; *Deshpande & Gupta*, 2012; *Yeh et al.*, 2014a; *Hameed et al.*, 2015; *Parlov et al.*, 2019]. Investigation of seasonal variation in the isotopic composition of groundwater, with reference to the corresponding variation in the isotopic composition of various probable water sources (rain, river, lakes, seawater), can provide valuable insights into groundwater recharge dynamics and interaction between groundwater and surface water. In this study, the shallow groundwater samples from unconfined aquifers tapping alluvium and laterite formation (maximum water table depth of 20 m bgl) were collected during pre-monsoon and post-monsoon seasons across Kerala under the aegis of the National Programme on Isotope Fingerprinting of Waters of India (IWIN) [*Deshpande & Gupta*, 2008; 2012]. A total of 450 samples were collected (i.e. 225 samples from pre-monsoon and 225 samples from post-monsoon were collected from the same locations).

6.2 Study area

- **Location, Physiography and Climate**

Situated on the southwestern tip of the Indian peninsula (Fig 6.1), the Indian state of Kerala (8.29º-12.79º N; 74.46º-77.62º E) covers an area of 38863 km^2 (1.2% of India's geographical area) and is home to 36 million people (2.76% of India's population). The state of Kerala is surrounded by the Arabian Sea in the west and the Western Ghats in the east and falls in the tropical monsoonal climate. As per the Climate Change and Disaster Management Report 2017, the temperature is maximum during the summer season (~40°C) and minimum during the winter season (~20°C). Diurnal and seasonal variation in temperature depends on location, height, and proximity to the ocean. Kerala receives a total of ~3060 mm of annual rainfall during three rainy periods (1) South-West Monsoon (SWM; June to September; average ~2049 mm); (2) North-East Monsoon (NEM; October to November; average ~610 mm); and (3) Pre-monsoon seasons (March-May; average ~401 mm),

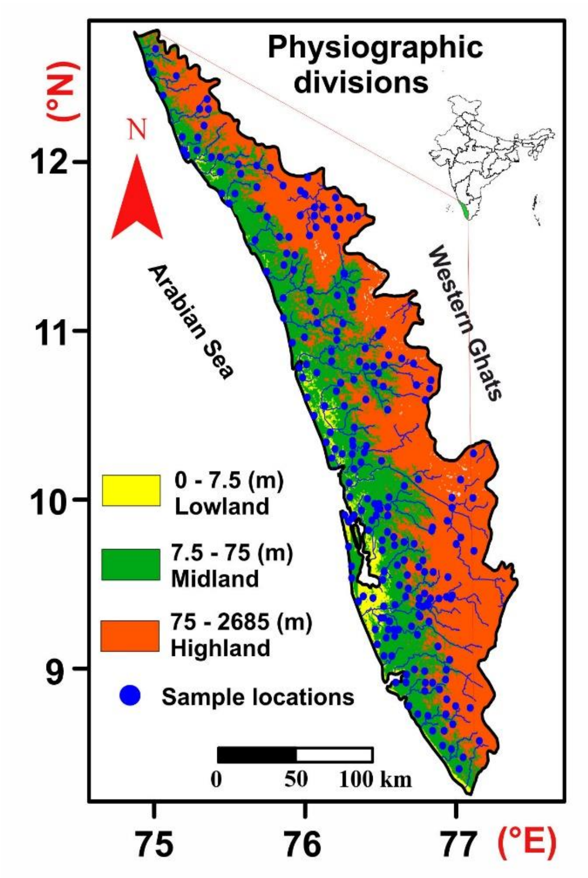

Fig 6.1: Physiographic divisions of the state of Kerala, located in southwestern coastal India. Based on the elevation, it is divided into lowland, midland, and highland; with elevations ranging from sea level to 2682m. Blue circles represent the sample locations.

with highest (70%) contribution from SWM (Dynamic Groundwater Resources of Kerala, 2017). The amount of rainfall varies spatially, with more rainfall in the northern part compared to southern Kerala. Mean monthly relative humidity varies between 55% to 75% *[Nair et al., 2018]*. The above information can be seen in the link below:

(http://www.kerenvis.nic.in/Database/ENVIRONMENT_824.aspx).

(https://spb.kerala.gov.in/sites/default/files/inline-files/1.10Climate%20Change.pdf).

Physiographically the state is divided into three broad units [*Sujith*, 2016] ((Fig 6.1) (1) Lowland (altitude: < 7.5 m) covered by the coastal alluvium, having the highest open well density in the country (200/km^2); (2) Midland (altitude: 7.5 to 75 m) covered by laterite; (3) Highland (altitude: 75 to 2600 m) covered by crystalline and weathered crystalline rocks. Besides these three physiographic zones, a Foothill zone is covered by weathered crystalline rocks.

- **Hydrogeology**

Kerala has four hydrogeologically different aquifers (Fig 6.2a), namely (1) crystalline or hard rock aquifers, (2) Laterite aquifers, (3) Alluvial aquifers, and (4) Tertiary rock aquifers [*Swetha et al.*, 2017].

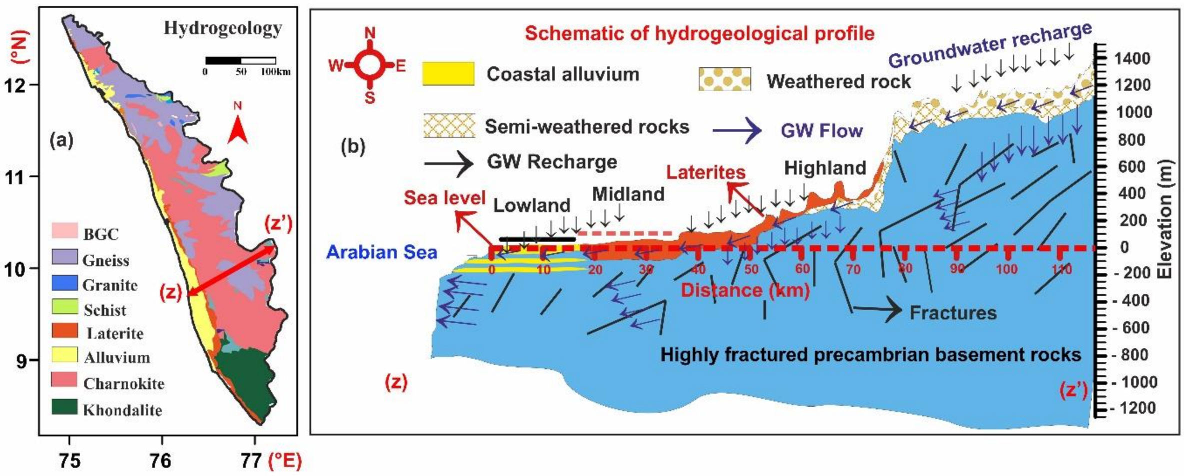

Fig 6.2: (a) Hydrogeological map of Kerala, redrawn from https://indiawris.gov.in/wris/#/ Aquifer. The alluvial and lateritic aquifers run along the west coast in the lowlands. Charnokite constitutes the largest aquifers. In some areas, either Khondalite or the Gneissic aquifers stretch from highland to coast, these all come under crystalline hard rock aquifers (b) Schematic of a hydrogeological profile along the red arrow in fig(a) of the study area, lateral movement of groundwater occurs from shallow as well deeper aquifers because of the higher slope.

Crystalline or hard rock aquifers are mainly composed of Charnokite, Khondalite, and schistose rocks in which Charnokite is the major aquifer and covers 41% of the geographical area of Kerala [*Nandakumaran & Balakrishnan*, 2020]. These rocks are caped with weathered and semi-weathered materials and form a potential aquifer in highland areas. These weathered materials are highly permeable and form shallow aquifers favouring the lateral and vertical movement of groundwater present in phreatic conditions Fig (6.2b) [*Jesiya & Gopinath*, 2019]. Groundwater in these aquifers is present from 2 to 16 m bgl, and the yield of these shallow aquifers is 2 to 10 m^3 per day (Dynamic Groundwater Resources of Kerala 2013). These hard rock aquifers with highly irregular fractures are hydraulically connected with upper aquifers on the regional scale [*Varma*, 2017; *Nandakumaran & Balakrishnan*, 2020].

Laterite is widely distributed in the study area, but it forms a potential aquifer in lowland and midland areas. Lateritic aquifers cover approximately 3.7% of the geographical area of Kerala. The thickness of these aquifers reaches up to 30 m; moreover, in some of the boreholes, it goes up to 74 m. These aquifers have very high porosity, due to which water can easily drain from them. The water level varies from 2 to 25 m bgl, and the yield of these aquifers varies from 0.5 to 30 m^3 per day.

The Alluvial aquifers lie along the coastal area of the state and form a potential aquifer whose thickness goes up to 100 m. Groundwater is present in phreatic and semi-confined conditions, with the depth of water varying from 1 to 6 m bgl. The yield of these aquifers varies from 5 to 35 m^3 per day [*Varma*, 2017]. The alluvial and lateritic aquifers form the coastal aquifers and cover the low and midland region in which the density of both the population as well as open wells (200 to 150 open wells per km^2), are very high. The groundwater is extracted for drinking and irrigation purposes from these aquifers.

The Tertiary rock aquifers lie in the SW coastal part of the state. The groundwater occurs in the phreatic condition in the shallow part, while at a deeper level, groundwater occurs in semiconfined and confined conditions. The yield of these aquifers varies from 0.5 to 20 m^3 per day, and the water level ranges from 3 to 27 m. The detailed information about the aquifer can be seen in the report (Dynamic Groundwater Resources of Kerala, 2013). All the four aquifers have water present in phreatic, semiconfined and confined conditions at different depths, but this study is based on phreatic water samples where the water table depth varies from less than 1m to 20 m bgl.

6.3 Results and discussion

- **Pre-monsoon signatures**

The isotopic composition of pre-monsoon groundwater samples (N = 225) ranges from -5.4‰ to -1.1‰ in $\delta^{18}O$ with an average of -3.2‰; from -32.0‰ to -3.0‰ in δD with an average of -15.0‰; and from 3.0‰ to 15.0‰ in d-excess with an average of 10.3‰ (Table 6. 1). The least-square linear regression between the δD and $\delta^{18}O$ for pre-monsoon groundwater is plotted in Fig 6.3a and that between the d-excess and $\delta^{18}O$ is plotted in Fig 6.3b. The regression line for δD vs $\delta^{18}O$ of pre-monsoon groundwater samples has a slope of (6.1 ± 0.2) and intercept of (4.3 ± 0.5). The much lower slope and intercept values of δD-$\delta^{18}O$ regression line for groundwater, compared to that for GMWL (Slope = 8; Intercept = 10) and the LMWL (Fig 6.3a; slope = 7.5; intercept = 12), indicate that the pre-monsoon groundwater has undergone substantial evaporation through capillary fringe zone because the water table is very shallow in this region even during pre-monsoon season.

Table 6.1: Statistical details of the pre-monsoon GW, post-monsoon GW and rainwater samples along with slope and intercept of regression lines. The amount of rainfall and its isotopic composition were taken from (http://hdl.handle.net/10603/132722).

	Post-monsoon (GW)			**Pre-monsoon (GW)**			**NEM**			**May-October Rain**		
	$\delta^{18}O$ (‰)	**δD (‰)**	**d-excess (‰)**	**$\delta^{18}O$ (‰)**	**δD (‰)**	**d-excess (‰)**	**$\delta^{18}O$ (‰)**	**δD (‰)**	**d-excess (‰)**	**$\delta^{18}O$ (‰)**	**δD (‰)**	**d-excess (‰)**
Min	-5.3	-30.0	7.1	-5.4	-32.0	3.0	-10.4	-66.0	10.8	-8.7	-60.0	9.3
Max	-2.2	-7.0	15.6	-1.1	-3.0	15.0	-2.0	-5.0	18.6	-0.8	8.0	18.5
Mean	-3.6	-18.0	10.9	-3.2	-15.0	10.3	-6.0	-34.0	14.5	-3.9	-19.0	12.5
standard deviation	0.5	4.0	1.5	0.7	5.0	2.2	2.3	17.0	2.3	1.8	14.0	2.2
Slope	(6.9 ± 0.2)			(6.1± 0.2)			(7.5 ± 0.2)			(7.7 ± 0.2)		
Intercept	(7.1 ± 0.6)			(4.3 ± 0.5)			(12.0 ± 1.2)			(11.5 ± 0.8)		

It is noteworthy that there is a cluster of pre-monsoon groundwater samples (Fig 6.3a), distinguishable from the rest of the groundwater samples due to their enriched $\delta^{18}O$ (>-2.5‰) and lower d-excess (< 8‰). Some of these samples (8 samples) are located in the coastal region (samples represented in a diamond shape in inset Fig 6.3b). These locations are the probable sites of seawater intrusion as seawater in this region has $\delta^{18}O$ values of 0‰ to 0.8‰

[*Deshpande et al.*, 2013]. The remaining 8 samples are lying in the inland region (Fig 6.3b) where the observed enriched isotopic signatures are only possible when they are directly recharged through evaporated surface water bodies (lakes, ponds or reservoirs) [*Jasechko*, 2019; *Saranya et al.*, 2020].

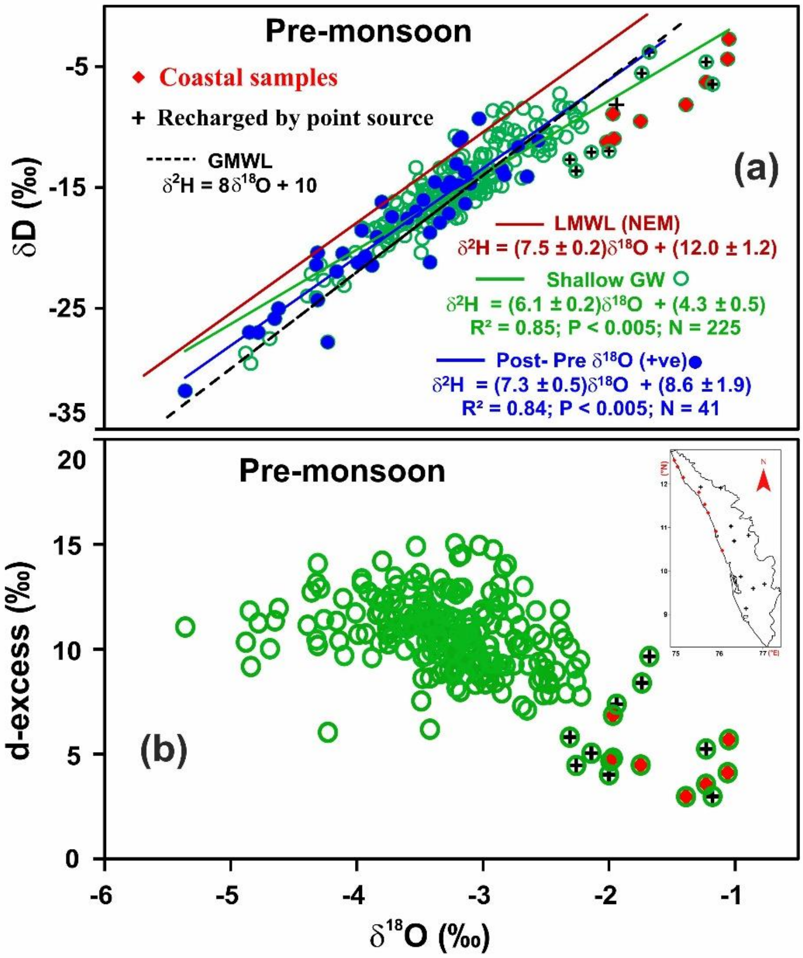

Fig 6.3:(a) The plot of δD vs. $\delta^{18}O$ (b) and d-excess vs. $\delta^{18}O$ of pre-monsoon groundwater and LMWL. The isotopic data of Northeast monsoon rainfall (NEM) are from (http://hdl.handle.net/10603/132722). Samples with conspicuous isotopic composition (enriched $\delta^{18}O$ and lower d-excess) are identified by diamond and plus signs. These signatures are associated with groundwater recharge from an isotopically enriched source which would be the seawater (samples represent by diamond, their location can be seen in inset Fig 6.3b) or highly evaporated surface water (samples represented by plus sign and their location can be seen in Fig 6.3b).

The pre-monsoon groundwater samples are influenced by the NEM rainfall from November to December (~ 600mm). Therefore, a comparison of the isotopic composition of pre-monsoon groundwater with NEM rainfall can provide useful information about the recharging source water, and also spatially varying recharge characteristics. The isotopic composition of NEM rainwater samples ranges in $\delta^{18}O$ from -10.4‰ to -2.0‰ with an amount weighted average of -6.0‰; in δD from -66.0‰ to -5.0‰ with an amount weighted of -34.0‰; and in d-excess from 10.8‰ to 18.6‰ with an amount weighted value of 14.5‰ (Table 6.1). To understand the interaction between NEM rainfall and pre-monsoon groundwater, a linear regression between the δD and δ^{18}O for pre-monsoon groundwater has been compared with LMWL for NEM rainfall in Fig 6.3a. The LMWL for NEM rainfall has a slope of (7.5 ± 0.2) and an intercept of (12.0 ± 1.2).

A comparison of isotopic values and regression line slopes for pre-monsoon groundwater and NEM rainfall (Fig 6.3a and Table 6.1) reveals that the average isotopic composition of pre-monsoon groundwater (δ^{18}O: -3.2‰; δD: -15.0‰) is about 2.8‰ enriched in δ^{18}O and about 19.0 ‰ enriched in δD compared to the NEM rainwater (δ^{18}O: -6.0 ‰; δD: -34.0‰). Thus, isotopically depleted NEM rainwater does not seem to impart depleted isotopic character to groundwater. Further, the δD-δ^{18}O regression line for pre-monsoon groundwater samples has a slope (6.1 ± 0.2) and intercept (4.3 ± 0.5) smaller than those for NEM rainfall (slope: 7.5 ± 0.2; intercept: 12.0 ± 1.2). These two observations indicate that groundwater recharge from isotopically depleted NEM rainfall is limited and insufficient to isotopically deplete the pre-monsoon groundwater and erase its evaporative signatures from the entire region. It is, therefore, inferred that NEM rainfall is not contributing substantially to pre-monsoon groundwater.

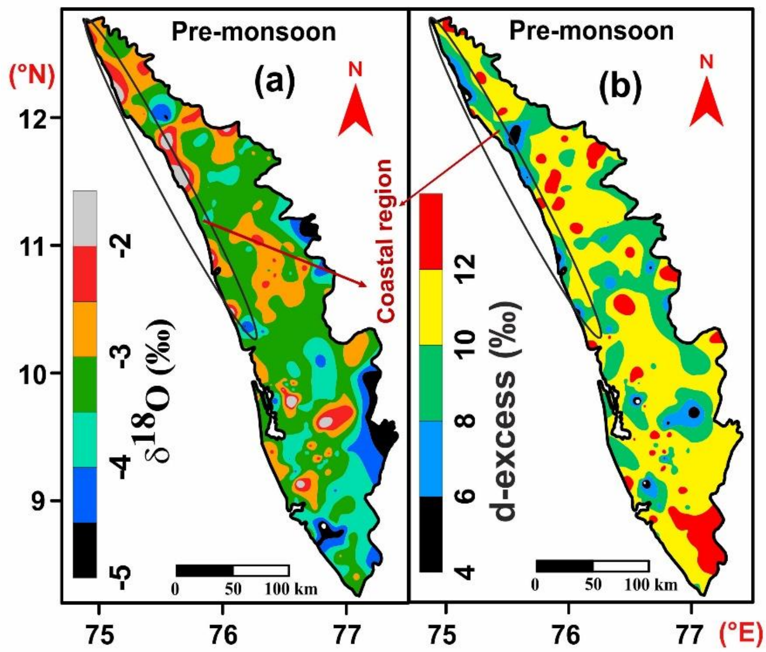

Fig 6. 4:(a) Spatial distribution of δ^{18}O (b) and d-excess in pre-monsoon groundwater samples of Kerala. The sample locations are marked in Fig 6.1.

The spatial distribution of δ^{18}O and d-excess in pre-monsoon groundwater samples in Kerala is shown in Fig 6.4a and b, respectively. The groundwater with enriched values of δ^{18}O (-1.5‰ to -2.5‰) and lower value of d-excess (4.0‰ to 8.0‰) occurs along the coast north of 10º latitude. These enriched δ^{18}O and lower d-excess values of groundwater in certain coastal patches north of 10º latitude are possibly affected by seawater intrusion. This kind of signature was also found in the coastal area of different parts of the world [*Gonfiantini & Araguás*, 1988; *Edmunds & Droubi*, 1998; *Carreira et al.*, 2014; *Carreira et al.*, 2018]. Seawater intrusion has also been reported earlier in these regions based on chemical characteristics [*Shaji et al.*, 2009; *Prasanth et al.*, 2012; *Kumar, K A et al.*, 2015; *Sajeena et al.*, 2020; *Saranya et al.*, 2020]. The possible reason why seawater intrusion is noticed prominently north of 10° latitude is that NEM rainfall is more prominent in the south of 10° latitude and influences the groundwater more significantly there [*Sreekala et al.*, 2012]. The higher d-excess (>12‰) values in groundwater are observed in the southern part (below 10º latitude) of Kerala and in some patches in the northern part. The only way in which pre-monsoon groundwater can have higher values of d-excess compared to surrounding areas is preferential recharge by the NEM rainfall [*Sukhija et al.*, 1996; *Gupta & Deshpande*, 2003; *Agarwal et al.*, 2006]. This indicates that NEM rainfall is more prominently affecting groundwater south of 10° latitude resulting in higher d-excess and depleted isotopic values in groundwater. The signatures of NEM are also recorded in the depleted $\delta^{18}O$ (< -4.5‰) and comparatively higher d-excess (>10‰) values in the groundwaters in the higher elevation areas in the eastern margin of Kerala (Fig 6.4a).

- **4.2. Post-monsoon signatures**

The isotopic composition of post-monsoon groundwater samples (N = 225) ranges in $\delta^{18}O$ from -5.3‰ to -2.2‰ with an average of -3.6‰; in δD from -30.0‰ to -7.0‰ with an average of -18.0‰; and in d-excess from 7.1‰ to 15.6‰ with an average of 10.9‰ (Table 6.1). The regression line between the δD and $\delta^{18}O$ for post-monsoon groundwater is plotted in Fig 6.5a, and that between the d-excess and $\delta^{18}O$ is plotted in Fig 6.5b. The regression line for δD vs $\delta^{18}O$ of post-monsoon groundwater samples has a slope of (6.9 ± 0.2) and an intercept of (7.1 ± 0.6).

It is noteworthy that the cluster of enriched $\delta^{18}O$ and lower d-excess groundwater samples observed in the coastal and inland region in the pre-monsoon season (Fig 6.3a and b) is not so distinctly visible during the post-monsoon season (Fig 6.5a and b). This suggests that the enriched isotopic character of pre-monsoon groundwater samples due to marine ingression in the coastal area and preferential recharge from evaporated surface water bodies is completely changed in the post-monsoon season due to fresh recharge.

During the period between collection of the pre-monsoon groundwater sample in April and collection of the post-monsoon groundwater sample in November, the groundwater is

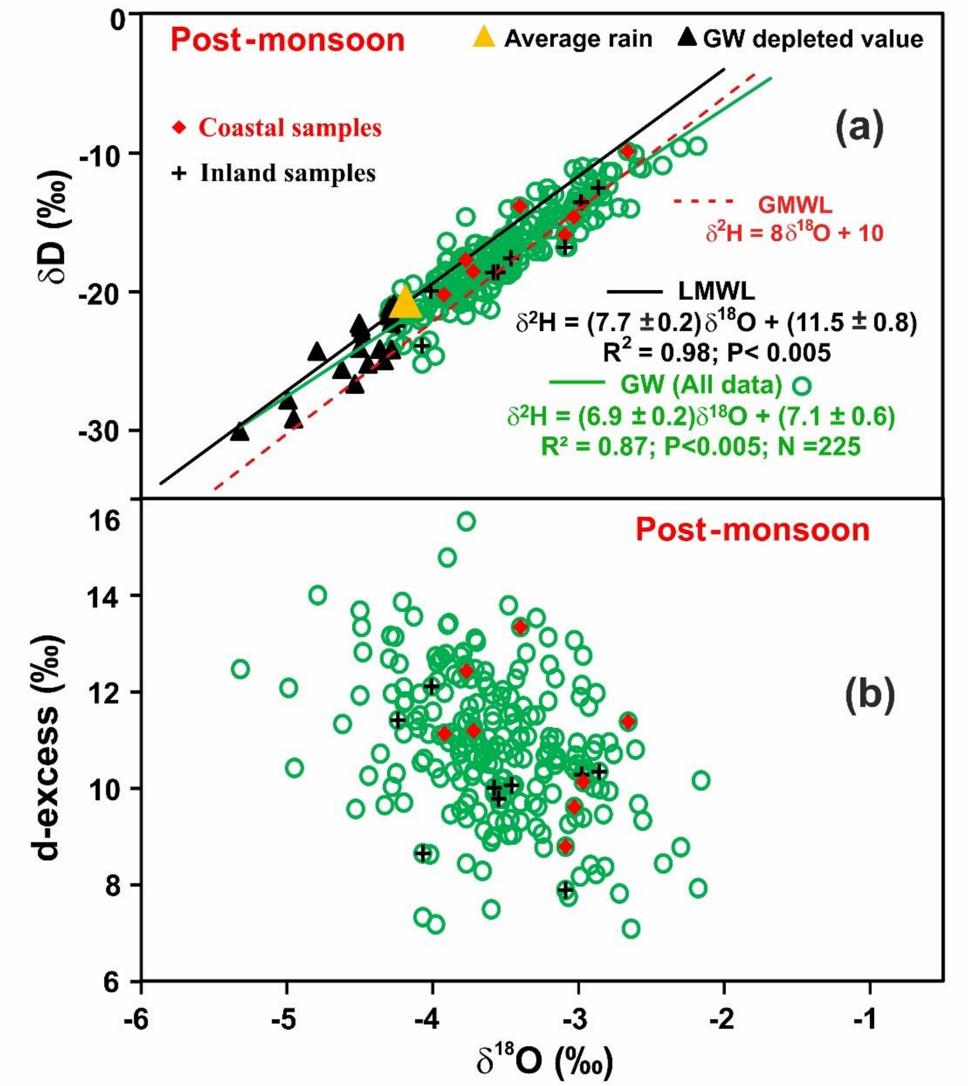

Fig 6.5: The plot of δD vs. δ^{18}O (a) and d-excess vs. δ^{18}O (b) of post-monsoon groundwater and LMWL for Post-monsoon rainwater samples along with GMWL. The samples having enriched δ^{18}O and lower d-excess during pre-monsoon (Diamond and Plus shape samples) show depleted δ^{18}O and higher d-excess in the post-monsoon season. This signature suggests the seasonal freshwater influx during the monsoon season.

likely to be recharged by the variable magnitude of rainfall received during pre-monsoon showers (May), southwest monsoon (June-September), and retreating monsoon (October). Therefore, a comparison of the isotopic composition of post-monsoon groundwater with that of rainwater from May to October can provide useful information about the possible recharge source water and spatially variable recharge characteristics.

The amount of rainfall and the average isotopic composition of these three phases of rainfall are distinctly different. The amount of rainfall and the average $\delta^{18}O$ and δD values for three different rainy phases of the year 2010 are respectively: ~ 143 mm, $\delta^{18}O$: -1.7‰ and δD: -0.7‰ for pre-monsoon showers; ~1742 mm, $\delta^{18}O$: -4.0‰ and δD: -20.0 ‰ for the southwest monsoon; and ~500mm, $\delta^{18}O$: -5.6‰ and δD: -29.0‰ for retreating monsoon rainfall in October. Overall, from May to October, the study area received ~2385 mm of rainfall, having it's $\delta^{18}O$ values ranging from -8.7‰ to -0.8‰, with an amount weighted average of -4.0‰, and δD values ranging from -60.0‰ to 8.0‰ with an amount weighted average of -19.0‰. The d-excess of rain from May to October varied from 9.3‰ to 18.5‰ with an amount-weighted average value of 12.8‰. The LMWL for rainwater during May to October months has a slope of (7.7 ± 0.2) and an intercept of (11.5 ± 0.8) (Fig 6.5a).

It is seen (Table 6.1) that the average values of the isotopic composition of post-monsoon groundwater ($\delta^{18}O$ = -3.6‰; δD = -18.0‰) is depleted compared to pre-monsoon showers ($\delta^{18}O$ = -1.7‰; δD = -0.7‰); only marginally enriched compared to southwest monsoon rains ($\delta^{18}O$ = -4.0‰; δD = -20.0‰); and significantly enriched compared to retreating monsoon rains ($\delta^{18}O$ = -5.6‰; δD = -29.0‰). Overall, the post-monsoon groundwater ($\delta^{18}O$: -3.6‰; δD -18.0‰) is enriched by 0.4‰ in $\delta^{18}O$ and 1.0 ‰ in δD compared to average rain from May to October ($\delta^{18}O$: -4.0‰; δD: -19.0‰). On the other hand, post-monsoon groundwater has become isotopically lighter compared to pre-monsoon groundwater ($\delta^{18}O$: -3.2‰; δD: -15.0‰).

It is seen from Fig 6.5a that δD vs $\delta^{18}O$ regression for post-monsoon groundwater samples has a lower slope (6.9 ± 0.2) than that for the LMWL (7.7 ± 0.2) of the rainfall from May to October, and most of the post-monsoon groundwater samples fall below the LMWL. This indicates post-precipitation evaporative enrichment of infiltrating rainwater and subsequent mixing with a large reservoir of isotopically enriched pre-monsoon groundwater. Normally the groundwater samples everywhere are expected to be slightly enriched in heavier isotopes compared to local rains, due to the evaporation, before and during infiltration. However, a small proportion (~ 6%) of post-monsoon groundwater samples presented by black triangles in Fig 6.5a have isotopically depleted $\delta^{18}O$ values (< 4.0‰) compared to the average local rain from May to October. These samples are mostly located at higher altitudes on the eastern side of the study area; some of the samples are also lying in the midland region (Fig 6.6a). This kind of signature is possible when groundwater is recharged at a higher altitude or recharged by allochthonous water, i.e. water originated at a distal place [*Jasechko*, 2019]. Comparison of isotopic composition and regression line slopes of post-monsoon groundwater with that of rainfall during May to October and the pre-monsoon groundwater suggests that there must be significant recharge by rainfall during May to October which isotopically depletes the enriched pre-monsoon groundwater and brings it almost close to rain's isotopic composition.

The spatial distribution of $\delta^{18}O$ and d-excess in post-monsoon groundwater samples in Kerala is given in Fig 6.6a and b, respectively. The observed spatial variations in the isotopic composition of groundwater are governed by the physiography, isotopic composition of rain, and the aquifer types. The coastal belt (north of 10ºN latitude; Fig 6.4a and b), which had enriched isotopic composition in pre-monsoon ($\delta^{18}O$: -2.5‰ to 1.5‰) and lower d-excess (4‰ to 8‰) is seen to be replaced by freshly recharged isotopically lighter groundwater ($\delta^{18}O$: -4‰ to -3‰; d-excess: 7‰ to 10‰) in Fig 6.6a and b. This indicates that pre-monsoon groundwater is recharged by fresh rainwater from May to October, and the recharge is significant enough to change the isotopic composition of groundwater. Another evidence of groundwater being recharged by local rainfall is the fact that the altitude gradient in the isotopic composition of SWM rainfall and post-monsoon groundwater is comparable.

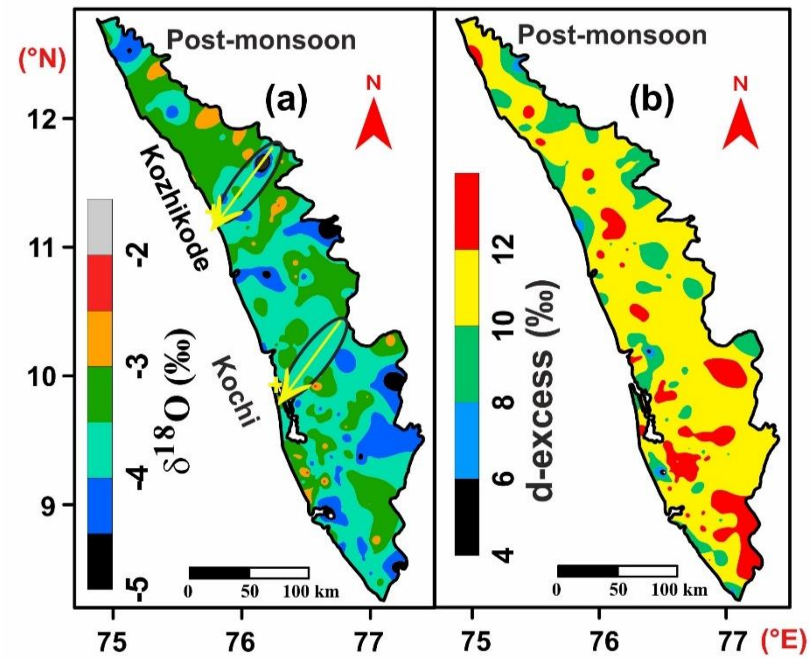

Fig 6.6: Spatial distribution of $\delta^{18}O$ (a) and d-excess (b) in post-monsoon groundwater samples of Kerala. The sample locations are marked in Fig 6.1.

There are, however, two regions marked in Fig 6.6a by an ellipse close to Kozhikode and another close to Kochi in which groundwater does not show any altitude gradient in isotopic composition, although there is a significant variation in altitude ranging from 10m in the coastal area in the west to 1000m in the inland area in the east, and receive a varying amount of rainfall from ~2071mm in the west to ~1613mm in the east, with different isotopic composition due to altitude effect. There is homogenous isotopic composition of groundwater over an altitude range of about 1000m, and comparatively depleted isotopic composition ($\delta^{18}O$: ~ -4.0‰) even in the coastal region in which comparatively enriched isotopic composition is observed in the adjoining region. This homogenous isotopic composition of groundwater in these two identified regions and their depleted value from high altitude to coastal areas indicate the significant inter-aquifer movement of groundwater from higher altitude to a lower altitude. The coastal aquifers may eventually release this regional groundwater flow into the ocean through Submarine Groundwater Discharge (SGD). It is noteworthy that the coastal regions of Kerala have already been identified as SGD sites [*Babu et al.*, 2009; *George et al.*, 2018; *Babu et al.*, 2021; *George et al.*, 2021].

The altitude gradient in $\delta^{18}O$ and δD for post-monsoon groundwater for Kerala is plotted in Fig 6.7a and b respectively. The altitude of groundwater sampling locations varies from 10m to 1200m, but most of the locations are below 600m altitudes, and only a few locations are above 600m. Therefore, for plotting the altitude gradient in isotopic composition, average $\delta^{18}O$ and δD for all groundwater samples within successive intervals of 100m have been considered up to the altitude of 600m and thereafter, up to 1200m all the available samples have been considered. It is seen from Fig 6.7a and b that there is a depletion of 0.1‰ in $\delta^{18}O$ and 0.9‰ in δD per 100m rise in elevation. This observed altitude effect in isotopic composition in groundwater closely resembles the altitude effect in rain reported earlier by *Resmi et al.* [2016] in the study area (0.1‰ for $\delta^{18}O$ and 0.8‰ for δD per 100m rise), is observation supports the inference that post-monsoon groundwater is recharged by local rains.

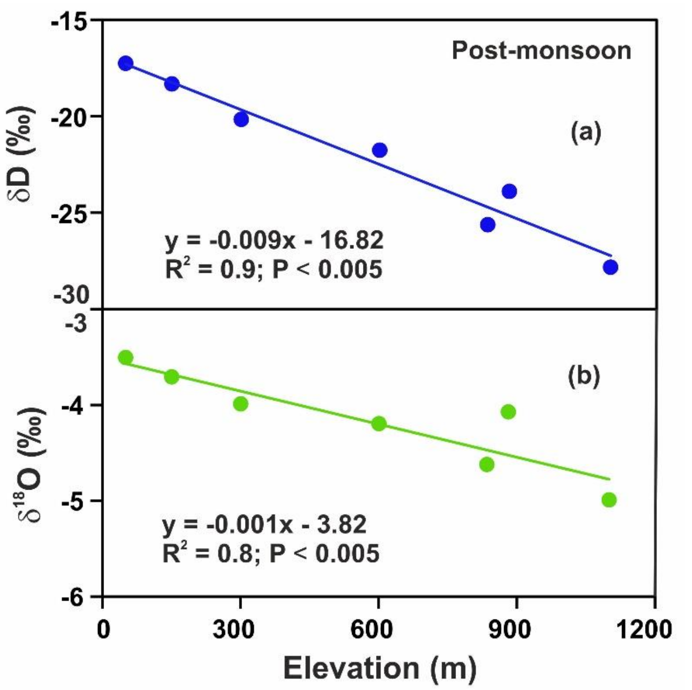

Fig 6.7: Altitudinal variation in (a) δD and (b) $\delta^{18}O$ of groundwater samples. Each point up to 600m altitudes is an average value of all samples around 100m interval. All three samples are plotted beyond 600m altitudes.

- **Temporal variation in $\delta^{18}O$**

From the foregoing, it is clear that there is a noticeable difference between the isotopic composition of pre-monsoon and post-monsoon groundwater (Table 6.1). Also, there is a significant difference between the isotopic composition of NEM rainfall and the rainfall from May to October, which affects the pre-monsoon and post-monsoon groundwater respectively (Table 6.1). In view of the above seasonally different isotopic character, the isotopic separation ($\Delta\delta = \delta_{post\text{-}monsoon} - \delta_{pre\text{-}monsoon}$)between post-monsoon and pre-monsoon groundwater can provide geographical information about areas with relatively dominant recharge by NEM rainfall vis-a-vis rainfall from May to October. The +ve values of $\Delta\delta$ signify groundwater recharges in the pre-monsoon season from isotopically depleted water compared to the post-monsoon groundwater, and such depleted source is the NEM rainfall in the region. The -ve values of $\Delta\delta$ signify the recharge of groundwater from isotopically depleted sources compared to pre-monsoon groundwater which is the rainfall that occurs during the SWM season. The geographical distribution of $\Delta\delta^{18}O$ is shown in Fig 6.8. It is seen that groundwater is only about 11% of the geographical area is recharged dominantly by NEM rainfall (or more correctly, the rainfall during November till March) although the entire region receives rainfall during NEM. Groundwater in the rest 63% of the geographical area seems to be recharged primarily by the SWM rainfall (or more correctly rainfall from May to October). This information is very useful for the assessment of the geographically different impact of monsoon performance on agriculture and other economic activities.

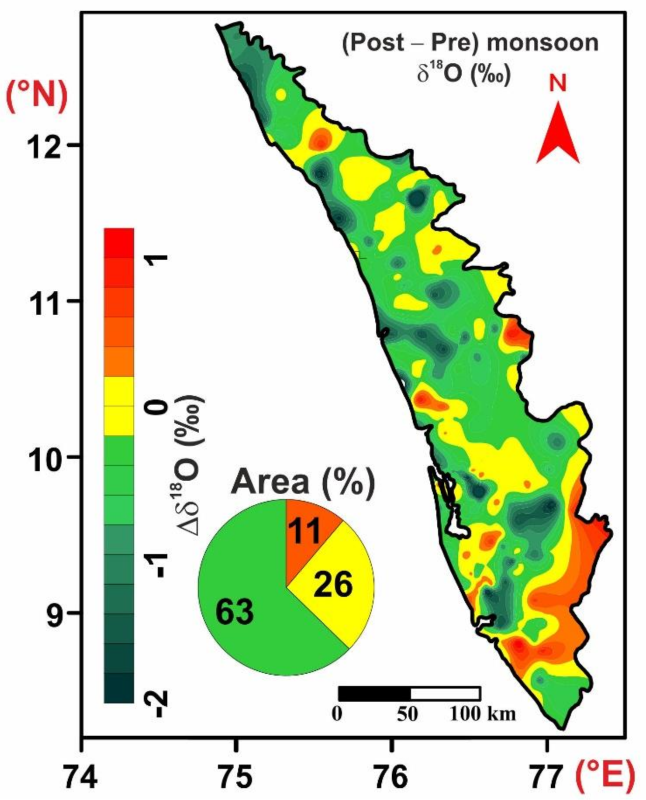

Fig 6.8: Seasonal variation in $\delta^{18}O$ plotted in terms of the isotopic difference between post-monsoon and pre-monsoon samples. Groundwater in ~11% of the geographical area is additionally recharged by NEM rainfall (post-pre difference >0.2‰), besides the monsoonal rainfall which affects the entire study area.

Comparison (Table 6.1) of the relative isotopic difference between; (1) the pre-monsoon and post-monsoon groundwater; (2) the two types of seasonal rainwaters; and (3) the groundwater and the corresponding seasonal rainwater feeding to it reveals that there is a significant difference between the isotopic composition of NEM rainfall and SWM rainfall, and both the pre-monsoon and post-monsoon groundwater has isotopic character closer to SWM rainfall. Thus, groundwater in Kerala is predominantly recharged by SWM. However, NEM rainfall does deplete the pre-monsoon groundwater, which indicates that it does certainly contribute to groundwater to a limited extent.

This seasonal isotopic difference in groundwater and rainfall, in conjunction with other hydrogeological data, has been advantageously used to estimate the volume of groundwater recharge as a percentage of rainfall, and also to understand the seasonally varying groundwater dynamics.

- **Estimation of groundwater recharge from rainfall**

Kerala receives ~3060 mm of rainfall (Groundwater Resources of Kerala, 2017, https://groundwater.kerala.gov.in/wp-content/uploads/2020/07/Dynamic-GW-Resources-of-Kerala-as-in-March-2017-Modified-18-04-2019.pdf) annually of which ~78% (2385mm) occurs from May to October 2010. From the similarity between the isotopic composition of post-monsoon groundwater and rainwater (May-October), it is evident that rainwater is the dominant source of groundwater recharge. A mixing model involving two components (pre-monsoon groundwater and rain during May-October) has been used in the following to estimate the contribution of rain to groundwater recharge in different physiographic divisions (Lowland, Midland, and Highland). The isotopic mass balance equations are:

$$\delta_{pre}\, M_{pre} + \delta_{rain}\, M_{rain} = \delta_{post} \; \dots\dots\dots\dots\dots.. \; Eq. 1$$

$$Where$$

$$M_{pre} + M_{rain} = 1 \dots\dots\dots\dots\dots. Eq. 2$$

Where δ_{pre} is the $\delta^{18}O$ of pre-monsoon groundwater and M_{pre} is the fraction of pre-monsoon groundwater, δ_{rain} is the $\delta^{18}O$ of rainwater from May to October and M_{rain} is the fraction of rainfall, δ_{post} is the $\delta^{18}O$ of the post-monsoon groundwater i.e. admixture of pre-monsoon groundwater and the rainfall. From the above equations, the percentage contribution of rainwater in post-monsoon groundwater recharge can be estimated by:

$$\text{Rainwater contribution in (\%)} = \left\{\frac{\delta_{post} - \delta_{pre}}{\delta_{rain} - \delta_{pre}}\right\} \times 100 \ldots\ldots\ldots . Eq. 3$$

From the earlier description of physiography, it is obvious that rainwater contribution to post-monsoon groundwater recharge will vary physiographically. This is because, in high-altitude areas (i.e. in highlands), the rainwater quickly drains down the slope and contributes relatively less to groundwater recharge. Conversely, in the lowland area towards the coastal belt, the rainwater contribution can be expected to be more. The end member $\delta^{18}O$ values (Table 6.2) of pre-monsoon and post-monsoon groundwater for three physiographic divisions have been considered based on their geographical distribution. The end member $\delta^{18}O$ values of rainfall from May to October in three physiographic divisions have been taken from (http://hdl.handle.net/10603/132722). The uncertainty analyses on the estimated rainfall contribution have been done using the formulations of *Genereux* [1998]. The uncertainty in the estimated recharge contribution from rainfall is given in (Table 6.2).

Table 6.2: The $\delta^{18}O$ end-member values of groundwater and rainwater in three physiographic divisions and the percentage contribution of rain to groundwater recharge are estimated by a two-component mixing model.

End members	**Physiographic Divisions**		
	Lowland	**Midland**	**Highland**
Pre-monsoon (GW) $\delta_{pre}{}^{18}O$ (‰)	-3.1	-3.2	-3.3
Rain (May-October) $\delta_{rain}{}^{18}O$ (‰)	-4.0	-4.2	-4.5
Post-monsoon (GW) $\delta_{post}{}^{18}O$ (‰)	-3.5	-3.5	-3.6
Contribution of rain in GW recharge (%)	45.0	30.0	25.0
Uncertainty values (%) using formulations of Genereux, (1998)	±13	±12	±10

The results of the two-component mixing model (Table 6.2) reveal that the percentage contributions of rain in recharging the post-monsoon groundwater in different physiographic divisions are different. Although the rainfall amount is maximum in the highland region the relative contribution of rain to post-monsoon groundwater recharge is minimum (25% rain; 75% pre-monsoon groundwater) due to the draining of rainwater down the slope. On the other hand, the lowland area receives a maximum relative contribution of rainfall (45% recharge from rainwater and 55% pre-monsoon groundwater) to post-monsoon groundwater recharge. The average contribution of rain in groundwater recharge for Kerala (covering lowland, midland, and highland) is 46% (i.e. 46% recharge from rainwater and 54% pre-monsoon groundwater). The reasons behind the unequal recharge in different physiographic divisions are high elevation and steeper slope in the highland region and very gentle slope and more suitable aquifer types in the lowland region.

As reported in the Dynamic groundwater Resources of India [*CGWB, 2011*], the state of Kerala is estimated to receive 4.85 Billion Cubic meters (BCM) of groundwater recharge directly from the rainfall from May to October and about 0.06 BCM of groundwater recharge indirectly from rainfall through temporary storage in lakes and reservoirs, surface water bodies and irrigation return flow. Thus, a total of 4.9 BCM of rainwater from May to October eventually goes underground, which is only 5.3% of the total rainfall (92.7 BCM) from May to October.

From the end-member mixing model, it is known that the rainwater contribution (4.91 BCM) equals 46% of the relative contribution in the mass balance, with the remaining 54% being the pre-monsoon groundwater whose volume works out to be 5.9 BCM. Thus, there is an estimated dynamic groundwater resource of 10.8 BCM (4.9 BCM recharge from rainwater + 5.9 BCM pre-monsoon groundwater) in the post-monsoon month of November for extraction. The annual groundwater extraction, however, is reported to be only 2.9 BCM (Dynamic Ground Water Resources of India, 2011). This implies that of the total 10.8 BCM of the annual replenishable groundwater resource, at least about 2.0 BCM (i.e. 10.8 BCM annual replenishable groundwater resource – 2.9 BCM extraction – 5.9 BCM of residual pre-monsoon groundwater) of groundwater is drained to sea as submarine groundwater discharge from shallow aquifers, or percolates into deeper aquifers, which too eventually drains into the ocean annually. This water constitutes ~18.5% of the annual replenishable groundwater resource and ~41% of the freshwater recharge.

6.4 Conclusion

In spite of receiving substantial rainfall of more than 3000 mm, the region is experiencing water scarcity and related environmental problems. In this backdrop, it is important to understand the overall groundwater dynamics in terms of the interaction between the rainwater and the groundwater, the annual water budget, the local hydrological cycle and the unutilised groundwater lost to the adjoining Arabian Sea through submarine groundwater discharge.

Interpretation of spatio-temporal variation in the oxygen and hydrogen isotopic composition of groundwater in conjunction with associated hydrogeological parameters has yielded new scientific insights which are very important for planning effective water management to tackle the existing and imminent water scarcity. Following are the valuable inferences from this study:

The rainfall during the southwest monsoon and retreating monsoon season is a major source of groundwater recharge in Kerala, accounting for ~46% (4.91 BCM) of freshly recharged groundwater. The volume of fresh recharge varies in different physiographic regions, with a maximum (~2.2 BCM) in the lowland region and a minimum (~1.2 BCM) in the highland region. The midland region accounts for the remaining ~1.5 BCM of annual recharge.

Of the total 10.8 BCM of the annual replenishable groundwater resource, ~ 18.5% is drained to sea as submarine groundwater discharge from a shallow aquifer which is ~41% of the freshwater recharge (4.9 BCM). This unutilised groundwater water, which is lost to the sea as SGD can be a very useful resource of fresh water that can be advantageously utilised. This study has identified two linear geographical belts, with similar isotopic composition from the highlands to the coast, indicating the groundwater recharges at a higher elevation and moves laterally from the highland to the coastal area. The coastal area where these belts intersect with the coastline is the most probable location of SGD. The Coastal area north of 10º N latitude is affected by marine water intrusion during the pre-monsoon season, which however is flushed out, back into the sea, due to the high throughflow of fresh groundwater after monsoonal rainfall. While the groundwater in the entire state of Kerala is recharged by SW monsoonal rainfall, there are specific areas (~11% of total area) in which groundwater is additionally recharged also by the NEM rainfall. These areas in which groundwater is likely to be recharged twice in a year are potential areas where systematic augmented groundwater extraction can be sustained if so planned.

Chapter 7

Seasonal recharge of groundwater and its spatiotemporal variation in central India (Madhya Pradesh)

7.1 Introduction

India is the highest extractor of groundwater in the world, extracting ~250 BCM (Billion Cubic Meters) of groundwater which is ~ 6% of the global extraction (3880 BCM). However, as per UN-Water Report 2022 (https://unesdoc.unesco.org/ark:/48223/pf0000380721), the annual groundwater recharge in India is only ~1% (436 BCM) compared to that of the global (37000 BCM). The groundwater recharge and extraction vary spatially and temporally because of highly seasonal and erratic rainfall patterns (which recharge the groundwater), variation in hydrogeological conditions and heterogeneous distribution of the surface water. Several studies have been carried out in the northern part of India, covering the Indo-Gangetic plains, to understand the surface water groundwater interactions, groundwater recharge, groundwater depletion, and their causes using satellite data and tracer methods [*Rodell et al.*, 2009; *Tiwari et al.*, 2009; *Chen, J et al.*, 2014; *Döll et al.*, 2014; *Long et al.*, 2016]. However, very few studies [*Gupta et al.*, 2005b] have been carried out in central India, which is home to a 70 million population and groundwater is a major source of fulfilling the water demand as per CGWB Report 2020-2021 (http://cgwb.gov.in/GW-Year-Book-State.html). The higher dependency on groundwater leads to overexploitation of dynamic groundwater resources [*Patil et al.*, 2019]. To overcome this situation, it is important to understand the groundwater recharge sources and their spatiotemporal variation.

In the present study, A total of 564 shallow groundwater samples were collected (i.e. 282 in pre-monsoon and 282 in post-monsoon from the same locations) from the state of Madhya Pradesh in central India under the aegis of a multi-institutional collaborative IWIN National Programme [*Deshpande & Gupta*, 2008; 2012] analysed for their oxygen and hydrogen isotopes compositions. The rainwater isotopic data for Jabalpur and Bhopal (located in Madhya Pradesh) were obtained from the doctoral thesis of [*Oza*, 2020]. The specific objective of the present study is to understand the spatiotemporal variation in the isotopic composition of groundwater and its relationship with the SWM rainfall, orography and tectonic framework and groundwater recharge processes in basaltic and sedimentary hard rock settings.

7.2 Study area

- **Location, Physiography, and Climate**

Located in the central part of India (Fig 7.1), the state of Madhya Pradesh lies between 21.06° N to 26.87° N latitude and 74.02° E to 82.80° E longitude. It occupies a geographical area of 308,252 km^2 (~9% of the country's area) and accommodates nearly 70 million people. Most of the State lies on the tableland of Central India, bounded by the Upper Gangetic plains in the north, the Godavari valley in the south, the plains of Gujarat in the west, and the plateau of Bundelkhand and Chhattisgarh in the east. The physiography of the study area is characterised by low hills, extensive plateaus, and river valleys. The study area is traversed by the Vindhyan and the Satpura hill ranges running east to west. Most of the State has an elevation of between 250 to 500 m above MSL. Low-lying areas (Narmada valley) lie between the Vindhyan and the Satpura Range and the northern and eastern sides of the study area. Madhya Pradesh experiences a subtropical climate with a mean annual temperature ranging between 22.5°C to 25°C. The rainfall mainly occurs during SWM, and it is highly heterogeneous, varying from 800 mm (northern and north-western side) to 1800 mm (south and south-east) [*Wani et al.*, 2010; *Kundu et al.*, 2015].

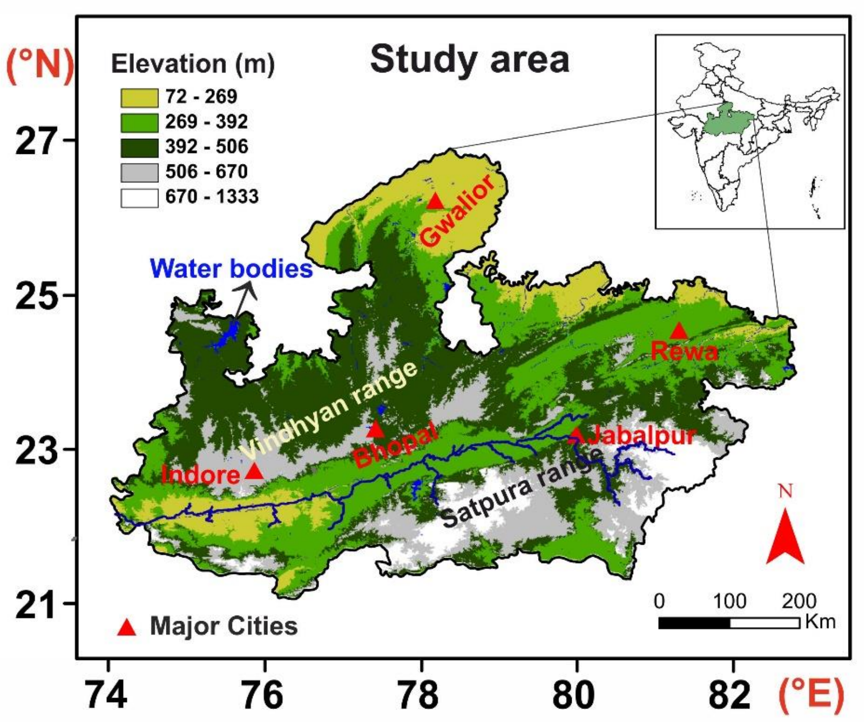

Fig 7.1: Physiography of Madhya Pradesh is characterized by low hills, extensive plateaus, and river valleys. Most of the area is covered by a tableland kind of topography; low lying area lies between the Vindhyan and the Satpura range.

- **Hydrogeology**

The study area has varied hydrogeological settings (Fig 7.2) that include an Alluvial system (8.4% of the geographical area), Sedimentary hard rocks (22.3%), Sedimentary soft rocks (7.2%), Crystalline systems (15.7%) and Volcanic systems (46%) [*Patil et al.*, 2019].

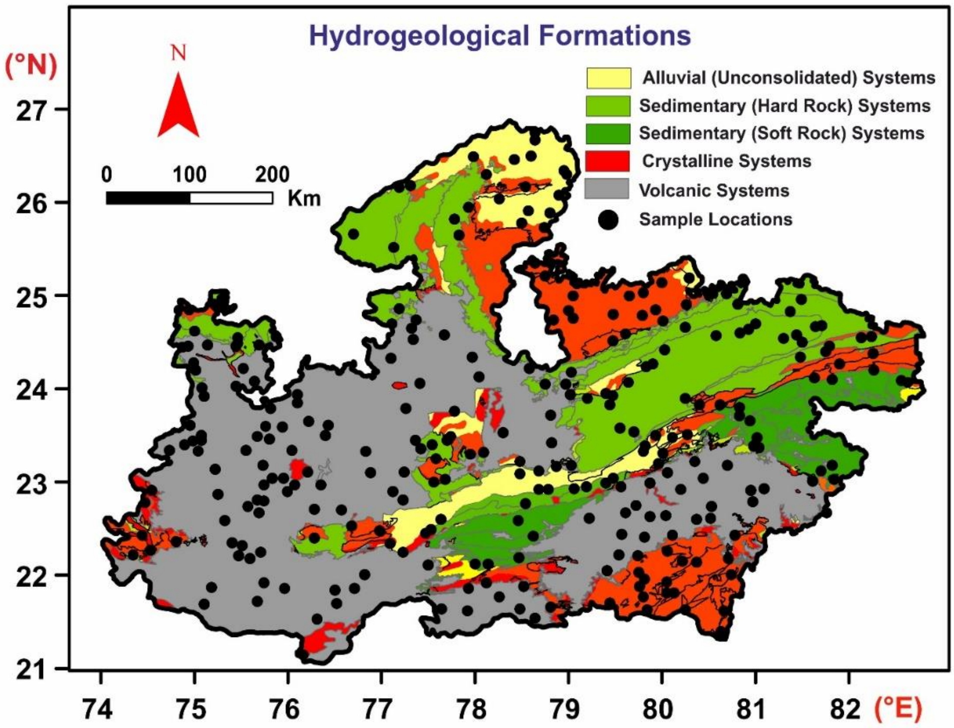

Fig 7.2: This figure represents sample locations and hydrogeological settings in the region. The study area has diverse hydrogeological settings but the volcanic system has the largest areal extent and covers 46% of the study area.

The hydrogeological settings of the region determine the rate of infiltration, recharge, yields of wells, the extent and depth of the aquifers, and the variable consequence of groundwater exploitation, which eventually controls the groundwater potential of the region [*Patil et al.*, 2019]. As per the Groundwater Year Book (2019-2020) published by CGWB (http://cgwb.gov.in/Regions/NCR/Reports/GW_Year_Book_2019-20_MadhyaPradesh.pdf), the upper weathered zone in Basaltic terrain forms moderate to good aquifers where water level varies from 2 to 14 m bgl, hydraulic conductivity and specific yield vary between 5 to 15m/d and 1% to 3% (2 to 30 m^3/hr) respectively, apart from this, other aquifers such as Sedimentary hard rock, Crystalline settings hold water in the weathered zone with almost similar yield (1% to 3%), only alluvial settings form the multilayered aquifers that has higher yield (30-50m^3/hr.). For details on the hydrogeology and groundwater resources of Madhya Pradesh, reference is made to the Groundwater Year Book of Madhya Pradesh 2019-20 (http://cgwb.gov.in/GW-

Assessment/GWR-2020-Reports%20State/2022-03-10GWRA_MP_2020_Final.pdf) and Dynamic Groundwater Resources of Madhya Pradesh (2020) (http://cgwb.gov.in/Regions/NCR/Reports/GW_Year_Book_2019-20_MadhyaPradesh.pdf.) published by the Central Ground Water Board (CGWB), Govt. of India and the Water Resources Department, Govt. of Madhya Pradesh.

- **Backward wind trajectory modelling**

To track the air parcels containing moisture for precipitation in the eastern (Rewa) and western (Indore) half of the study area, backward wind trajectories were analysed using Hybrid Single-Particle Lagrangian Integrated Trajectory (HYSPLIT) model downloaded from http://ready.arl.noaa.gov/HYSPLIT [*Draxler & Rolph*, 2003; *Stein et al.*, 2015]. For each rainy day, four trajectories were generated at every six hours interval for the last 120 hours, each starting at 1500m agl. The converging altitude of 1500m was considered because it is the approximate cloud base height reported around this region [*Deshpande et al.*, 2010; *Oza*, 2020]. Each backword trajectory contained information on five meteorological parameters namely (1) temperature (°C); (2) specific humidity (g/kg); (3) rainfall (mm/h); (4) height (m, agl); and (5) geographical coordinates provided by the HYSPLIT model. The percentage contribution of the sources for each 120 h back trajectory was calculated using the formula given by [*Oza*, 2020] and discussed in the methodology chapter.

7.3 Results and Discussion

- **δ^{18}O and δD regression lines**

A total of 564 groundwater samples were collected from shallow unconfined aquifers from the 282 locations during pre-monsoon (April-May) and post-monsoon (November) seasons for the analysis of its δ^{18}O and δD isotopic composition. During the pre-monsoon season, the δ^{18}O varies from -7.3‰ to 2.9‰ with an average of -3.6‰ and the δD vary from -50.0‰ to 4.0‰ with an average of -27.0‰. Whereas in the post-monsoon season, the δ^{18}O varies from -10.5‰ to 2.1‰ with an average of -4.2‰ and δD vary from -76.0‰ to 3.0‰ with an average of -30.0‰. Thus, the average isotopic composition of post-monsoon shallow groundwater is relatively depleted in heavy isotopes. The d-excess values range from -19.7‰ to 22.2‰ with an average of 2.3‰ for the pre-monsoon season and ranges from -13.4‰ to 15.1‰ with an average of 3.4‰ for the post-monsoon season. The low average values of the δ^{18}O and the δD, and higher values of d-excess during the post-monsoon season indicate that water mass in the aquifer is replenished with isotopically depleted water during the rainy season.

Between the pre-monsoon and post-monsoon seasons, the study area receives rainfall from SWM. The SWM samples were collected from two nearby locations, Bhopal and Jabalpur for the year 2010-2011 as part of the IWIN National Programme [*Oza*, 2020]. The rainfall has a very distinct isotopic character [Rainfall: $\delta^{18}O$: range -14.2‰ to 2.1‰ with an amounted weighted average of -6.4‰; δD: range -99‰ to 19‰ with an amounted weighted average of -43‰; d-excess: range -8‰ to 19‰ with an amounted weighted average of 8‰] compared to the groundwater. The amount weighted average $\delta^{18}O$ of SWM rainfall is highly depleted compared to the average $\delta^{18}O$ of pre-monsoon (-3.6‰) and post-monsoon (-4.2‰) groundwater. From pre-monsoon to post-monsoon, the average $\delta^{18}O$ (-3.6‰ to -4.2‰) of groundwater shifts towards the average value of rain which indicates seasonal recharge of groundwater from SWM rain.

The $\delta^{18}O$-δD regression line for SWM rain and groundwater (both post-monsoon and pre-monsoon) are plotted in Fig (7.3a), and d-excess vs. $\delta^{18}O$ are plotted in Fig (7.3b). The slope of the LMWL is (7.7 ± 0.1), which is close to the slope of GMWL, i.e. 8 [*Craig*, 1961]. Groundwater, both in the pre-monsoon and post-monsoon, has a lower slope compared to LMWL. The pre-monsoon groundwater has a lower slope (5.8 ± 0.1) compared to post-monsoon groundwater (6.5 ± 0.1). The d-excess vs. $\delta^{18}O$ plot for SWM rain shows no trend, and most samples fall in the range between 5‰ to15‰. In contrast, groundwater shows a decreasing trend in both seasons. The lower slope of $\delta^{18}O$ - δD regression line for groundwater combined with the inverse relationship between $\delta^{18}O$ and d-excess suggests significant evaporation of shallow groundwater [*Gupta et al.*, 2005a; *Yeh et al.*, 2014b; *Mao et al.*, 2021]. The higher $\delta^{18}O$-δD regression line slope of post-monsoon groundwater compared to the pre-monsoon groundwater and the inverse relationship between $\delta^{18}O$ and d-excess even during the post-monsoon season indicate a freshwater influx of isotopically lighter SWM rainfall that mixes with the existing large reservoir of isotopically enriched pre-monsoon groundwater.

Groundwater samples identified within ellipses 1 and 2 (Fig 7.3a & 7.3b) show conspicuously enriched and depleted samples, respectively compared to other samples in the same season. The samples in ellipses 1 and 2 geographically correspond with regions 1 and 2 (Fig 7.4a & 7.4b). The ellipse-1 contains mostly pre-monsoon groundwater samples having enriched $\delta^{18}O$ (> -2.0‰) and lower d-excess (< -7‰) values. The enriched groundwater in isolated patches can be ascribed to recharge by point sources such as lakes, ponds or reservoirs, which undergo substantial evaporative isotopic enrichment. The ellipse-2 contains post-monsoon groundwater samples having depleted $\delta^{18}O$ (< -4.5‰) and higher d-excess (> 0‰) compared to other post-monsoon samples. These depleted groundwater samples are ascribable

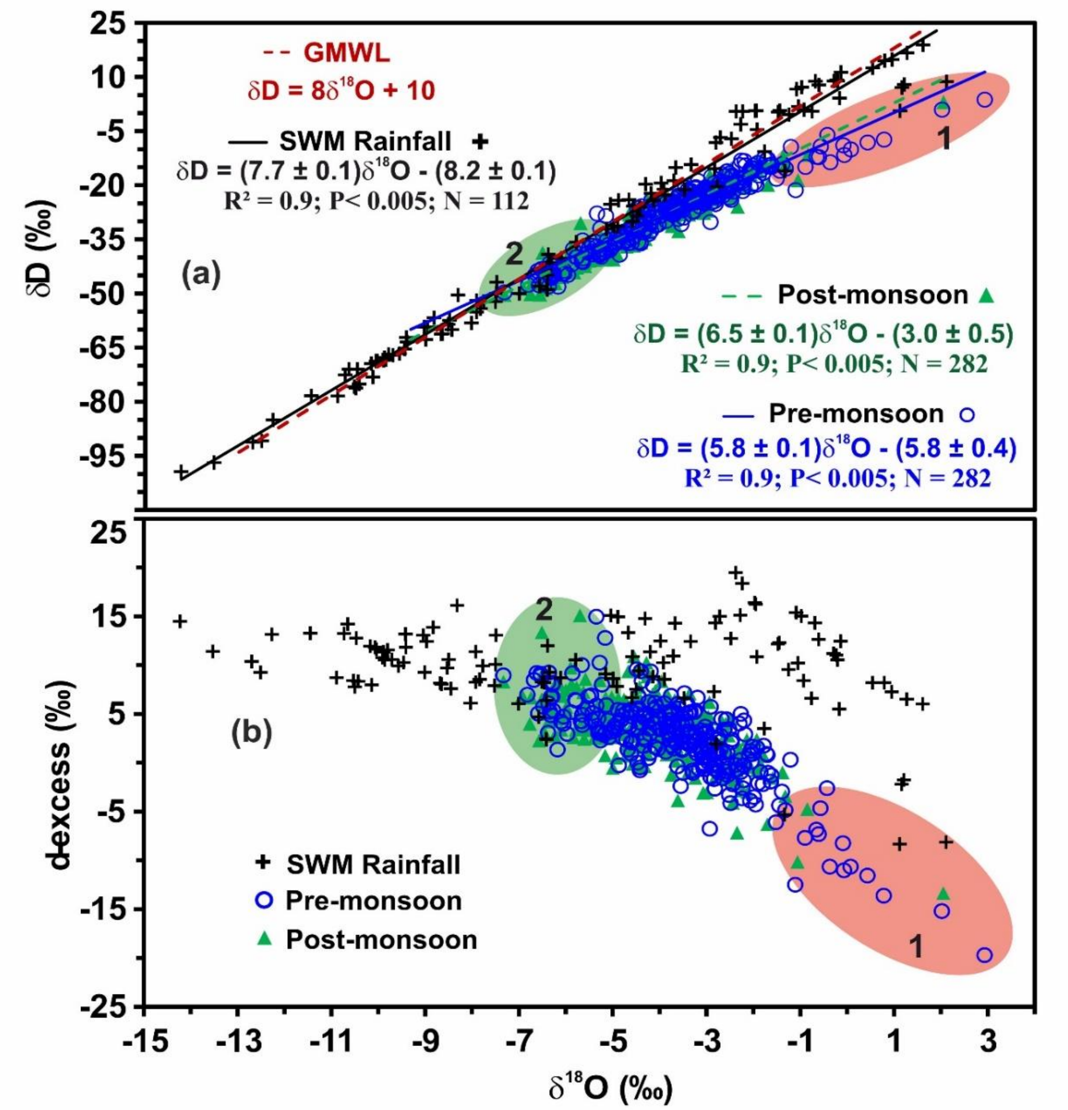

Fig 7.3: (a) $\delta^{18}O$-δD regression plot for shallow unconfined aquifer samples for both pre-monsoon and the post-monsoon seasons, along with LMWL based on daily rainfall samples collected at Bhopal and Jabalpur. (b) A plot of d-excess vs $\delta^{18}O$ for groundwater and SWM rainfall. The samples with extreme isotopic values in groundwater are marked by region 1 and region 2 and associated hydrogeological processes are discussed in the text.

to recharge by isotopically depleted SWM rains of different meteorological origins, discussed in the next section. The isotopically depleted groundwater also suggests relatively faster groundwater recharge, which favours the inheritance of pristine rainwater signatures without much modification during infiltration [*Jasechko*, 2019; *Mao et al.*, 2021].

The spatial variation in isotopic composition and its relationship with meteorological factors and vapour source variation have been discussed in the next section.

- **Spatial variation in δ^{18}O and d-excess and meteorological reasons**

The spatial distribution of δ^{18}O for pre-monsoon and post-monsoon groundwater is plotted in Fig 7.4a & 7.4b using the kriging method in Surfer 13 Software. The same for d-excess is plotted in Fig 7.5a & 7.5b. Based on spatial variation in δ^{18}O and d-excess, the study area can be divided into two isotopically distinguishable regions 1 and 2, marked by two ellipses. The groundwater in region-1 is isotopically enriched compared to region-2. The δ^{18}O values of groundwater are getting progressively depleted from -1‰ in the west up to -6.0‰ in the east, both during pre-monsoon and post-monsoon seasons. It is important to note that such an extent of depletion in δ^{18}O values of groundwater cannot be explained by the isotopic depletion in recharge source, i.e. SWM rainfall either due to continental effect (~2‰ /1000km. as reported by *Krishnamurthy &Bhattacharya* [1991] or elevation effect (-0.4‰ per 100 m. rise reported by *Deshpande et al.* [2003]. This calls for an alternate meteorological explanation for observed isotopic depletion in groundwater, which will be discussed later.

Groundwater also shows the spatial variation in d-excess in pre-monsoon and post-monsoon seasons (Fig 7.5a & 7.5b). During both seasons, groundwater in most of the areas shows d-excess between 0 to 6‰, which is lower than the global average value of +10‰, and suggests that the groundwater is prone to considerable evaporation or recharge by considerably evaporated source water. In the pre-monsoon season, there are a few localized pockets of groundwater in the study area which show the -ve d-excess (and also very high δ^{18}O). These localized pockets are not in one climatic zone or in hydrogeological settings (Fig 7.2), which suggests that some localised processes are active in that region which lowers the d-excess values. These processes could be evaporation from groundwater due to shallow water table, recharge from evaporated surface water, and mixing of evaporated surface water (having lower d-excess and higher δ^{18}O) with shallow groundwater [*Deshpande et al.*, 2003; *Krishan et al.*, 2020b]. The -ve d-excess patches turn into +ve d-excess in the post-monsoon season, which clearly indicates freshwater influx from SWM rain. The eastern side of the study area, marked by region-2 shows higher d-excess and correspondingly lower δ^{18}O compared to region-1 where d-excess is lower and δ^{18}O is relatively high in both seasons. The spatial variability of

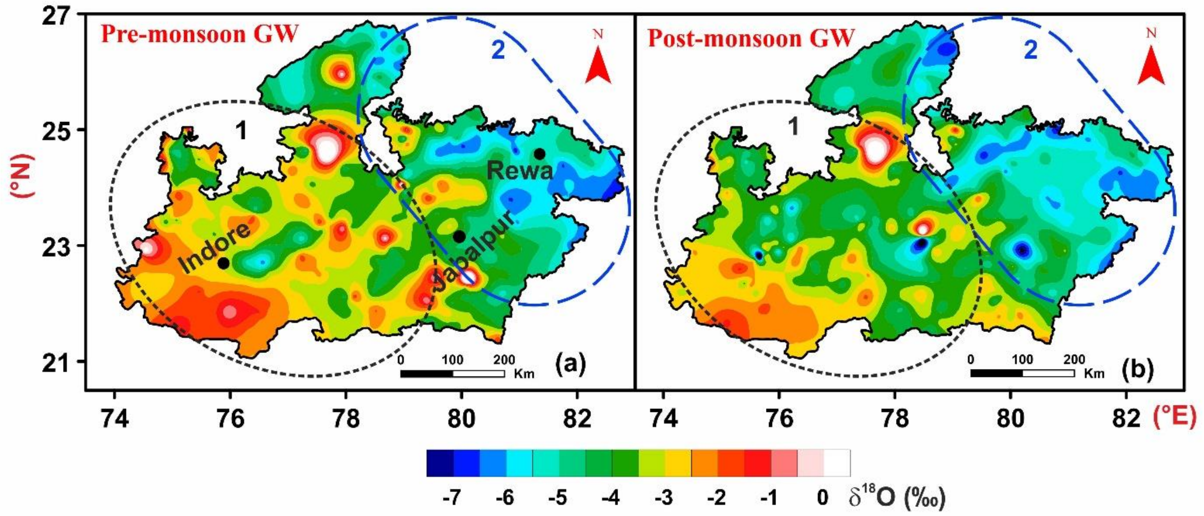

Fig 7.4: Spatial variation in δ^{18}O for (a) pre-monsoon and (b) post-monsoon is plotted in this figure, the two regions with different isotopic compositions in pre-monsoon and post-monsoon are marked by ellipses.

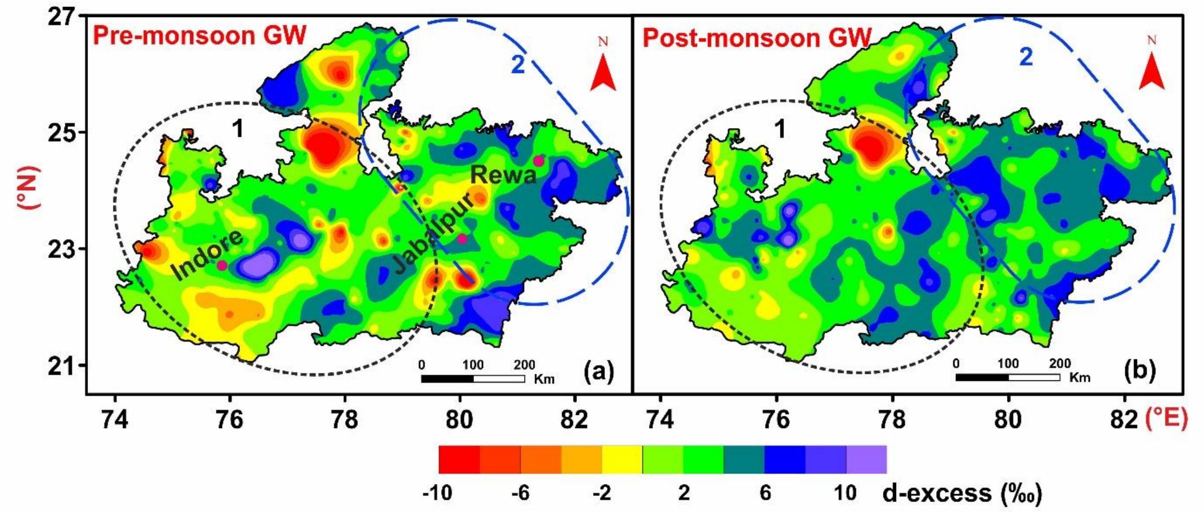

Fig 7.5: Spatial variation in d-excess for (a) pre-monsoon and (b) post-monsoon is plotted in this figure.

δ^{18}O and d-excess in groundwater from region-1 to region-2 indicates that, although SWM rainfall is known to be the source of groundwater recharge, the rainfall in the east and west must have different isotopic compositions. Since the observed spatial isotopic variation in groundwater is more than that accountable by continental effect or elevation effect in rainfall, we have examined other meteorological reasons such as moisture source and their transport history for regions 1 and 2.

To identify the moisture sources, their relative contribution, and transport history for the SWM rains (June-September) in the region-1 and region-2, backward wind trajectories for Indore (located in region 1) and Rewa (located in region 2) are shown in Fig (7.6a & 7.6b). The resultant backward wind trajectory map of specific humidity variation for all the rainfall events during SWM (representing groundwater recharge source) shows the direction of the moisture-containing air parcel. The percentage contribution of vapour by different sources such as the Arabian Sea (AS), the Bay of Bengal (BOB), and continentally recycled moisture estimated for each month of SWM season are given in Fig (7.6a' & 7.6b'). It is clearly seen from Fig 7.6a and 7.6b that almost all the rain-bearing backward wind trajectories at Indore

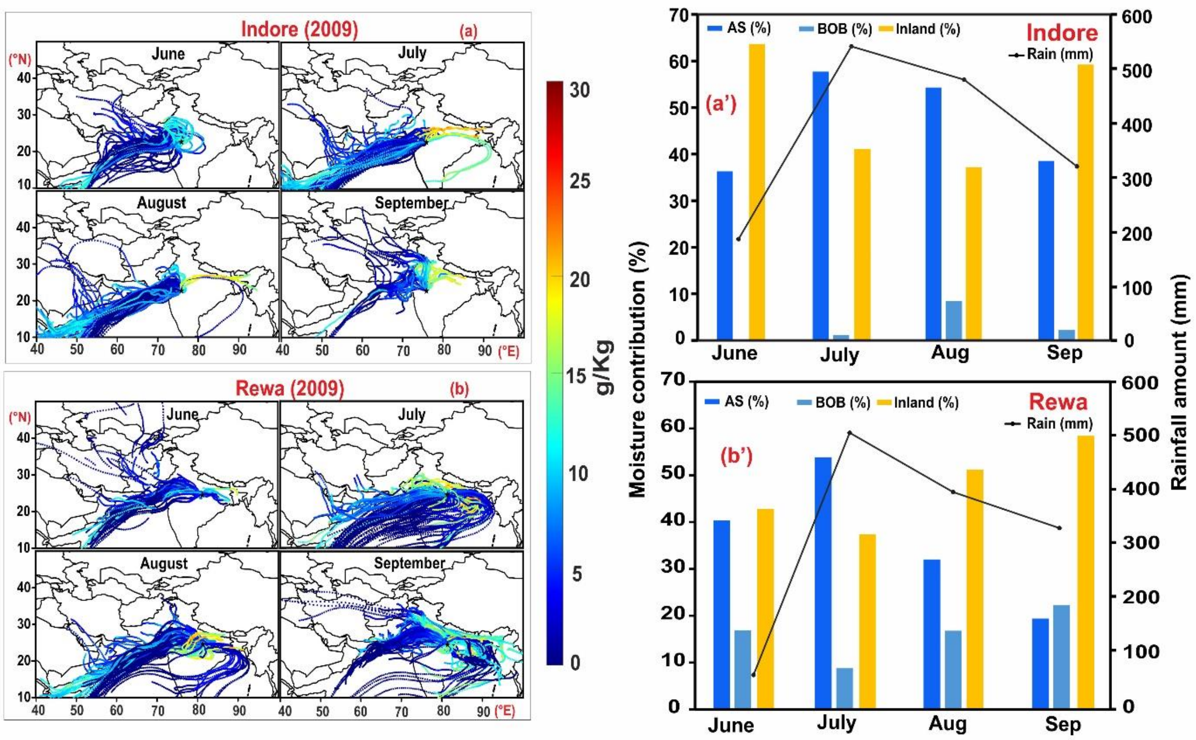

Fig 7.6: 120 hr backwards wind trajectories converging at 1500m above ground level, at every six hours interval for each rainy day for (a) Indore (located in region-1 of Fig 7.5) and (b) Rewa (located in region-2 of Fig 7.5). The estimated contribution of moisture from different sources, namely, the Arabian Sea, Bay of Bengal and continental recycling is shown in (Fig. a') for Indore and (Fig. b') for Rewa are calculated.

(Fig 6a) are coming from the AS side, with only a few trajectories coming from the BOB side. In contrast, at Rewa, a large number of backward wind trajectories are from the BOB side. It is also seen from Fig. 7.6a' and 7.6b' that the relative contribution of moisture (average of June to September) from the AS is 48% for Indore (Region-1) whereas it is only 33% for Rewa

(Region-2). Correspondingly, relative contribution of moisture combined from the BOB and the continental recycling is only 52% (i.e. 6% BOB + 46% continental) for Indore (Region-1), whereas that for the Rewa (Region-2) is 67 % (i.e. 16% BOB + 51% continental). The increased contribution of moisture from the BOB and continental recycling is reported [*Breitenbach et al.*, 2010; *Deshpande et al.*, 2010; *Oza,* 2020] to give rise to isotopically depleted rain elsewhere in the country. The same reason is responsible for the depleted rains and the depleted groundwater that it recharges in region-2.

- **Temporal variation in δ^{18}O and d-excess**

To understand the effect of SWM on groundwater recharge in the study area, the temporal variation in δ^{18}O ($\Delta\delta^{18}$O = δ^{18}Opost-mon - δ^{18}O pre-mon) and d-excess (Δd-excess = d-excess post-mon – d-excess pre-mon) contour is plotted in Fig (7.7a & 7.7b). Considering the 1σ measurement precision of better than ±0.1‰ for δ^{18}O and ±1.0‰ for δD as mentioned in the methodology section, the 2σ seasonal difference of ±0.2‰ for δ^{18}O and ±1.3‰ for d-excess is considered as a significant threshold value for evaluating the seasonal variations in these two parameters. In other words, a seasonal difference of more than ±0.2‰ in δ^{18}O and more than ±1.3‰ in d-excess is treated as a genuine seasonal isotopic difference caused by seasonal change in groundwater mass and not by any instrumental uncertainty [*Mao et al.*, 2021]. In the non-rainy pre-monsoon season, dry climatic conditions in the study area favour evaporation from the groundwater and with the non-availability of a recharge source, groundwater shows enrichment in δ^{18}O and lower d-excess values. During the rainy season, due to recharge by monsoonal rainwater, which has depleted δ^{18}O and higher d-excess values compared to pre-monsoon groundwater, the areas that receive freshwater influx show -veΔ^{18}O and +ve Δd-excess. A large part of the study area shows -veΔ^{18}O (~58%) or no variation (~27%). The -veΔ^{18}O is possible when groundwater receives isotopically lighter freshwater influx during SWM, suggesting that 58% of the study area recharges seasonally.

Some parts of the study show +veΔ^{18}O (15%), which meant during the pre-monsoon season, groundwater has depleted δ^{18}O compared to surrounding regions and the amount weighted average δ^{18}O of SWM. The lower δ^{18}O in the pre-monsoon season is possible only when groundwater is recharged by isotopically depleted sources such as deeper groundwater

[*Gonfiantini et al.*, 1998], rivers originating from higher altitude areas [*Liu & Yamanaka*, 2012], lateral movement of groundwater from higher elevation to lower area [*Jasechko*, 2019].

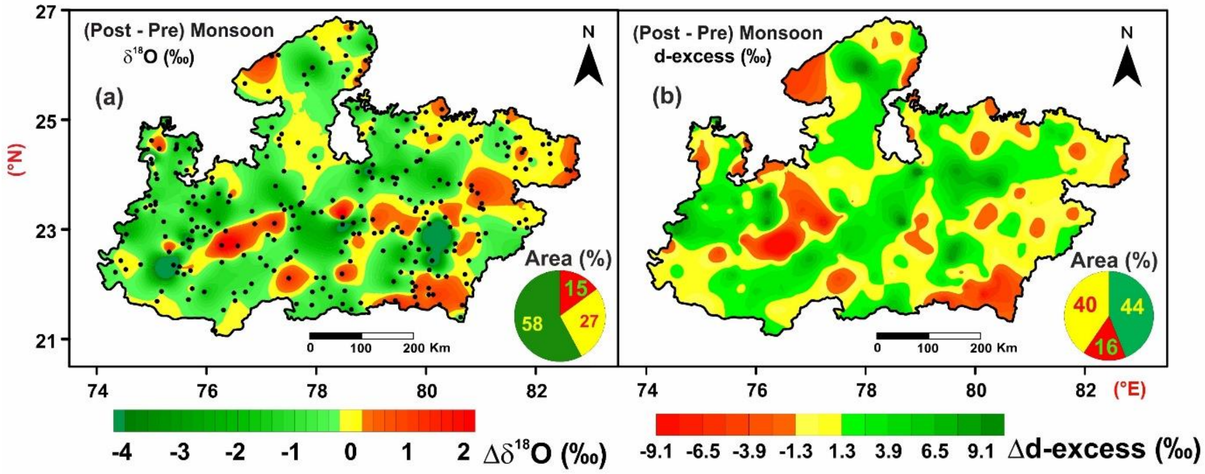

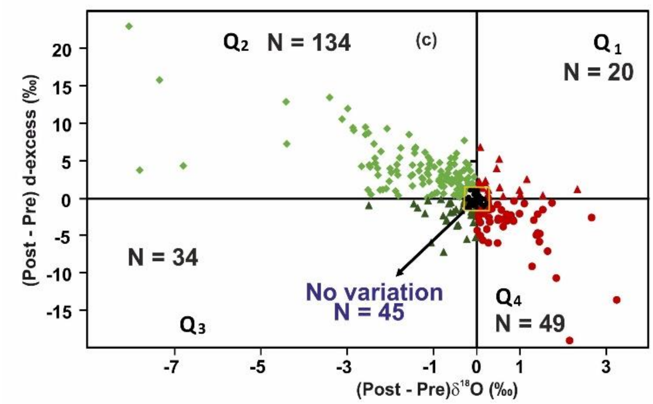

Fig 7.7: The seasonal difference (Δ = Post-monsoon minus Pre-monsoon) for (a) $\delta^{18}O$ (i.e. $\Delta\delta^{18}O$ $_{post-pre\text{-}monsoon}$), and (b) for d-excess (i.e. Δd-excess $_{post-pre\text{-}monsoon}$) of Groundwater sare shown in this figure. The inserted pie chart in (a) and (b) represents the area showing +ve, -ve or no variation. The values of seasonal variation in $\delta^{18}O$ ($\Delta\delta^{18}O$) and d-excess (Δd-excess) i.e. $\Delta\delta^{18}O$ versus Δd-excess are plotted in (c).

To discern the interpretative significance of seasonal isotopic variation in groundwater, the values of seasonal variation in $\delta^{18}O$ ($\Delta\delta^{18}O$) and d-excess (Δd-excess) are plotted as $\Delta\delta^{18}O$ versus Δd-excess in Fig (7.7c). Seasonal isotopic variation actually represents the variation in the groundwater mass. Groundwater mass can change both in the pre-monsoon season (due to direct evaporation from groundwater or recharge from evaporated sources such as irrigation return flow and evaporated surface water, long-distance transport of allochthonous rainwater) or in the post-monsoon season (due to recharge from fresh rainwater). Plotting the seasonal variation as $\Delta\delta^{18}O$ vs Δd-excess can provide insights into season changes in the groundwater mass during pre- and post-monsoon. In the following, based on the observed seasonal isotopic variation in groundwater, we hypothesize the possible geohydrological processes.

It is seen in Fig 7.7c that the maximum number (134) of groundwater samples fall in the second quadrant (Q_2: -ve $\Delta\delta^{18}O$ and +ve Δd-excess), which signifies enriched $\delta^{18}O$ and lower d-excess in groundwater in the pre-monsoon season compared to the post-monsoon season. These signatures can be ascribed to: (1) direct evaporation of GW during the warm and arid pre-monsoon season; or (2) recharge from the evaporated surface water in pre-monsoon; and/or (3) recharge from fresh rainwater during post-monsoon season.

The second highest number (49) of groundwater samples fall in the fourth quadrant (Q_4: +ve $\Delta\delta^{18}O$ and -ve Δd-excess), signifying lower $\delta^{18}O$ and higher d-excess in groundwater in the pre-monsoon season compared to post-monsoon. Such a seasonal isotopic difference is possible in two situations: (1) groundwater is recharged in the post-monsoon by isotopically enriched water with higher $\delta^{18}O$ and lower d-excess such as that stored in the surface reservoir and released when fresh influx is received; or (2) groundwater is recharged in the pre-monsoon season by the allochthonous monsoonal rainwater of previous season, having lower $\delta^{18}O$ and higher d-excess, which can be transported for a long distance through fractured terrain existing in the study area. Besides the above two possibilities, the influence of palaeowater with lower $\delta^{18}O$ and higher d-excess may also be there.

Thirty-four groundwater samples are falling in the third quadrant (Q_3: -ve $\Delta\delta^{18}O$ and -ve Δd-excess), which signifies lower $\delta^{18}O$ and lower d-excess in groundwater during the post-monsoon season compared to pre-monsoon. Such an isotopic composition is possible in the case of cyclonic precipitation [*Sun et al.*, 2022] or precipitation from a cloud parcel, highly diminished in its original moisture content [*Clark & Fritz*, 1997]. While such an isotopic composition is already reported in precipitation [*Müller et al.*, 2020], its signatures in groundwater are identified in this study.

There are only a small number (20) of groundwater samples falling in the first quadrant (Q_1: +ve $\Delta^{18}O$ and +ve Δd-excess) which signify lower $\delta^{18}O$ and lower d-excess in groundwater in pre-monsoon season compared to post-monsoon. This is possible when groundwater in a particular area is recharged in the pre-monsoon season by allochthonous rainwater of the previous monsoon in higher altitude regions. Such higher altitude rainwater has lower $\delta^{18}O$ and lower d-excess due to the elevation effect [*Araguás-Araguás et al.*, 1998; *Kumar, B et al.*, 2010], which can be transported for a long distance through fractured terrain existing in the study area and is detected in pre-monsoon sampling of the next year.

Various hypotheses regarding the recharge mechanism suggested above are based exclusively on seasonal variation in isotopic composition and highlight the importance of seasonal sampling.

- **Seasonal groundwater recharge in two adjoining aquifers**

The Basaltic rock forms the major aquifer system in the study area. It covers nearly 46% of the geographical area [*Patil et al.*, 2019] and the rest of the area is covered with lithified sandstone, shale, unconsolidated alluvium, and crystalline hard rocks. These two major aquifers have different hydrogeological properties as discussed earlier, which governs the groundwater availability in these aquifers. The aquifers are recharged in general by the SWM rainfall, but the recharge varies spatially depending upon the aquifer types and recharge processes. To understand and estimate the magnitude of seasonal SWM rainfall contribution to groundwater recharge, two adjoining aquifer systems (basalt and sedimentary hard rocks) were selected close to the rainfall sampling location, and the isotope mass balance was carried out (Fig 7.8a).

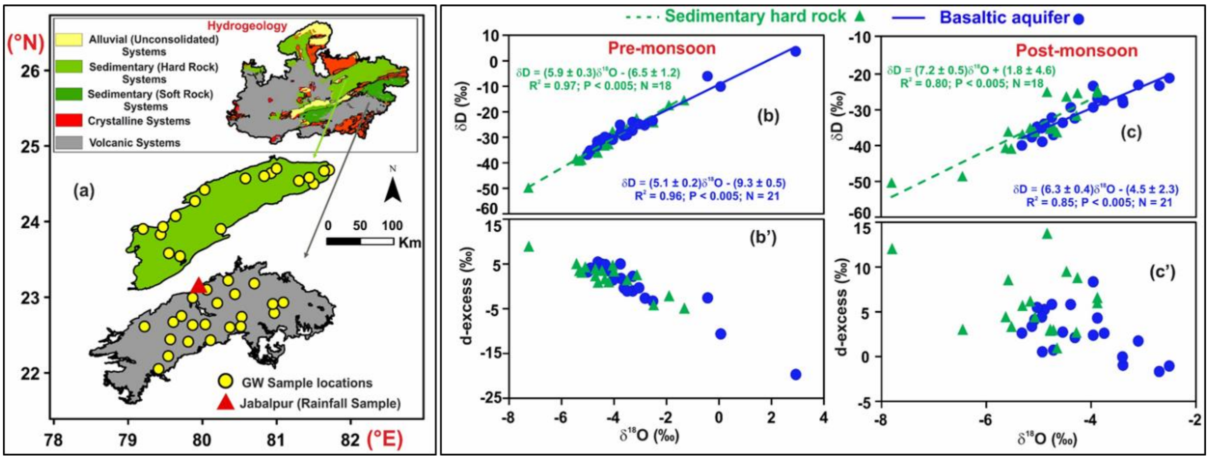

Fig 7.8: (a) Represents two distinct aquifers falling in region 2 and groundwater sample locations in these aquifers. The δD vs. δ^{18}O and d-excess vs. δ^{18}O for pre-monsoon are given in (b and b') and post-monsoon in (c and c').

In basaltic aquifers, the isotopic composition of groundwater in the pre-monsoon season is δ^{18}O: -5.0‰ to 2.9‰ with an average of -3.2‰; δD: -37.0‰ to 4.0‰ with an average of -27.0‰; and d-excess: -19.7‰ to 5.4‰ with an average of 0.5‰. In this aquifer, the isotopic composition of groundwater for the post-monsoon season is δ^{18}O: -5.3‰ to -2.5‰ with an average of -4.2‰; δD: -40.0‰ to -21.0‰ with an average of -31.0‰; and d-excess: -1.7‰ to 8.3‰ with an average of 2.3‰.

In sedimentary hard rock aquifers, the groundwater has a different isotopic composition compared to basaltic aquifers in both seasons. In the pre-monsoon season, the isotopic composition of groundwater in the sedimentary aquifer is δ^{18}O: -7.2‰ to -1.3‰ with an average of-4.2; δD: -50.0‰ to -15.0‰ with an average of -32.0‰; and d-excess: -4.8‰ to

8.9‰ with an average of 2.2‰. In the post-monsoon season, the isotopic composition of groundwater in the sedimentary aquifer is: [$\delta^{18}O$: -7.8‰ to -3.9‰ with an average of -5.1‰; δD: -50.0‰ to -24.0‰ with an average of -35.0‰; d-excess: 1.0‰ to 13.8‰ with an average of 5.8‰].

The δD vs $\delta^{18}O$ and d-excess vs $\delta^{18}O$ for both the aquifers in pre-monsoon and post-monsoon seasons have been plotted in Fig 7.8b, b' and Fig 7.8c, c'. The slopes of the regression lines in the pre-monsoon season for basaltic aquifer and sedimentary hard rock are respectively (5.1 ± 0.2) and (5.9 ± 0.3). In the post-monsoon season, the regression line slopes for the basaltic and sedimentary aquifers increase to respectively (6.3 ± 0.4) and (7.2 ± 0.5), which is similar to the slope of LMWL (7.7 ± 0.1). The depletion in the average isotopic composition of groundwater in the post-monsoon season and increase in the regression line slope confirms the groundwater recharge during the monsoon season.

The SWM rainwater contributions to groundwater recharge in two aquifers are calculated using two end-member isotopic mixing models using the seasonal isotopic composition of groundwater in the two aquifers and the local rainwater [*Phillips*, 2001; *Hameed et al.*, 2015; *Sakakibara et al.*, 2017]:

$$\delta_{pre}\, M_{pre} + \delta_{rain}\, M_{rain} = \delta_{post} \ \dots\dots\dots\dots\dots\,.\ Eq. 1$$

$$Where$$

$$M_{pre} + M_{rain} = 1 \dots\dots\dots\dots\dots . Eq. 2$$

Where δ_{pre} is the $\delta^{18}O$ of pre-monsoon groundwater and M_{pre} is the mass fraction of pre-monsoon groundwater, δ_{rain} is the $\delta^{18}O$ of SWM rainwater and M_{rain} is the mass fraction of rainfall, δpost is the $\delta^{18}O$ of post-monsoon groundwater, which is the admixture of pre-monsoon groundwater and the rainfall. From the above equation, the percentage contribution of rain in groundwater is calculated using the following equation:

$$\text{Rainwater contribution in (\%)} = \left\{\frac{\delta_{post} - \delta_{pre}}{\delta_{rain} - \delta_{pre}}\right\} \times 100 \dots\dots\dots . Eq. 3$$

For basaltic aquifer, the end member values are $\delta^{18}O_{pre}$ = -3.2‰, and $\delta^{18}O_{post}$ = -4.2‰. For sedimentary aquifers, the end member values are $\delta^{18}O_{pre}$ = -4.2‰, and $\delta^{18}O_{post}$ = -5.1‰. The end member values for groundwater are the average $\delta^{18}O$ value for pre-monsoon and post-monsoon seasons, whereas for rain, it is the amount weighted average value ($\delta^{18}O_{rain}$ = -6.4 ‰).

Uncertainty in rainwater contribution in the above equations is calculated by the uncertainty propagation technique [*Genereux*, 1998], which is less than 5%. The above end-member mixing model reveals that in the case of the basaltic aquifer, the post-monsoon groundwater mass consists of an admixture of 32% of rainwater which mixes with 68% of the pre-monsoon groundwater, and in sedimentary hard rock aquifer, it is 39% of rainwater and 61% of pre-monsoon residual groundwater. As discussed in the following, these estimated mass fractions of rainwater and pre-monsoon groundwater can be advantageously used for the volumetric estimation of other hydrological components of the eastern part of the study area where these aquifers are situated.

As per the Dynamic Groundwater Resource of India 2011 [*Cgwb*, 2011], the basaltic aquifer is spread in three districts (Jabalpur, Mandla, and Seoni) of Madhya Pradesh and covers a 22727 km^2 area and receives nearly 1.7 BCM (Billion Cubic Meter) of groundwater recharge in the monsoon season while sedimentary hard rock aquifer covers 21048 km^2 area in Damoha, Rewa and Satna districts of Madhya Pradesh and receives 1.2 BCM of groundwater recharge in monsoon season. As per the mass balance calculation, in the basaltic aquifer, 32% of the groundwater is rainfall recharge which in volumetric terms becomes 1.7 BCM. The rest 68% (3.7 BCM) is pre-monsoon residual water. The total groundwater potential calculated by the mass balance of this aquifer is 5.4 BCM (1.7 rainfall recharge + 3.7 pre-monsoon residual water). The annual groundwater abstraction, natural discharge and pre-monsoon residual water in the basaltic aquifer are 0.6 BCM, 0.1BCM (reported by CGWB), and 3.7 BCM (calculated) respectively, so the remaining 1.0 BCM (5.4 minus 0.6 minus 0.1 minus 3.7) groundwater is estimated to percolate into deeper aquifers through faults present in the area. This inference is justifiable considering the known faults in this region [*Deshpande & Gupta*, 2013].

In sedimentary hard rock aquifer, groundwater has a 39% freshwater influx from monsoonal rain, which is nearly 1.2 BCM as per the CGWB report (2011), so the groundwater potential in this aquifer is 3.2 BCM (1.2 BCM freshwater influx + 1.9 BCM pre-monsoon residual water). The annual groundwater abstraction, natural discharge, and pre-monsoon residual water in this aquifer are 0.9 BCM, 0.07 BCM (given by CGWB), and 1.9 BCM (calculated) respectively, so the remaining 0.3 BCM of groundwater percolates into the deeper aquifer. This additional water can be advantageously used for some other purposes.

7.4 Conclusion

This study uses seasonal variations in the isotopic composition of groundwater to understand the interaction between the SWM rainwater and the groundwater and estimate the relative contribution of SWM rainfall to two adjoining aquifers.

There are distinct differences in the isotopic composition of groundwater in the western and eastern parts of the study area, with significant isotopic depletion on the eastern side. Since the observed differences cannot be accounted by the isotopic difference in the rainwater due to continental effect or altitude effect, backward wind trajectory analyses were performed to estimate the relative contribution of vapour sources (the Arabian Sea, Bay of Bengal and the continental recycling) for rainfall in the eastern and western regions of the study area. It is observed that due to meteorological reasons, the contribution of moisture from the Bay of Bengal and the continental recycling is higher (67 % = 16% BOB + 51% continental) for rainfall in the eastern part compared to the western part (52% = 6% BOB + 46% continental). The signatures of this meteorological process are discerned in the groundwater.

The temporal difference in the isotopic composition of groundwater ($\delta^{18}O$) reveals the seasonal recharge by different sources, with 58% of the study area recharged by monsoonal rain and 15% of the area recharged in the pre-monsoon season by isotopically depleted rain which could be irrigation return flow of deeper static water, recharge by an allochthonous source such as rainfall in higher altitude region. Approximately 27% of the study area shows no variation in isotopic composition which suggests longer residence time and a lower rate of recharge. This finding also conveys that if the groundwater in this 27% area is overexploited or polluted, it would be difficult to restore or replenish it. This is a societally useful input for groundwater development and management. The rainwater contribution to groundwater recharge was also calculated for two adjoining aquifers (basaltic aquifer and sedimentary hard rock) using two end-member mixing models suggesting that groundwater recharge occurs at a higher rate in the sedimentary hard aquifer.

Chapter 8

Conclusion and Way Forward

8.1 Conclusion

This doctoral study is aimed at understanding the surface water groundwater interaction, seasonality in groundwater recharge and its spatial variation, and the contribution of different sources for groundwater recharge. The main tool used for this study is the seasonal differences in the oxygen and hydrogen stable isotopic composition of groundwater and the interpretation of isotope data in conjunction with the isotopic composition of rainfall and hydrogeological settings of the region. Conventionally, the seasonal water level fluctuation is used to estimate groundwater recharge, and an increase in water level in the post-monsoon season is ascribed to fresh groundwater influx. However, the seasonal difference in water level depends on aquifer properties and seasonal variation in groundwater extraction. Therefore, the water level increase in the post-monsoon season does not necessarily represent the actual recharge. To discern the processes governing the seasonality in the groundwater recharge, this study uses oxygen and hydrogen isotopic composition of groundwater from 2527 locations for pre-monsoon (April-May) and the post-monsoon (Oct-Nov) seasons across India. The isotope dataset was generated under the aegis of the National Programme on Isotope Fingerprinting of Waters of India (IWIN). All the inferences drawn from this study have been described and explained in detail in individual chapters, but some of the major conclusions of this study are summarized in the bulleted form in the following:

1. **Seasonal isoscapes ($\delta^{18}O$ and δD) of India**

The study provides an integrated synoptic snapshot of spatial variation in the isotopic composition of shallow groundwater and underlying hydrogeological processes in different hydrogeological settings of India for pre-monsoon and post-monsoon seasons. Based on the seasonal variability of the isotopic composition of groundwater along with hydrogeology and climate settings, some of the areas in western (Gujarat), southwestern (Kerala), and central (Madhya Pradesh) India have been identified for detailed study.

- Post precipitation and pre-infiltration modification in the isotopic composition of rainwater by evaporation, evaporation of shallow groundwater through the capillary fringe zone, and groundwater recharge by substantially evaporated open surface water (lakes, ponds, reservoirs) are the dominant natural processes concerning groundwater recharge and impart characteristics isotopic signature to pre-monsoon groundwater with lower $\delta^{18}O$-δD regression slope of groundwater compared to the composite Indian meteoric water line (IMWL) in case of all India data. For regional datasets, the pre-monsoon isotopic composition of groundwater of a region has a lower regression line slope compared to the local meteoric water line.

- The spatial variation in the isotopic composition of groundwater (seasonal isoscapes) is governed by SWM rainfall, although in some of the areas, particularly the southeastern coast of India and the western part of Rajasthan affected by NEM rainfall and irrigation return flow through Indira Gandhi Canal water that can be identified by the depleted isotopic composition of groundwater compared to SWM rainfall.
- In 45% of the geographical area, seasonal groundwater recharge takes place by SWM rainfall, while in 25% of the area, groundwater recharge takes place through irrigation return flow or some other sources, and 30% of the area does not receive the seasonal recharge.

2. Semi-arid western India (Gujarat)

- Isotopic enrichment in groundwater during the post-monsoon season in 25% of the geographical area of Gujarat is ascribable to deep static non-replenishable groundwater extracted for irrigation which finds its way into shallower aquifers.
- ~28% (0.6 Billion Cubic Meters) of the available dynamic groundwater resource in South Gujarat is lost as submarine groundwater discharges into the Arabian Sea.
- Depletion in the isotopic composition of groundwater over the last ten years in north Gujarat is caused by the lower abstraction of groundwater and recharge from rainfall. Due to the availability of Narmada water through the Narmada Canal overall evaporative regime that existed in 2009 has become milder (less evaporative) during 2019.
- It is observed that regions which were not fed by the Narmada Canal water in 2009 had isotopically enriched groundwater in 2009 compared to 2019, when the canal has now been available for the last ten years. Narmada canal is known to have isotopically depleted water compared to local rain and groundwater in Gujarat.

3. Coastal southwestern India (Kerala)

- The rainfall from May to October accounts for ~46% (4.91 BCM) of fresh recharge in Kerala, which mixes with the 54% (5.90 BCM) of the residual pre-monsoon groundwater.
- 11% of the geographical area is additionally recharged by the NE monsoon rainfall.
- On an annual basis, a huge 41% (~2.0 BCM) of replenishable groundwater is lost into the coastal water of the Arabian Sea as submarine groundwater discharge (SGD).
- The estimated annual groundwater recharge varies physiographically from ~2.2 BCM in the lowland region to ~1.5 BCM in the midland and ~1.2 BCM in the highland areas of Kerala.

4. Central India (Madhya Pradesh)

- The seasonal difference in the isotopic composition of groundwater ($\delta^{18}O$) reveals the seasonal recharge by different sources, with 58% of the study area recharged by monsoonal rain and 15% of the area recharged in the pre-monsoon season by the isotopically depleted source, which could be irrigation return flow of deeper static water or the recharge by an allochthonous source such as rainfall from the higher altitude region or from the different meteorological regime.
- Approximately 27% of the study area in Madhya Pradesh shows no variation in isotopic composition, which suggests longer residence time and a lower rate of recharge. This finding also conveys that if the groundwater in this 27% area is overexploited or polluted, it would be difficult to restore or replenish it at a faster rate.
- The rainwater contribution to groundwater recharge was also calculated for two adjoining aquifers (basaltic aquifer and sedimentary hard rock) using two end-member mixing models suggesting that groundwater recharge occurs at a higher rate in the sedimentary hard aquifer.

8.2 Limitations

The present study provides some new insights into various hydrogeological processes governing surface water groundwater interactions and their spatiotemporal variation across India. There can be substantial heterogeneity of processes on different spatial scales, which is determined by spatial variation in climate (rainfall, temperature, and relative humidity), topography, lithology, tectonic settings, vegetation cover, and urbanisation. Therefore, there are limitations of upscaling inferences from a local scale study to regional or basinal scale. This is precisely the reason why stable isotopes of oxygen and hydrogen have emerged as a very convenient and useful pair of tracers which integrate the resultant effect of several spatially variable features and provide an overall impression of major processes operating in a particular area over which the isotope data are available. This is also the reason why isotope data are always interpreted in conjunction with associated hydrogeological and climatic parameters. This study also has a few limitations which are: (1) the entire study is based mainly on the stable isotope characterization of groundwater and its seasonal variation. In some cases, it would have been more advantageous to have additional chemical characterization to support the isotope-based inferences with chemistry data; (2) In order to isotopically characterize the groundwater from a large number of stations across the entire country, the samples were collected from the available well within a given area even if it was not possible to ascertain the depth information about the well. This fact entails a limitation that the groundwater has to be treated as shallow first unconfined groundwater, without referring to its depth or without differentiating based on its depth information; (3) Isotope data of groundwater needs to be compared with isotope data of rainfall. However, it is not possible to set up rainfall collection stations as closely spaced locations as the groundwater sampling locations. Therefore, rainfall isotopes data is available from a limited number of representative locations in each region across the country collected under the IWIN National Programme; (4) Spatial heterogeneity related to hydrogeology was not taken into consideration while doing the regression analysis; (5) Such a countrywide network of sampling over more than 2500 locations was operated for only one seasonal cycle of pre-monsoon and post-monsoon.

8.3 Future Scope

The present study gave new insights into the groundwater recharge processes in different hydrogeological units across India based on spatial and seasonal variability of the isotopic composition of groundwater in conjunction with the isotopic composition of rainfall. Seasonal isoscapes ($\delta^{18}O$ and δD) of India provide a base to find out an area that shows the deviation in the isotopic composition of groundwater compared to the recharge source. Some of the salient points which need to be pursued to advance the understanding are (1) Interaction between different groundwater masses in multilayered aquifer settings; (2) Seasonal variation in the isotopic composition of soil moisture and its interaction with shallow groundwater; (3)

Improved correlation study between temporal variation in the isotopic composition of groundwater, groundwater recharge sources and factor governing groundwater recharge. (4) In order to test the hypothesis that deeper static groundwater extracted for irrigation is feeding the shallow groundwater, it will be an important research component in future to date the deeper and shallower groundwaters, and to compare the difference in groundwater ages of shallow groundwater between of the regions in which deep groundwater is extracted, and the one in which it is no extracted.

The concept of deeper static groundwater being brought to a shallower level has a lot of significance in terms of the water budget of dynamic groundwater resources of a region. Similarly, the dynamic groundwater, annually recharged but getting out of dynamic resource through submarine groundwater discharge and/or percolation to deeper static aquifers through deep fractures and faults is another important groundwater research topic emerging from this study which can be pursued in future.

References

Adams, S., R. Titus, K. Pietersen, G. Tredoux, and C. Harris (2001), Hydrochemical characteristics of aquifers near Sutherland in the Western Karoo, South Africa, *Journal of Hydrology*, *241*(1-2), 91-103.

Agarwal, M., S. Gupta, R. Deshpande, and M. Yadava (2006), Helium, radon and radiocarbon studies on a regional aquifer system of the North Gujarat–Cambay region, India, *Chemical Geology*, *228*(4), 209-232.

Aggarwal, P. K., K. Froehlich, and K. M. Kulkarni (2009), Environmental isotopes in groundwater studies, *Groundwater*, *2*, 69.

Alley, W. M., R. W. Healy, J. W. LaBaugh, and T. E. Reilly (2002), Flow and storage in groundwater systems, *Science*, *296*(5575), 1985-1990.

Alley, W. M., and S. A. Leake (2004), The journey from safe yield to sustainability, *Groundwater*, *42*(1), 12-16.

Allison, G. (1988), A review of some of the physical, chemical and isotopic techniques available for estimating groundwater recharge, *Estimation of Natural Groundwater Recharge*, 49-72.

Andharia, P. B. (2013), Salt pan workers in Gujarat: examining the need for a special legislation, *GNLU JL Dev. & Pol.*, *3*, 88.

Apodaca, L. E., J. B. Bails, and C. M. Smith (2002), Water Quality in Shallow Alluvial Aquifers, Upper Colorado River Basin, Colorado, 1997 1, *JAWRA Journal of the American Water Resources Association*, *38*(1), 133-149.

Araguás-Araguás, L., K. Froehlich, and K. Rozanski (1998), Stable isotope composition of precipitation over southeast Asia, *Journal of Geophysical Research: Atmospheres*, *103*(D22), 28721-28742.

Arjun, K. M. (2013), Indian agriculture-status, importance and role in Indian economy, *International Journal of Agriculture and Food Science Technology*, *4*(4), 343-346.

Asoka, A., T. Gleeson, Y. Wada, and V. Mishra (2017), Relative contribution of monsoon precipitation and pumping to changes in groundwater storage in India, *Nature Geoscience*, *10*(2), 109-117.

Babu, D. S., M. Anish, K. Vivekanandan, N. Ramanujam, K. N. Murugan, and A. A. Ravindran (2009), An account of submarine groundwater discharge from the SW Indian coastal zone, *Journal of Coastal Research*, *25*(1), 91-104.

Babu, D. S., A. Khandekar, C. Bhagat, A. Singh, V. Jain, M. Verma, B. K. Bansal, and M. Kumar (2021), Evaluation, effect and utilization of submarine groundwater discharge for coastal population and ecosystem: A special emphasis on Indian coastline, *Journal of Environmental Management*, *277*, 111362.

Bagheri, R., F. Bagheri, G. H. Karami, and H. Jafari (2019), Chemo-isotopes (18O & 2H) signatures and HYSPLIT model application: Clues to the atmospheric moisture and air mass origins, *Atmospheric Environment*, *215*, 116892.

Bandyopadhyay, N., C. Bhuiyan, and A. Saha (2020), Drought mitigation: Critical analysis and proposal for a new drought policy with special reference to Gujarat (India), *Progress in Disaster Science, 5*, 100049.

Banks, D., B. Frengstad, A. K. Midtgård, J. R. Krog, and T. Strand (1998), The chemistry of Norwegian groundwaters: I. The distribution of radon, major and minor elements in 1604 crystalline bedrock groundwaters, *Science of the Total Environment, 222*(1-2), 71-91.

Barker, R., B. Van Koppen, and T. Shah (2000), A global perspective on water scarcity and poverty: achievements and challenges for water resource management.

Bhagat, C., P. K. Mohapatra, and M. Kumar (2021), Unveiling the extent of salinization to delineate the potential submarine groundwater discharge zones along the North-western coast of India, *Marine Pollution Bulletin, 172*, 112773.

Bhanja, S. N., P. Malakar, A. Mukherjee, M. Rodell, P. Mitra, and S. Sarkar (2019), Using satellite-based vegetation cover as indicator of groundwater storage in natural vegetation areas, *Geophysical Research Letters*, *46*(14), 8082-8092.

Bhanja, S. N., A. Mukherjee, and M. Rodell (2020), Groundwater storage change detection from in situ and GRACE-based estimates in major river basins across India, *Hydrological Sciences Journal*, *65*(4), 650-659.

Bhanja, S. N., A. Mukherjee, M. Rodell, Y. Wada, S. Chattopadhyay, I. Velicogna, K. Pangaluru, and J. S. Famiglietti (2017), Groundwater rejuvenation in parts of India influenced by water-policy change implementation, *Scientific Reports*, *7*(1), 1-7.

Bhanja, S. N., A. Mukherjee, D. Saha, I. Velicogna, and J. S. Famiglietti (2016), Validation of GRACE based groundwater storage anomaly using in-situ groundwater level measurements in India, *Journal of Hydrology*, *543*, 729-738.

Bhattacharya, S., K. Froehlich, P. Aggarwal, and K. Kulkarni (2003), Isotopic variation in Indian Monsoon precipitation: records from Bombay and New Delhi, *Geophysical Research Letters*, *30*(24).

Bierkens, M. F., and Y. Wada (2019), Non-renewable groundwater use and groundwater depletion: a review, *Environmental Research Letters*, *14*(6), 063002.

Bouwer, H. (1977), Land subsidence and cracking due to ground-water depletion a, *Groundwater, 15*(5), 358-364.

Bowen, G. J., Z. Cai, R. P. Fiorella, and A. L. Putman (2019), Isotopes in the water cycle: regional-to global-scale patterns and applications, *Annual Review of Earth and Planetary Sciences*, *47*(1).

Bowen, G. J., and J. Revenaugh (2003), Interpolating the isotopic composition of modern meteoric precipitation, *Water Resources Research*, *39*(10).

Breitenbach, S. F., J. F. Adkins, H. Meyer, N. Marwan, K. K. Kumar, and G. H. Haug (2010), Strong influence of water vapor source dynamics on stable isotopes in precipitation observed in Southern Meghalaya, NE India, *Earth and Planetary Science Letters*, *292*(1-2), 212-220.

Carpenter, S. R., E. H. Stanley, and M. J. Vander Zanden (2011), State of the world's freshwater ecosystems: physical, chemical, and biological changes, *Annual review of Environment and Resources, 36*, 75-99.

Carreira, P. M., M. Bahir, O. Salah, P. G. Fernandes, and D. Nunes (2018), Tracing salinization processes in coastal aquifers using an isotopic and geochemical approach: comparative studies in western Morocco and southwest Portugal, *Hydrogeology Journal*, *26*(8), 2595-2615.

Carreira, P. M., J. M. Marques, and D. Nunes (2014), Source of groundwater salinity in coastline aquifers based on environmental isotopes (Portugal): natural vs. human interference. A review and reinterpretation, *Applied Geochemistry*, *41*, 163-175.

CGWB (2011), Dynamic Ground Water Resources of India, edited, Central Ground Water Board, Ministry of Water Resources, Government of India ….

Chakraborty, M., S. Sarkar, A. Mukherjee, M. Shamsudduha, K. M. Ahmed, A. Bhattacharya, and A. Mitra (2020), Modeling regional-scale groundwater arsenic hazard in the transboundary Ganges River Delta, India and Bangladesh: Infusing physically-based model with machine learning, *Science of the Total Environment*, *748*, 141107.

Chamyal, L., D. Maurya, and R. Raj (2003), Fluvial systems of the drylands of western India: a synthesis of Late Quaternary environmental and tectonic changes, *Quaternary International*, *104*(1), 69-86.

Changming, L., Y. Jingjie, and E. Kendy (2001), Groundwater exploitation and its impact on the environment in the North China Plain, *Water International*, *26*(2), 265-272.

Charatkar, S., D. Mitra, R. Biradar, and M. Pikle (2005), Study of Salt Pan Increment in Gulf of Cambay using GIS, paper presented at 25th Annual ESRI User International Conference at San Diego, California, USA, July.

Chen, C., S. Pei, and J. Jiao (2003), Land subsidence caused by groundwater exploitation in Suzhou City, China, *Hydrogeology Journal*, *11*(2), 275-287.

Chen, J., J. Li, Z. Zhang, and S. Ni (2014), Long-term groundwater variations in Northwest India from satellite gravity measurements, *Global and Planetary Change*, *116*, 130-138.

Clark, and Fritz (1997), Environmental isotopes in hydrogeology.

Coplen, T. B., A. L. Herczeg, and C. Barnes (2000), Isotope engineering—using stable isotopes of the water molecule to solve practical problems, in *Environmental Tracers in Subsurface Hydrology*, edited, pp. 79-110, Springer.

Coudrain, A., B. Fourcade, and J. Touma (2003), Evaporative flux of the phreatic water table in arid regions], *International Association of Hydrological Sciences, Publication*(278), 82-86.

Craig, H. (1961), Isotopic variations in meteoric waters, *Science*, *133*(3465), 1702-1703.

Currell, M. J., I. Cartwright, D. C. Bradley, and D. Han (2010), Recharge history and controls on groundwater quality in the Yuncheng Basin, north China, *Journal of Hydrology*, *385*(1-4), 216-229.

Custodio, E. (2002), Aquifer overexploitation: what does it mean?, *Hydrogeology Journal*, *10*(2), 254-277.

Dansgaard, W. (1964), Stable isotopes in precipitation, *Tellus*, *16*(4), 436-468.

Darling, W. G., A. Bath, and J. Talbot (2003), The O and H stable isotope composition of freshwaters in the British Isles. 2. Surface waters and groundwater, *Hydrology and Earth System Sciences*, *7*(2), 183-195.

Dave, H., and M. E. James (2017), Characteristics of intense rainfall over Gujarat State (India) based on percentile criteria, *Hydrological Sciences Journal*, *62*(12), 2035-2048.

Deshpande, R., S. Bhattacharya, R. Jani, and S. Gupta (2003), Distribution of oxygen and hydrogen isotopes in shallow groundwaters from Southern India: influence of a dual monsoon system, *Journal of Hydrology*, *271*(1-4), 226-239.

Deshpande, R., and S. Gupta (2008), National programme on isotope fingerprinting of waters of India (IWIN), *Glimpses of Geosciences Research in India, the Indian Report to IUGS, Indian National Science Academy (eds Singhvi, AK, Bhattacharya, A. and Guha, S.), INSA, New Delhi*, 10-16.

Deshpande, R., and S. Gupta (2012), Oxygen and hydrogen isotopes in hydrological cycle: new data from IWIN national programme, *Proceedings of the Indian National Science Academy*, *78*(3), 321-331.

Deshpande, R., and S. Gupta (2013), Groundwater helium: an indicator of active tectonic regions along Narmada River, central India, *Chemical Geology*, *344*, 42-49.

Deshpande, R., A. Maurya, B. Kumar, A. Sarkar, and S. Gupta (2010), Rain-vapor interaction and vapor source identification using stable isotopes from semiarid western India, *Journal of Geophysical Research: Atmospheres*, *115*(D23).

Deshpande, R., P. Muraleedharan, R. L. Singh, B. Kumar, M. S. Rao, M. Dave, K. Sivakumar, and S. Gupta (2013), Spatio-temporal distributions of δ18O, δD and salinity in the Arabian Sea: Identifying processes and controls, *Marine Chemistry*, *157*, 144-161.

Döll, P., H. Hoffmann-Dobrev, F. T. Portmann, S. Siebert, A. Eicker, M. Rodell, G. Strassberg, and B. Scanlon (2012), Impact of water withdrawals from groundwater and surface water on continental water storage variations, *Journal of Geodynamics*, *59*, 143-156.

Döll, P., H. Müller Schmied, C. Schuh, F. T. Portmann, and A. Eicker (2014), Global-scale assessment of groundwater depletion and related groundwater abstractions: Combining hydrological modeling with information from well observations and GRACE satellites, *Water Resources Research*, *50*(7), 5698-5720.

Draxler, R., and G. Rolph (2003), HYSPLIT (HYbrid Single-Particle Lagrangian Integrated Trajectory) Model Access via NOAA ARL READY Website. NOAA Air Resources Laboratory, Silver Spring, MD, edited.

Edmunds, W., and A. Droubi (1998), Groundwater salinity and environmental change, in *Isotope techniques in the study of environmental change*, edited.

Elango, L., and R. Kannan (2007), Rock–water interaction and its control on chemical composition of groundwater, *Developments in Environmental Science*, *5*, 229-243.

Epstein, S., and T. Mayeda (1953), Variation of O18 content of waters from natural sources, *Geochimica et Cosmochimica Acta*, *4*(5), 213-224.

Esquivel-Hernández, G., G. M. Mosquera, R. Sánchez-Murillo, A. Quesada-Román, C. Birkel, P. Crespo, R. Célleri, D. Windhorst, L. Breuer, and J. Boll (2019), Moisture transport and seasonal variations in the stable isotopic composition of rainfall in Central American and Andean Páramo during El Niño conditions (2015–2016), *Hydrological Processes*, *33*(13), 1802-1817.

Famiglietti, J. S. (2014), The global groundwater crisis, *Nature Climate Change*, *4*(11), 945-948.

Famiglietti, J. S., M. Lo, S. L. Ho, J. Bethune, K. Anderson, T. H. Syed, S. C. Swenson, C. R. de Linage, and M. Rodell (2011), Satellites measure recent rates of groundwater depletion in California's Central Valley, *Geophysical Research Letters*, *38*(3).

Figueroa, A. J., and M. Smilovic (2021), Groundwater irrigation and implication in the Nile river basin, in *Global Groundwater*, edited, pp. 81-95, Elsevier.

Fishman, R. M., T. Siegfried, P. Raj, V. Modi, and U. Lall (2011), Over-extraction from shallow bedrock versus deep alluvial aquifers: Reliability versus sustainability considerations for India's groundwater irrigation, *Water Resources Research*, *47*(6).

Förstel, H., and H. Hützen (1983), Oxygen isotope ratios in German groundwater, *Nature*, *304*(5927), 614-616.

Foster, S., and P. Chilton (2003), Groundwater: the processes and global significance of aquifer degradation, *Philosophical Transactions of the Royal Society of London. Series B: Biological Sciences*, *358*(1440), 1957-1972.

Frits, P., R. Drimmie, S. Frape, and K. O'shea (1987), The isotopic composition of precipitation and groundwater in Canada, in *Isotope Techniques in Water Resources Development*, edited.

Gat, J. R. (1971), Comments on the stable isotope method in regional groundwater investigations, *Water Resources Research*, *7*(4), 980-993.

Gat, J. R. (1996), Oxygen and hydrogen isotopes in the hydrologic cycle, *Annual Review of Earth and Planetary Sciences*, *24*, 225-262.

Gat, J. R. (2010), *Isotope hydrology: a study of the water cycle*, World scientific.

Gautam, M. K., B.-Y. Song, W.-J. Shin, Y.-S. Bong, and K.-S. Lee (2020), Spatial variations in oxygen and hydrogen isotopes in waters and human hair across South Korea, *Science of the Total Environment*, *726*, 138365.

Genereux, D. (1998), Quantifying uncertainty in tracer-based hydrograph separations, *Water Resources Research*, *34*(4), 915-919.

George, M. E., T. Akhil, R. Remya, M. Rafeeque, and D. S. Babu (2021), Submarine groundwater discharge and associated nutrient flux from southwest coast of India, *Marine Pollution Bulletin*, *162*, 111767.

George, M. E., D. Babu, T. Akhil, and M. Rafeeque (2018), Investigation on submarine groundwater discharge at Kozhikkode coastal aquifer, SW western Ghats, *Journal of the Geological Society of India*, *92*(5), 626-633.

Gimenez, E., and I. Morell (1997), Hydrogeochemical analysis of salinization processes in the coastal aquifer of Oropesa (Castellon, Spain), *Environmental Geology*, *29*(1), 118-131.

Gleeson, T., K. M. Befus, S. Jasechko, E. Luijendijk, and M. B. Cardenas (2016), The global volume and distribution of modern groundwater, *Nature Geoscience*, *9*(2), 161-167.

Gleeson, T., K. Novakowski, and T. K. Kyser (2009), Extremely rapid and localized recharge to a fractured rock aquifer, *Journal of Hydrology*, *376*(3-4), 496-509.

Gleeson, T., J. VanderSteen, M. A. Sophocleous, M. Taniguchi, W. M. Alley, D. M. Allen, and Y. Zhou (2010), Groundwater sustainability strategies, *Nature Geoscience*, *3*(6), 378-379.

Gleeson, T., Y. Wada, M. F. Bierkens, and L. P. Van Beek (2012), Water balance of global aquifers revealed by groundwater footprint, *Nature*, *488*(7410), 197-200.

Gonfiantini, R. (1986), Environmental isotopes in lake studies, *Handbook of Environmental Isotope Geochemistry*, *2*, 113-168.

Gonfiantini, R., and L. Araguás (1988), Los isótopos ambientales en el estudio de la intrusión marina, paper presented at Tecnología de la intrusión en acuíf¸ eros costeros.

Gonfiantini, R., K. Fröhlich, L. Araguás-Araguás, and K. Rozanski (1998), Isotopes in groundwater hydrology, in *Isotope Tracers in Catchment Hydrology*, edited, pp. 203-246, Elsevier.

Govender, Y., E. Cuevas, L. Sternberg, and M. Jury (2013), Temporal variation in stable isotopic composition of rainfall and groundwater in a tropical dry forest in the northeastern Caribbean, *Earth Interactions*, *17*(27), 1-20.

Gupta, S., and R. Deshpande (2003), Origin of groundwater helium and temperature anomalies in the Cambay region of Gujarat, India, *Chemical Geology*, *198*(1-2), 33-46.

Gupta, S., and R. Deshpande (2005a), Groundwater isotopic investigations in India: What has been learned?, *Current Science*, 825-835.

Gupta, S., and R. Deshpande (2005b), The need and potential applications of a network for monitoring of isotopes in waters of India, *Current Science*, 107-118.

Gupta, S., R. Deshpande, M. Agarwal, and B. Raval (2005a), Origin of high fluoride in groundwater in the North Gujarat-Cambay region, India, *Hydrogeology Journal*, *13*(4), 596-605.

Gupta, S., R. Deshpande, S. Bhattacharya, and R. Jani (2005b), Groundwater δ18O and δD from central Indian Peninsula: influence of the Arabian Sea and the Bay of Bengal branches of the summer monsoon, *Journal of Hydrology*, *303*(1-4), 38-55.

Hameed, A. S., T. Resmi, S. Suraj, C. U. Warrier, M. Sudheesh, and R. Deshpande (2015), Isotopic characterization and mass balance reveals groundwater recharge pattern in Chaliyar river basin, Kerala, India, *Journal of Hydrology: Regional Studies*, *4*, 48-58.

Hao, S., F. Li, Y. Li, C. Gu, Q. Zhang, Y. Qiao, L. Jiao, and N. Zhu (2019), Stable isotope evidence for identifying the recharge mechanisms of precipitation, surface water, and groundwater in the Ebinur Lake basin, *Science of the Total Environment*, *657*, 1041-1050.

Healy, R. W. (2010), *Estimating groundwater recharge*, Cambridge university press.

Hendry, M., and F. Schwartz (1988), An alternative view on the origin of chemical and isotopic patterns in groundwater from the Milk River Aquifer, Canada, *Water Resources Research*, *24*(10), 1747-1763.

Herczeg, A. L., C. J. Barnes, P. G. Macumber, and J. M. Olley (1992), A stable isotope investigation of groundwater-surface water interactions at Lake Tyrrell, Victoria, Australia, *Chemical Geology*, *96*(1-2), 19-32.

Horita, J., and D. J. Wesolowski (1994), Liquid-vapor fractionation of oxygen and hydrogen isotopes of water from the freezing to the critical temperature, *Geochimica et Cosmochimica Acta*, *58*(16), 3425-3437.

Huang, T., and Z. Pang (2012), The role of deuterium excess in determining the water salinisation mechanism: a case study of the arid Tarim River Basin, NW China, *Applied Geochemistry*, *27*(12), 2382-2388.

Hunt, R. J., T. B. Coplen, N. L. Haas, D. A. Saad, and M. A. Borchardt (2005), Investigating surface water–well interaction using stable isotope ratios of water, *Journal of Hydrology*, *302*(1-4), 154-172.

Ingraham, N. L., and B. E. Taylor (1991), Light stable isotope systematics of large-scale hydrologic regimes in California and Nevada, *Water Resources Research*, *27*(1), 77-90.

Jackson, P. E. (2000), Ion chromatography in environmental analysis, *Encyclopedia of Analytical Chemistry*, *2779*.

Jackson, R. B., S. R. Carpenter, C. N. Dahm, D. M. McKnight, R. J. Naiman, S. L. Postel, and S. W. Running (2001), Water in a changing world, *Ecological applications*, *11*(4), 1027-1045.

Jasechko, S. (2019), Global isotope hydrogeology―Review, *Reviews of Geophysics*, *57*(3), 835-965.

Jeelani, G., and R. Deshpande (2017), Isotope fingerprinting of precipitation associated with western disturbances and Indian summer monsoons across the Himalayas, *Journal of Earth System Science*, *126*(8), 1-13.

Jeelani, G., U. S. Kumar, and B. Kumar (2013), Variation of δ18O and δD in precipitation and stream waters across the Kashmir Himalaya (India) to distinguish and estimate the seasonal sources of stream flow, *Journal of Hydrology*, *481*, 157-165.

Jesiya, N., and G. Gopinath (2019), Hydrogeochemical and isotopic investigations on phreatic aquifers of urban and peri-urban clusters of Kozhikode District Kerala Southern India, Cochin University of Science and Technology.

Joshi, S. K., S. P. Rai, and R. Sinha (2021), Understanding groundwater recharge processes in the Sutlej-Yamuna plain in NW India using an isotopic approach, *Geological Society, London, Special Publications*, *507*(1), 133-147.

Jung, Y.-Y., D.-C. Koh, Y.-Y. Yoon, H.-I. Kwon, J. Heo, K. Ha, and S.-T. Yun (2019), Using stable isotopes and tritium to delineate groundwater flow systems and their relationship to streams in the Geum River basin, Korea, *Journal of Hydrology*, *573*, 267-280.

Jung, Y.-Y., W.-J. Shin, K.-H. Seo, D.-C. Koh, K.-S. Ko, and K.-S. Lee (2022), Spatial distributions of oxygen and hydrogen isotopes in multi-level groundwater across South Korea: A case study of mountainous regions, *Science of The Total Environment*, *812*, 151428.

Keesari, T., D. A. Sharma, M. S. Rishi, D. Pant, H. V. Mohokar, A. K. Jaryal, and U. Sinha (2017), Isotope investigation on groundwater recharge and dynamics in shallow and deep alluvial aquifers of southwest Punjab, *Applied Radiation and Isotopes*, *129*, 163-170.

Kendall, C., and J. J. McDonnell (2012), *Isotope Tracers in Catchment Hydrology*, Elsevier.

Konikow, L. F. (2011), Contribution of global groundwater depletion since 1900 to sea-level rise, *Geophysical Research Letters*, *38*(17).

Konikow, L. F., and E. Kendy (2005), Groundwater depletion: A global problem, *Hydrogeology Journal*, *13*(1), 317-320.

Kortelainen, N. M. (2011), Isotope tracing in groundwater applications, *Geological Survey of Finland Special Paper*, *49*, 279-284.

Kortelainen, N. M., and J. A. Karhu (2004), Regional and seasonal trends in the oxygen and hydrogen isotope ratios of Finnish groundwaters: a key for mean annual precipitation, *Journal of Hydrology*, *285*(1-4), 143-157.

Krishan, G., N. Ghosh, C. Kumar, L. M. Sharma, B. Yadav, M. L. Kansal, S. Singh, S. Verma, and G. Prasad (2020a), Understanding stable isotope systematics of salinity affected groundwater in Mewat, Haryana, India, *Journal of Earth System Science*, *129*(1), 1-9.

Krishan, G., G. Prasad, C. Kumar, N. Patidar, B. K. Yadav, M. L. Kansal, S. Singh, L. Sharma, A. Bradley, and S. Verma (2020b), Identifying the seasonal variability in source of groundwater salinization using deuterium excess-a case study from Mewat, Haryana, India, *Journal of Hydrology: Regional Studies*, *31*, 100724.

Krishan, G., M. S. Rao, C. Kumar, S. Kumar, and M. R. A. Rao (2015), A study on identification of submarine groundwater discharge in Northern East Coast of India, *Aquatic Procedia*, *4*, 3-10.

Krishnamurthy, R., and S. Bhattacharya (1991), Stable oxygen and hydrogen isotope ratios in shallow ground waters from India and a study of the role of evapotranspiration in the Indian monsoon, *Stable Isotope Geochemistry: A Tribute to Samuel Epstein*, *3*, 187-193.

Kumar, B., S. P. Rai, U. S. Kumar, S. Verma, P. Garg, S. V. Kumar, R. Jaiswal, B. Purendra, S. Kumar, and N. Pande (2010), Isotopic characteristics of Indian precipitation, *Water Resources Research*, *46*(12).

Kumar, K. A., C. Priju, and N. N. Prasad (2015), Study on saline water intrusion into the shallow coastal aquifers of Periyar River Basin, Kerala using hydrochemical and electrical resistivity methods, *Aquatic Procedia*, *4*, 32-40.

Kumar, K. R., G. Pant, B. Parthasarathy, and N. Sontakke (1992), Spatial and subseasonal patterns of the long-term trends of Indian summer monsoon rainfall, *International Journal of climatology*, *12*(3), 257-268.

Kumar, R. V. S. (2018), Characteristics of Brown Carbon Present in Ambient Aerosols Over Different Regions in India, Mohanlal Sukhadia University, Udaipur.

Kumar, U. S., S. Sharma, and S. Navada (2008), Recent studies on surface water–groundwater relationships at hydro-projects in India using environmental isotopes, *Hydrological Processes: An International Journal*, *22*(23), 4543-4553.

Kundu, S., D. Khare, A. Mondal, and P. Mishra (2015), Analysis of spatial and temporal variation in rainfall trend of Madhya Pradesh, India (1901–2011), *Environmental Earth Sciences*, *73*(12), 8197-8216.

Lakshmanan, E., R. Kannan, and M. S. Kumar (2003), Major ion chemistry and identification of hydrogeochemical processes of ground water in a part of Kancheepuram district, Tamil Nadu, India, *Environmental Geosciences*, *10*(4), 157-166.

Lawson, M., C. Ballentine, D. Polya, A. Boyce, D. Mondal, D. Chatterjee, S. Majumder, and A. Biswas (2008), The geochemical and isotopic composition of ground waters in West Bengal:

tracing ground-surface water interaction and its role in arsenic release, *Mineralogical Magazine*, *72*(1), 441-444.

Li, P., H. Qian, J. Wu, Y. Zhang, and H. Zhang (2013), Major ion chemistry of shallow groundwater in the Dongsheng Coalfield, Ordos Basin, China, *Mine Water and the Environment*, *32*(3), 195-206.

Lin, L., and C. N. Garzione (2017), Spatial distribution and controlling factors of stable isotopes in meteoric waters on the Tibetan Plateau: Implications for paleoelevation reconstruction, *Earth and Planetary Science Letters*, *460*, 302-314.

Liotta, M., F. Grassa, W. D'Alessandro, R. Favara, E. G. Candela, A. Pisciotta, and C. Scaletta (2013), Isotopic composition of precipitation and groundwater in Sicily, Italy, *Applied Geochemistry*, *34*, 199-206.

Liu, Y., and T. Yamanaka (2012), Tracing groundwater recharge sources in a mountain–plain transitional area using stable isotopes and hydrochemistry, *Journal of Hydrology*, *464*, 116-126.

Long, D., X. Chen, B. R. Scanlon, Y. Wada, Y. Hong, V. P. Singh, Y. Chen, C. Wang, Z. Han, and W. Yang (2016), Have GRACE satellites overestimated groundwater depletion in the Northwest India Aquifer?, *Scientific Reports*, *6*(1), 1-11.

Loni, O. A., F. K. Zaidi, M. S. Alhumimidi, O. A. Alharbi, M. T. Hussein, M. Dafalla, K. A. AlYousef, and O. M. Kassem (2015), Evaluation of groundwater quality in an evaporation dominant arid environment; a case study from Al Asyah area in Saudi Arabia, *Arabian Journal of Geosciences*, *8*(8), 6237-6247.

Mahmoudpour, M., M. Khamehchiyan, M. R. Nikudel, and M. R. Ghassemi (2016), Numerical simulation and prediction of regional land subsidence caused by groundwater exploitation in the southwest plain of Tehran, Iran, *Engineering Geology*, *201*, 6-28.

Majoube, M. (1971), Fractionnement en oxygène 18 et en deutérium entre l'eau et sa vapeur, *Journal de Chimie Physique*, *68*, 1423-1436.

Manivannan, V., and L. Elango (2019), Seawater intrusion and submarine groundwater discharge along the Indian coast, *Environmental Science and Pollution Research*, *26*(31), 31592-31608.

Mao, H., G. Wang, Z. Shi, F. Liao, and Y. Xue (2021), Spatiotemporal variation of groundwater recharge in the lower reaches of the Poyang Lake Basin, China: insights from stable hydrogen and oxygen isotopes, *Journal of Geophysical Research: Atmospheres*, *126*(6), e2020JD033760.

Margat, J., and J. Van der Gun (2013), *Groundwater Around the World: a Geographic Synopsis*, Crc Press.

Maurya, A. S., M. Shah, R. Deshpande, R. Bhardwaj, A. Prasad, and S. Gupta (2011), Hydrograph separation and precipitation source identification using stable water isotopes and conductivity: River Ganga at Himalayan foothills, *Hydrological Processes*, *25*(10), 1521-1530.

McGUIRE, K., and J. McDONNELL (2007), Stable isotope tracers in watershed hydrology, *Stable isotopes in Ecology and Environmental Science*, 334-374.

Mehr, S. (1995), Geology of Gujarat (p. 222), *Bangalore: Geological Society of India*.

Merlivat, L., and G. Nief (1967), Fractionnement isotopique lors des changements d ‘état solide-vapeur et liquide-vapeur de l'eau à des températures inférieures à 0° C, *Tellus*, *19*(1), 122-127.

Miller, M. P., S. G. Buto, D. D. Susong, and C. A. Rumsey (2016), The importance of base flow in sustaining surface water flow in the Upper Colorado River Basin, *Water Resources Research*, *52*(5), 3547-3562.

Mohanty, M., K. Ray, and K. Chakravarthy (2015), Analysis of increasing heavy rainfall activity over Western India, particularly Gujarat State, in the past decade, in *High-impact weather events over the SAARC region*, edited, pp. 259-276, Springer.

Morales, J. A., L. S. de Graterol, and J. Mesa (2000), Determination of chloride, sulfate and nitrate in groundwater samples by ion chromatography, *Journal of Chromatography A*, *884*(1-2), 185-190.

Mukherjee, A. (2018), Overview of the groundwater of South Asia, in *Groundwater of South Asia*, edited, pp. 3-20, Springer.

Mukherjee, A., S. N. Bhanja, and Y. Wada (2018), Groundwater depletion causing reduction of baseflow triggering Ganges river summer drying, *Scientific Reports*, *8*(1), 1-9.

Mukherjee, A., A. E. Fryar, and H. D. Rowe (2007), Regional-scale stable isotopic signatures of recharge and deep groundwater in the arsenic affected areas of West Bengal, India, *Journal of Hydrology*, *334*(1-2), 151-161.

Mukherjee, A., D. Saha, C. F. Harvey, R. G. Taylor, K. M. Ahmed, and S. N. Bhanja (2015), Groundwater systems of the Indian sub-continent, *Journal of Hydrology: Regional Studies*, *4*, 1-14.

Mukherjee, A., B. R. Scanlon, A. Aureli, S. Langan, H. Guo, and A. A. McKenzie (2020), *Global groundwater: source, scarcity, sustainability, security, and solutions*, Elsevier.

Müller, T., J. Friesen, S. M. Weise, O. Al Abri, A. B. A. Bait Said, and N. Michelsen (2020), Stable isotope composition of cyclone Mekunu rainfall, southern Oman, *Water Resources Research*, *56*(12), e2020WR027644.

Nakaya, S., K. Uesugi, Y. Motodate, I. Ohmiya, H. Komiya, H. Masuda, and M. Kusakabe (2007), Spatial separation of groundwater flow paths from a multi-flow system by a simple mixing model using stable isotopes of oxygen and hydrogen as natural tracers, *Water Resources Research*, *43*(9).

Nandakumaran, P., and K. Balakrishnan (2020), Groundwater quality variations in Precambrian hard rock aquifers: a case study from Kerala, India, *Applied Water Science*, *10*(1), 1-13.

Nimmo, J. R., R. W. Healy, and D. A. Stonestrom (2005), Aquifer recharge, *Encyclopedia of Hydrological Science*, *4*, 2229-2246.

O'Driscoll, M., D. DeWalle, K. McGuire, and W. Gburek (2005), Seasonal 18O variations and groundwater recharge for three landscape types in central Pennsylvania, USA, *Journal of Hydrology*, *303*(1-4), 108-124.

O'Neil, J. R. (1968), Hydrogen and oxygen isotope fractionation between ice and water, *The Journal of Physical Chemistry*, *72*(10), 3683-3684.

Oza, H. (2020), Understanding hydrometeorological processes concerning Indian precipitation: insights from oxygen and hydrogen stable isotopes in conjunction with meteorological parameters, Indian Institute of Technology Gandhinagar.

Oza, H., A. Ganguly, V. Padhya, and R. Deshpande (2020a), Hydrometeorological processes and evaporation from falling rain in Indian sub-continent: Insights from stable isotopes and meteorological parameters, *Journal of Hydrology*, *591*, 125601.

Oza, H., V. Padhya, A. Ganguly, and R. Deshpande (2022), Investigating hydrometeorology of the Western Himalayas: Insights from stable isotopes of water and meteorological parameters, *Atmospheric Research*, *268*, 105997.

Oza, H., V. Padhya, A. Ganguly, K. Saikranthi, T. Rao, and R. Deshpande (2020b), Hydrometeorological processes in semi-arid western India: insights from long term isotope record of daily precipitation, *Climate Dynamics*, *54*(5), 2745-2757.

Pahuja, S., C. Tovey, S. Foster, and H. Garduno (2010), Deep wells and prudence: towards pragmatic action for addressing groundwater overexploitation in India, *Deep wells and prudence: towards pragmatic action for addressing groundwater overexploitation in India.*

Pande, K., J. Padia, R. Ramesh, and K. Sharma (2000), Stable isotope systematics of surface water bodies in the Himalayan and Trans-Himalayan (Kashmir) region, *Journal of Earth System Science*, *109*(1), 109-115.

Parlov, J., Z. Kovač, Z. Nakić, and J. Barešić (2019), Using water stable isotopes for identifying groundwater recharge sources of the unconfined alluvial Zagreb aquifer (Croatia), *Water*, *11*(10), 2177.

Parthasarathy, B., and S. Yang (1995), Relationships between regional Indian summer monsoon rainfall and Eurasian snow cover, *Advances in Atmospheric Sciences*, *12*(2), 143-150.

Patel, P. M., D. Saha, and T. Shah (2020), Sustainability of groundwater through community-driven distributed recharge: An analysis of arguments for water scarce regions of semi-arid India, *Journal of Hydrology: Regional Studies*, *29*, 100680.

Patil, S., N. Bhave, and H. Kulkarni (2019), Situation Analysis of Groundwater.

Phillips, D. L. (2001), Mixing models in analyses of diet using multiple stable isotopes: a critique, *Oecologia*, *127*(2), 166-170.

Pohl, E., M. Knoche, R. Gloaguen, C. Andermann, and P. Krause (2015), Sensitivity analysis and implications for surface processes from a hydrological modelling approach in the Gunt catchment, high Pamir Mountains, *Earth Surface Dynamics*, *3*(3), 333-362.

Postel, S. L. (2000), Entering an era of water scarcity: the challenges ahead, *Ecological applications*, *10*(4), 941-948.

Prakash, R., K. Srinivasamoorthy, S. Gopinath, and K. Saravanan (2018), Measurement of submarine groundwater discharge using diverse methods in Coleroon Estuary, Tamil Nadu, India, *Applied Water Science*, *8*(1), 1-11.

Prasanth, S. S., N. Magesh, K. Jitheshlal, N. Chandrasekar, and K. Gangadhar (2012), Evaluation of groundwater quality and its suitability for drinking and agricultural use in the coastal stretch of Alappuzha District, Kerala, India, *Applied Water Science*, *2*(3), 165-175.

Priyan, K. (2015), Spatial and temporal variability of rainfall in Anand District of Gujarat State, *Aquatic Procedia*, *4*, 713-720.

Prusty, P., S. Farooq, D. Swain, and D. Chandrasekharam (2020), Association of geomorphic features with groundwater quality and freshwater availability in coastal regions, *International journal of Environmental Science and Technology*, *17*(6), 3313-3328.

Raidla, V., Z. Kern, J. Pärn, A. Babre, K. Erg, J. Ivask, A. Kalvāns, B. Kohán, M. Lelgus, and T. Martma (2016), A δ18O isoscape for the shallow groundwater in the Baltic Artesian Basin, *Journal of Hydrology*, *542*, 254-267.

Rajmohan, N., M. H. Masoud, and B. A. Niyazi (2021), Impact of evaporation on groundwater salinity in the arid coastal aquifer, Western Saudi Arabia, *Catena*, *196*, 104864.

Rastogi, N., A. Singh, M. Sarin, and D. Singh (2016), Temporal variability of primary and secondary aerosols over northern India: Impact of biomass burning emissions, *Atmospheric Environment*, *125*, 396-403.

Ray, K., M. Mohanty, and J. Chincholikar (2009), Climate variability over Gujarat, India, *ISPRS archives*, *38*(8), W3.

Resmi, T., K. Sudharma, and A. S. Hameed (2016), Stable isotope characteristics of precipitation of Pamba River basin, Kerala, India, *Journal of Earth System Science*, *125*(7), 1481-1493.

Rodell, M., J. S. Famiglietti, D. N. Wiese, J. Reager, H. K. Beaudoing, F. W. Landerer, and M.-H. Lo (2018), Emerging trends in global freshwater availability, *Nature*, *557*(7707), 651-659.

Rodell, M., I. Velicogna, and J. S. Famiglietti (2009), Satellite-based estimates of groundwater depletion in India, *Nature*, *460*(7258), 999-1002.

Rozanski, K. (1985), Deuterium and oxygen-18 in European groundwaters—links to atmospheric circulation in the past, *Chemical Geology: Isotope Geoscience Section*, *52*(3-4), 349-363.

Rozanski, K., L. Araguás-Araguás, and R. Gonfiantini (1993), Isotopic patterns in modern global precipitation, *Geophysical Monograph-American Geophysical Union*, *78*, 1-1.

Rubenstein, D. R., and K. A. Hobson (2004), From birds to butterflies: animal movement patterns and stable isotopes, *Trends in Ecology & Evolution*, *19*(5), 256-263.

Saha, D., Y. Dhar, and S. Vittala (2010), Delineation of groundwater development potential zones in parts of marginal Ganga Alluvial Plain in South Bihar, Eastern India, *Environmental Monitoring and Assessment*, *165*(1), 179-191.

Saha, D., S. Marwaha, and A. Mukherjee (2018), Groundwater resources and sustainable management issues in India, in *Clean and sustainable groundwater in India*, edited, pp. 1-11, Springer.

Saha, D., and R. K. Ray (2019), Groundwater resources of India: Potential, challenges and management, in *Groundwater Development and Management*, edited, pp. 19-42, Springer.

Saha, D., A. K. Sikka, and R. Goklani (2022), Artificial recharge endeavours in India: A review, *Water Security*, *16*, 100121.

Sajeena, S., P. Swathy, and A. H. VM (2020), Studies on saline water intrusion in the coastal stretch of Kadalundi river basin, Malappuram district, Kerala using visual MODFLOW–A case study.

Sakakibara, K., M. Tsujimura, X. Song, and J. Zhang (2017), Spatiotemporal variation of the surface water effect on the groundwater recharge in a low-precipitation region: Application of the multi-tracer approach to the Taihang Mountains, North China, *Journal of Hydrology*, *545*, 132-144.

Salam, M., M. J. M. Cheema, W. Zhang, S. Hussain, A. Khan, M. Bilal, A. Arshad, S. Ali, and M. A. Zaman (2020), Groundwater storage change estimation using grace satellite data in Indus Basin, *Big data in water resources engineering (BDWRE)*, *1*, 13-18.

Salameh, E. (2008), Over-exploitation of groundwater resources and their environmental and socio-economic implications: the case of Jordan, *Water International*, *33*(1), 55-68.

Saranya, P., A. Krishnakumar, S. Kumar, and K. A. Krishnan (2020), Isotopic study on the effect of reservoirs and drought on water cycle dynamics in the tropical Periyar basin draining the slopes of Western Ghats, *Journal of Hydrology*, *581*, 124421.

Sarkar, T., S. Kannaujiya, A. K. Taloor, P. K. C. Ray, and P. Chauhan (2020), Integrated study of GRACE data derived interannual groundwater storage variability over water stressed Indian regions, *Groundwater for Sustainable Development*, *10*, 100376.

Scanlon, B. R., K. E. Keese, A. L. Flint, L. E. Flint, C. B. Gaye, W. M. Edmunds, and I. Simmers (2006), Global synthesis of groundwater recharge in semiarid and arid regions, *Hydrological Processes: An International Journal*, *20*(15), 3335-3370.

Scanlon, B. R., A. Mukherjee, J. Gates, R. C. Reedy, and A. K. Sinha (2010), Groundwater recharge in natural dune systems and agricultural ecosystems in the Thar Desert region, Rajasthan, India, *Hydrogeology Journal*, *18*(4), 959-972.

Schilling, O. S., A. Parajuli, C. Tremblay Otis, T. Müller, W. Antolinez Quijano, Y. Tremblay, M. S. Brennwald, D. F. Nadeau, S. Jutras, and R. Kipfer (2021), Quantifying groundwater recharge dynamics and unsaturated zone processes in snow-dominated catchments via on-site dissolved gas analysis, *Water Resources Research*, *57*(2), e2020WR028479.

Scott, C. A., and T. Shah (2004), Groundwater overdraft reduction through agricultural energy policy: insights from India and Mexico, *International Journal of Water Resources Development*, *20*(2), 149-164.

Sengupta, T., A. Deshpande Mukherjee, R. Bhushan, F. Ram, M. Bera, H. Raj, A. J. Dabhi, R. Bisht, Y. Rawat, and S. Bhattacharya (2020), Did the Harappan settlement of Dholavira (India) collapse during the onset of Meghalayan stage drought?, *Journal of Quaternary Science*, *35*(3), 382-395.

Shah, T. (2014), *Groundwater governance and irrigated agriculture*, Global Water Partnership (GWP) Stockholm.

Shah, T., S. Bhatt, R. K. Shah, and J. Talati (2008), Groundwater governance through electricity supply management: Assessing an innovative intervention in Gujarat, western India, *Agricultural Water Management*, *95*(11), 1233-1242.

Shaji, E., N. Vinayachandran, and D. Thambi (2009), Hydrogeochemical characteristics of groundwater in coastal phreatic aquifers of Alleppey district, Kerala, *Journal of the Geological Society of India*, *74*(5), 585-590.

Shiklomanov, I. A., and A. I. Shiklomanov (1999), Assessment of the impacts of climate variability and change on the hydrology of Asia and Australia.

Siebert, S., J. Burke, J.-M. Faures, K. Frenken, J. Hoogeveen, P. Döll, and F. T. Portmann (2010), Groundwater use for irrigation–a global inventory, *Hydrology and earth system sciences*, *14*(10), 1863-1880.

Simmers, I. (2013), *Estimation of natural groundwater recharge*, Springer Science & Business Media.

Singh, D. K., and A. K. Singh (2002), Groundwater situation in India: Problems and perspective, *International Journal of Water Resources Development*, *18*(4), 563-580.

Sodemann, H., C. Schwierz, and H. Wernli (2008), Interannual variability of Greenland winter precipitation sources: Lagrangian moisture diagnostic and North Atlantic Oscillation influence, *Journal of Geophysical Research: Atmospheres*, *113*(D3).

Soderberg, K., S. P. Good, M. O'Connor, L. Wang, K. Ryan, and K. K. Caylor (2013), Using atmospheric trajectories to model the isotopic composition of rainfall in central Kenya, *Ecosphere*, *4*(3), 1-18.

Song, X., S. Wang, G. Xiao, Z. Wang, X. Liu, and P. Wang (2009), A study of soil water movement combining soil water potential with stable isotopes at two sites of shallow groundwater areas in the North China Plain, *Hydrological Processes: An International Journal*, *23*(9), 1376-1388.

Sreekala, P., S. V. B. Rao, and M. Rajeevan (2012), Northeast monsoon rainfall variability over south peninsular India and its teleconnections, *Theoretical and Applied Climatology*, *108*(1), 73-83.

Stallard, R., and J. Edmond (1983), Geochemistry of the Amazon: 2. The influence of geology and weathering environment on the dissolved load, *Journal of Geophysical Research: Oceans*, *88*(C14), 9671-9688.

Stein, A., R. R. Draxler, G. D. Rolph, B. J. Stunder, M. Cohen, and F. Ngan (2015), NOAA's HYSPLIT atmospheric transport and dispersion modeling system, *Bulletin of the American Meteorological Society*, *96*(12), 2059-2077.

Subramani, T., N. Rajmohan, and L. Elango (2010), Groundwater geochemistry and identification of hydrogeochemical processes in a hard rock region, Southern India, *Environmental Monitoring and Assessment*, *162*(1), 123-137.

Sudheer, A., M. Aslam, M. Upadhyay, R. Rengarajan, R. Bhushan, J. Rathore, S. Singh, and S. Kumar (2016), Carbonaceous aerosol over semi-arid region of western India: Heterogeneity in sources and characteristics, *Atmospheric Research*, *178*, 268-278.

Sujith, K. (2016), Access controlled high speed corridor and urban development of Kerala, *Procedia Technology*, *24*, 1851-1857.

Sukhija, B., P. Nagabhushanam, and D. Reddy (1996), Groundwater recharge in semi-arid regions of India: an overview of results obtained using tracers, *Hydrogeology Journal*, *4*(3), 50-71.

Sun, C., T. M. Shanahan, and J. Partin (2019), Controls on the isotopic composition of precipitation in the South-Central United States, *Journal of Geophysical Research: Atmospheres*, *124*(14), 8320-8335.

Sun, C., L. Tian, T. M. Shanahan, J. W. Partin, Y. Gao, N. Piatrunia, and J. Banner (2022), Isotopic variability in tropical cyclone precipitation is controlled by Rayleigh distillation and cloud microphysics, *Communications Earth & Environment*, *3*(1), 1-10.

Suzuoki, T., and T. Kimura (1973), D/H and 18O/16O fractionation in ice-water system, *Journal of the Mass Spectrometry Society of Japan*, *21*(3), 229-233.

Swetha, T., G. Gopinath, and T. Resmi (2020), Isotope mass balance estimation of groundwater recharge in a hard rock tropical river basin in Kerala, India, *Groundwater for Sustainable Development*, *11*, 100422.

Swetha, T., G. Gopinath, K. Thrivikramji, and N. Jesiya (2017), Geospatial and MCDM tool mix for identification of potential groundwater prospects in a tropical river basin, Kerala, *Environmental Earth Sciences*, *76*(12), 1-17.

Taylor, R. G., B. Scanlon, P. Döll, M. Rodell, R. Van Beek, Y. Wada, L. Longuevergne, M. Leblanc, J. S. Famiglietti, and M. Edmunds (2013), Ground water and climate change, *Nature Climate Change*, *3*(4), 322-329.

Tiwari, V., J. Wahr, and S. Swenson (2009), Dwindling groundwater resources in northern India, from satellite gravity observations, *Geophysical Research Letters*, *36*(18).

Van Loon, A. F. (2015), Hydrological drought explained, *Wiley Interdisciplinary Reviews: Water*, *2*(4), 359-392.

Varma, A. (2017), Groundwater resource and governance in Kerala: Status, issues and prospects, Forum for Policy Dialogue on Water Conflicts in India.

Vogel, J., and H. Van Urk (1975), Isotopic composition of groundwater in semi-arid regions of southern Africa, *Journal of Hydrology*, *25*(1-2), 23-36.

Wada, Y., L. P. van Beek, and M. F. Bierkens (2012), Nonsustainable groundwater sustaining irrigation: A global assessment, *Water Resources Research*, *48*(6).

Wada, Y., L. P. Van Beek, C. M. Van Kempen, J. W. Reckman, S. Vasak, and M. F. Bierkens (2010), Global depletion of groundwater resources, *Geophysical Research Letters*, *37*(20).

Wada, Y., L. P. Van Beek, N. Wanders, and M. F. Bierkens (2013), Human water consumption intensifies hydrological drought worldwide, *Environmental Research Letters*, *8*(3), 034036.

Wani, N., A. Velmurugan, and V. Dadhwal (2010), Assessment of agricultural crop and soil carbon pools in Madhya Pradesh, India.

Warrier, C. U., M. P. Babu, P. Manjula, K. Velayudhan, A. S. Hameed, and K. Vasu (2010), Isotopic characterization of dual monsoon precipitation–evidence from Kerala, India, *Current Science*, 1487-1495.

Wassenaar, L. I., S. L. Van Wilgenburg, K. Larson, and K. A. Hobson (2009), A groundwater isoscape (δD, δ18O) for Mexico, *Journal of Geochemical Exploration*, *102*(3), 123-136.

West, A., E. February, and G. Bowen (2014), Spatial analysis of hydrogen and oxygen stable isotopes (“isoscapes”) in ground water and tap water across South Africa, *Journal of Geochemical Exploration*, *145*, 213-222.

West, J. B., G. J. Bowen, T. E. Dawson, and K. P. Tu (2009), *Isoscapes: understanding movement, pattern, and process on Earth through isotope mapping*, Springer.

West, J. B., A. Sobek, and J. R. Ehleringer (2008), A simplified GIS approach to modeling global leaf water isoscapes, *PLoS one*, *3*(6), e2447.

Weyhenmeyer, C. E., S. J. Burns, H. N. Waber, P. G. Macumber, and A. Matter (2002), Isotope study of moisture sources, recharge areas, and groundwater flow paths within the eastern Batinah coastal plain, Sultanate of Oman, *Water Resources Research*, *38*(10), 2-1-2-22.

Wilcox, W. M., H. M. Solo-Gabriele, and L. O. R. Sternberg (2004), Use of stable isotopes to quantify flows between the Everglades and urban areas in Miami-Dade County Florida, *Journal of Hydrology*, *293*(1-4), 1-19.

Winter, T. C. (2007), The Role of Ground Water in Generating Streamflow in Headwater Areas and in Maintaining Base Flow 1, *JAWRA Journal of the American Water Resources Association*, *43*(1), 15-25.

Wu, H., X. Zhang, L. Xiaoyan, G. Li, and Y. Huang (2015), Seasonal variations of deuterium and oxygen-18 isotopes and their response to moisture source for precipitation events in the subtropical monsoon region, *Hydrological Processes*, *29*(1), 90-102.

Yang, L., X. Song, Y. Zhang, D. Han, B. Zhang, and D. Long (2012), Characterizing interactions between surface water and groundwater in the Jialu River basin using major ion chemistry and stable isotopes, *Hydrology and Earth System Sciences*, *16*(11), 4265-4277.

Yao, Y., C. Zheng, C. B. Andrews, B. R. Scanlon, X. Kuang, Z. Zeng, S. J. Jeong, M. Lancia, Y. Wu, and G. Li (2021), Role of groundwater in sustaining Northern Himalayan Rivers, *Geophysical Research Letters*, *48*(10), e2020GL092354.

Yeh, H.-F., C.-H. Lee, and K.-C. Hsu (2011), Oxygen and hydrogen isotopes for the characteristics of groundwater recharge: a case study from the Chih-Pen Creek basin, Taiwan, *Environmental Earth Sciences*, *62*(2), 393-402.

Yeh, H.-F., H.-I. Lin, C.-H. Lee, K.-C. Hsu, and C.-S. Wu (2014a), Identifying seasonal groundwater recharge using environmental stable isotopes, *Water*, *6*(10), 2849-2861.

Yeh, H.-F., H.-I. Lin, S.-T. Lee, M.-H. Chang, K.-C. Hsu, and C.-H. Lee (2014b), GIS and SBF for estimating groundwater recharge of a mountainous basin in the Wu River watershed, Taiwan, *Journal of Earth System Science*, *123*(3), 503-516.

Yuan, X., M. Zhang, L. Wang, and T. Zhou (2017), Understanding and seasonal forecasting of hydrological drought in the Anthropocene, *Hydrology and Earth System Sciences*, *21*(11), 5477-5492.

Zhao, M., Y. Hu, C. Zeng, Z. Liu, R. Yang, and B. Chen (2018), Effects of land cover on variations in stable hydrogen and oxygen isotopes in karst groundwater: A comparative study of three karst catchments in Guizhou Province, Southwest China, *Journal of hydrology*, *565*, 374-385.

Publications:

- Pandey, A., Padhya, V., Ganguly, A., Chakra, S. and Deshpande, R.D., 2023. Surface water groundwater interaction in water-stressed semi-arid western India: Insights from environmental isotopes. ***Journal of Arid Environments***, *208*, p.104879.
- Pandey, A., Padhya, V., Chakra, S., Ganguly, A. and Deshpande, R.D., 2022. Groundwater recharge in Central India and its spatio-temporal variation: Insights and implications from oxygen and hydrogen isotopes. ***Journal of Hydrology,*** p.129040.